NASA TECHNICAL REPORT

NASA TR R-436

A CUBIC SPLINE APPROXIMATION FOR PROBLEMS IN FLUID MECHANICS

Stanley G. Rubin and Randolph A. Graves, Jr.

Langley Research Center

Hampton, Va. 23665

NATIONAL AERONAUTICS AND SPACE ADMINISTRATION • WASHINGTON, D. C. • OCTOBER 1975

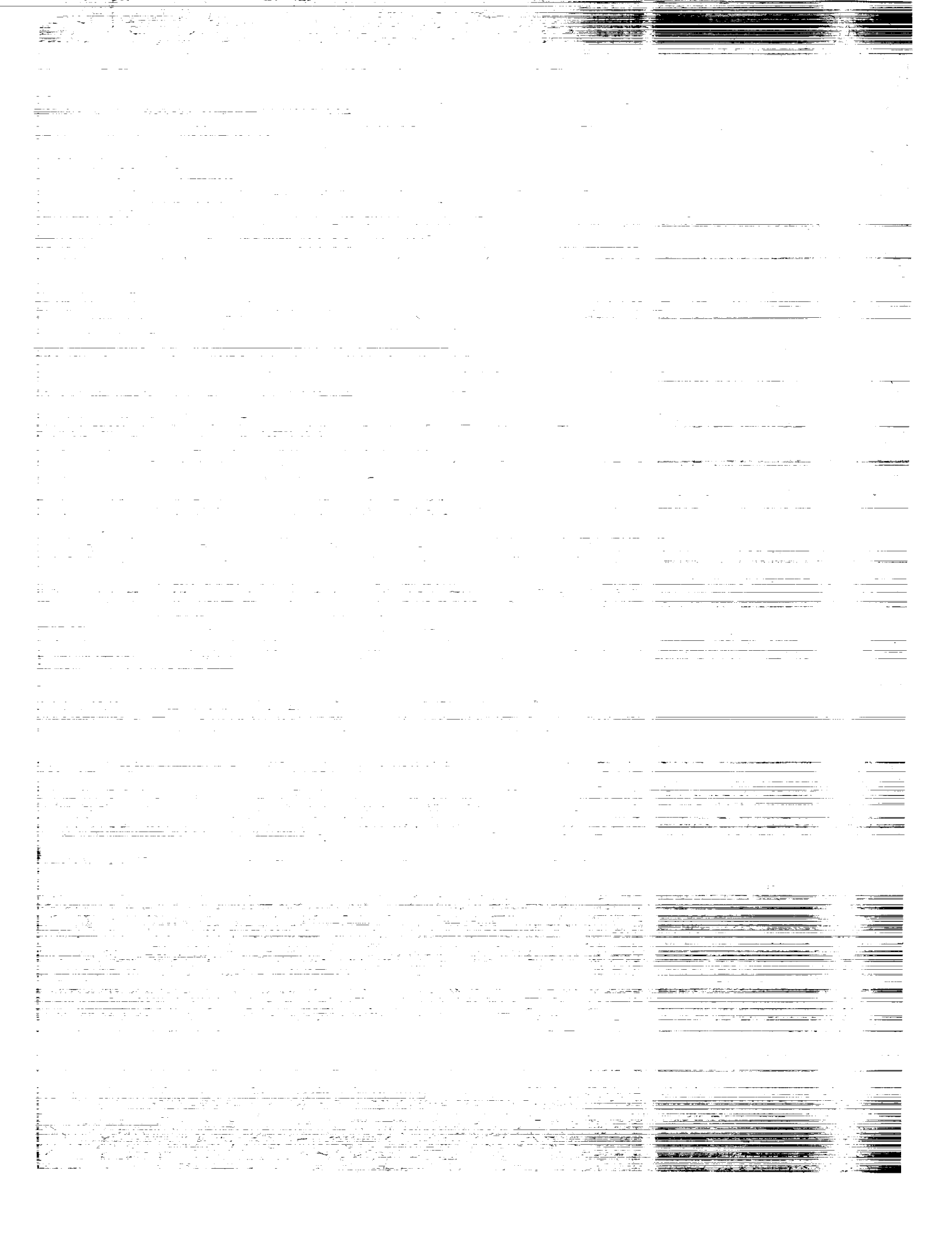

1. Report No.	2. Government Accession No.	3. Recipient's Catalog No.
NASA TR R-436		

4. Title and Subtitle	5. Report Date
A CUBIC SPLINE APPROXIMATION FOR PROBLEMS IN FLUID MECHANICS	October 1975
	6. Performing Organization Code

7. Author(s)	8. Performing Organization Report No.
Stanley G. Rubin and Randolph A. Graves, Jr.	L-9929
	10. Work Unit No.
9. Performing Organization Name and Address	506-26-20-05
NASA Langley Research Center	11. Contract or Grant No.
Hampton, Va. 23665	
	13. Type of Report and Period Covered
12. Sponsoring Agency Name and Address	Technical Report
National Aeronautics and Space Administration	14. Sponsoring Agency Code
Washington, D.C. 20546	

15. Supplementary Notes

Stanley G. Rubin is professor of aerospace engineering, Polytechnic Institute of New York, Farmingdale, N.Y. Work performed as visiting professor at Old Dominion University, Norfolk, Va.

16. Abstract

A cubic spline approximation is presented which is suited for many fluid-mechanics problems. This procedure provides a high degree of accuracy, even with a nonuniform mesh, and leads to an accurate treatment of derivative boundary conditions. The truncation errors and stability limitations of several implicit and explicit integration schemes are presented. For two-dimensional flows, a spline-alternating-direction-implicit (SADI) method is evaluated. The spline procedure is assessed, and results are presented for the one-dimensional nonlinear Burgers' equation, as well as the two-dimensional diffusion equation and the vorticity-stream function system describing the viscous flow in a driven cavity. Comparisons are made with analytic solutions for the first two problems and with finite-difference calculations for the cavity flow.

17. Key Words (Suggested by Author(s))	18. Distribution Statement
Cubic splines Burgers' equation Cavity flow Numerical analysis Splines under tension Stream function and vorticity	Unclassified – Unlimited Subject Category 12

19. Security Classif. (of this report)	20. Security Classif. (of this page)	21. No. of Pages	22. Price*
Unclassified	Unclassified	93	$4.75

*For sale by the National Technical Information Service, Springfield, Virginia 22161

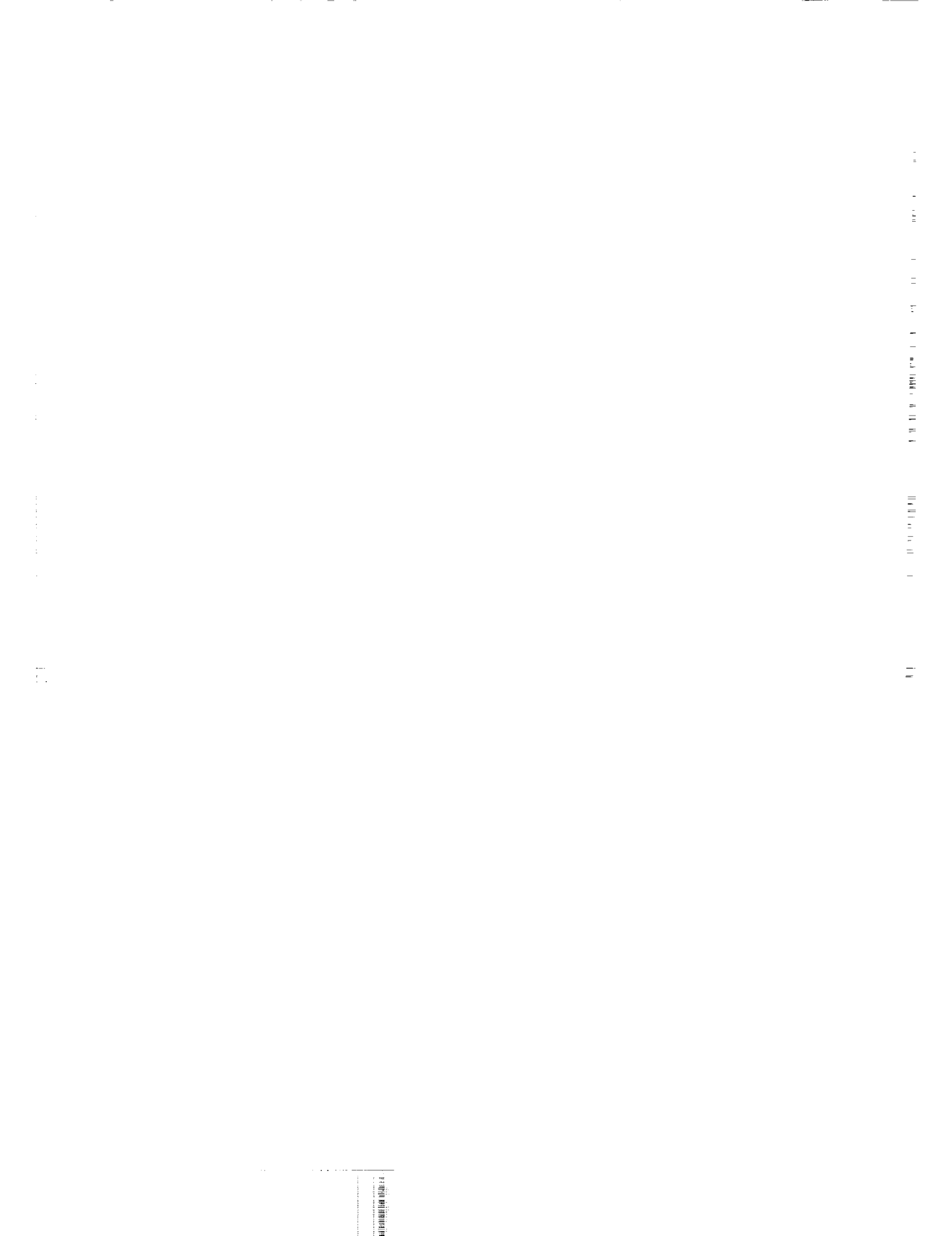

CONTENTS

A CUBIC SPLINE APPROXIMATION FOR PROBLEMS IN FLUID MECHANICS

Stanley G. Rubin* and Randolph A. Graves, Jr.
Langley Research Center

SUMMARY

A cubic spline approximation is presented which is suited for many fluid-mechanics problems. This procedure provides a high degree of accuracy, even with a nonuniform mesh, and leads to an accurate treatment of derivative boundary conditions. The truncation errors and stability limitations of several implicit and explicit integration schemes are presented. For two-dimensional flows, a spline-alternating-direction-implicit (SADI) method is evaluated. The spline procedure is assessed, and results are presented for the one-dimensional nonlinear Burgers' equation, as well as the two-dimensional diffusion equation and the vorticity-stream function system describing the viscous flow in a driven cavity. Comparisons are made with analytic solutions for the first two problems and with finite-difference calculations for the cavity flow.

INTRODUCTION

The numerical treatment of many problems in fluid mechanics is complicated by three conditions: (1) local singular regions where the flow gradients are much larger than typically found over the remainder of the domain, e.g., in the limit of large Reynolds number (particular examples of this singular behavior are given by shock waves, boundary and shear layers, entropy layers, etc.); (2) curvilinear boundaries that do not pass directly through the nodal points of a fixed uniform mesh. (Here, both geometric surfaces, as well as discrete shock waves, are referred to as they appear in a numerical shock fitting procedure with a fixed mesh and moving shock, Moretti, ref. 1); and (3) derivative boundary conditions as occur for vorticity or pressure (see Roache, ref. 2).

In some cases, coordinate transformations can alleviate the difficulties associated with conditions (1) and (2), but this generally requires a priori knowledge of the local or asymptotic flow behavior, which is not always available. Moreover, suitable transformations are difficult to formulate if multiple shocks or other singular regions appear, if

*Professor of aerospace engineering, Polytechnic Institute of New York, Farmingdale, N.Y. Work performed as visiting professor at Old Dominion University, Norfolk, Va.

a number of geometric configurations must be considered simultaneously, or if a singular region is multilayered, i.e., singular regions within singular regions. Some examples of the latter are the trailing-edge boundary layer (Messiter, ref. 3), the laminar sublayer within a turbulent boundary layer (ref. 4), oscillating boundary layers (Ackerberg, ref. 5), and corner boundary regions (Rubin, ref. 6).

The accuracy of a numerical calculation can be improved by suitable mesh reduction or by increasing the order of the truncation error. However, higher order methods generally require the introduction of additional nodal points in the discretization formulas, thereby increasing the coupling in the system of algebraic difference equations. For implicit methods the number of nonzero entries in the inversion matrix is increased so that the tridiagonal form associated with a three-point formulation no longer occurs. Since the very efficient tridiagonal inversion algorithms can no longer be applied, a significant increase in computer time results.

Higher order discretizations can also be used for accurately representing derivative boundary conditions (Briley, ref. 7). However, these may be inadequate if the mesh dimension is too large; i.e., if the local surface gradients are $0(\Delta^{-1})$ and the mesh dimension is $0(\Delta)$, the accuracy will remain poor regardless of the number of terms retained in a Taylor series expansion. In many problems a surface layer grows from zero thickness initially to some finite thickness in a steady state. In the initial stages, inaccuracy near the boundary can lead to a divergence that is suppressed only by an under-relaxation procedure (Bozeman and Dalton, ref. 8).

Uniform mesh reduction improves accuracy but results in a significant increase in the number of algebraic difference equations and is particularly inefficient from the point of view of computer storage and calculation time. A nonuniform mesh that is adjusted to reflect the appearance of singular regions and irregular boundaries should be optimal. Unfortunately, with a three-point finite-difference approximation the order of the truncation error will be significantly decreased with even a moderate variation in the mesh dimension (Crowder and Dalton, ref. 9). Therefore, the expected increase in accuracy associated with mesh reduction is not achieved.

The present paper describes a cubic spline procedure for the solution of second-order quasi-linear partial differential equations in one or two spatial dimensions. A finite-difference discretization is used for the marching or time-like direction. Unlike a finite-element or Galerkin procedure, there are no quadratures to evaluate, and the coefficient matrix is tridiagonal. Implicit and explicit spline fitting is examined for a one-dimensional Burgers' equation; a spline-alternating-direction-implicit (SADI) procedure is formulated for two-dimensional flows. The spline approximation is second-order accurate, even with relatively large variations in the mesh, so that singular regions and irregular boundaries can be considered without loss of accuracy and with a minimum

of computer storage and time. Moreover, for inviscid flows where the system of differential equations becomes first order, the spline procedure is third-order accurate with a nonuniform mesh and of fourth-order accuracy with a uniform mesh. This result is consistent with the increased accuracy of lower order derivatives in a spline curve fit (Ahlberg, Nilson, and Walsh in ref. 10). For a uniform mesh, a particular combination of splines and finite differences results in a fourth-order accurate procedure for viscous flows as well. The tridiagonal form is maintained.

Since the spline approximation provides a direct relation between the derivatives and the functional values evaluated at the nodal points, a finite-difference discretization is unnecessary. Derivative boundary conditions are imposed directly without incurring large local discretization errors due to inaccurate higher order one-sided difference approximations. This represents a significant advantage of the spline technique over conventional finite-difference procedures. Finally, unlike finite-difference or Galerkin techniques, with a spline approximation there appears to be no particular advantage gained with the divergence form of the equations. This fact, previously noted by Douglas and Dupont in reference 11 in their collocation procedure, can prove extremely important for flow problems where shock waves are captured during the numerical computation.

The spline formulation and the procedure for solving second-order quasi-linear partial differential equations are reviewed; the truncation errors for second derivatives, i.e., diffusion, and first derivatives, i.e., convection, are explicitly elucidated; the stability of explicit, implicit, and combined two-step procedures, with a uniform mesh, is discussed for a linearized Burgers' equation in one dimension and with the SADI procedure in two dimensions; and the concepts of splines under tension as a smoothing procedure are reviewed. The effects of tension, mesh variation, and divergence form on the resolution of a spline curve fit are discussed. Also, results are presented for the one-dimensional nonlinear Burgers' equation, the two-dimensional diffusion equation, and the viscous flow in a driven cavity. Comparisons are made with exact solutions and finite-difference solutions where available.

SYMBOLS

a,b	end points of interval or dimensions of cavity
a_i,b_i,c_i,d_i	scalar coefficients in equation (10)
c	stability coefficient, $\bar{u}\,\Delta t/h$
e_i	truncation error

$g(x)$	initial conditions on velocity
h_{ij}, h_i, h	mesh width, $x_i - x_{i-1}$
$\bar{h}$	average mesh width
k_{ij}, k_i, k	mesh width, $y_i - y_{i-1}$
ℓ_i, m_i	spline first derivative in y- and x-direction, respectively
L_i, M_i, P	spline second derivative in y-, x-, and z-direction, respectively
$\tilde{m}_i$	spline first derivative of $u^2/2$
R	Reynolds number
R_c	cell Reynolds number, $\bar{u}h/\nu$
t	time
Δt	time step increment
T_i, P_i	matrices in equation (27)
T_r, P_r	matrices in SADI stability analysis
u, v	velocity in x- and y-direction, respectively
$\bar{u}$	coefficient in linear Burgers' equation
U	wave speed in Burgers' equation
V_i	vector
x, y, z	spatial coordinates
x_i	nodal points
Y, Z	normalized coordinates

Δ_i coefficient in spline solution procedure

ζ vorticity

η transformed coordinate, x - ut

$\theta, \theta_1, \theta_2$ finite-difference scheme (0 for explicit, 1/2 for Crank-Nicolson, 1 for implicit)

λ_i eigenvalue

ν kinematic viscosity

σ tension factor

σ_i spacing factor

τ fictitious time

$\Delta\tau$ fictitious time step increment

υ amplification factor (see eq. (27))

ψ stream function

ω wave number

Superscripts:

n time step number

s fictitious time step number

Subscripts:

i,j indices for x- and y-direction, respectively

N number of nodes on $[a,b]$ excluding the boundaries

t differentiation with respect to time

x,y,z differentiation with respect to spatial coordinates

SPLINE FORMULATION

Basic Spline Theory

Consider a mesh with nodal points (knots) x_i such that

$$a = x_0 < x_1 < x_2 \cdot \cdot \cdot < x_N < x_{N+1} = b$$

and with

$$h_i = x_i - x_{i-1} > 0$$

Consider a function $u(x)$ such that at the mesh points x_i

$$u(x_i) = u_i$$

The cubic spline is a function $S_\Delta(u;x) = S_\Delta(x)$ which is continuous together with its first and second derivatives on the interval $[a,b]$, corresponds to a cubic polynomial in each subinterval $x_{i-1} \leq x \leq x_i$, and satisfies $S_\Delta(u_i;x_i) = u_i$.

If the function $u(x)$ belongs to $C^4[a,b]$, it has been shown that the spline function $S_\Delta(x)$ approximates $u(x)$ at all points in $[a,b]$ to fourth order in maximum h_i. First and second derivatives of $S_\Delta(x)$ approximate $u'(x)$ and $u''(x)$ to third and second order, respectively. See Ahlberg, Nilson, and Walsh in reference 10 for detailed proofs of convergence and for a discussion concerning the relationship of this spline approximation with a mechanical spline.

If $S_\Delta(x)$ is cubic on $[x_{i-1},x_i]$, then

$$S''_\Delta(x) = M_{i-1}\left(\frac{x_i - x}{h_i}\right) + M_i\left(\frac{x - x_{i-1}}{h_i}\right)$$

where $M_i \equiv S''_\Delta(x_i)$.

Integrating twice leads to the useful interpolation formula on $[x_{i-1},x_i]$ as follows:

$$S_\Delta(x) = M_{i-1}\frac{(x_i - x)^3}{6h_i} + M_i\frac{(x - x_{i-1})^3}{6h_i} + \left(u_{i-1} - \frac{M_{i-1}h_i^2}{6}\right)\frac{x_i - x}{h_i} + \left(u_i - \frac{M_i h_i^2}{6}\right)\frac{x - x_{i-1}}{h_i} \qquad (1)$$

The constants of integration have been evaluated from $S_\Delta(x_i) = u_i$ and $S_\Delta(x_{i-1}) = u_{i-1}$ where $S_\Delta(x)$ on $[i,i+1]$ is obtained with $i+1$ replacing i in equation (1).

The unknown derivatives M_i are related by enforcing the continuity condition on $S'_\Delta(x)$. With $S'(x_i^-) = m_i^-$ on $[i-1,i]$ and $S'_\Delta(x_i^+) = m_i^+$ on $[i,i+1]$,

$$m_i^- = m_i^+ = m_i$$

For $i = 1, \ldots, N$,

$$\frac{h_i}{6} M_{i-1} + \frac{h_i + h_{i+1}}{3} M_i + \frac{h_{i+1}}{6} M_{i+1} = \frac{u_{i+1} - u_i}{h_{i+1}} - \frac{u_i - u_{i-1}}{h_i} \tag{2}$$

Additional relationships obtained from equations (1) and (2), which prove useful later herein, are listed as follows:

$$\frac{1}{h_i} m_{i-1} + 2\left(\frac{1}{h_i} + \frac{1}{h_{i+1}}\right) m_i + \frac{1}{h_{i+1}} m_{i+1} = \frac{3(u_{i+1} - u_i)}{h_{i+1}^2} + \frac{3(u_i - u_{i-1})}{h_i^2} \tag{3}$$

$$m_{i+1} - m_i = \frac{h_{i+1}}{2}(M_i + M_{i+1}) \tag{4}$$

$$m_i = \frac{h_i}{3} M_i + \frac{h_i}{6} M_{i-1} + \frac{u_i - u_{i-1}}{h_i} \tag{5}$$

or

$$m_i = -\frac{h_{i+1}}{3} M_i - \frac{h_{i+1}}{6} M_{i+1} + \frac{u_{i+1} - u_i}{h_{i+1}} \tag{6}$$

Therefore, given the values u_i, the equations (2) and (3) with appropriate boundary conditions form a closed system for m_i and M_i; and with equation (1) the values $S_\Delta(x)$ can be found at all intermediate locations. Equation (2) or (3) lead to a system of N equations for the $N + 2$ unknowns M_i or m_i, respectively. The additional two equations are obtained from boundary conditions on m_0 and m_{N+1} or M_0 and M_{N+1}. The resulting tridiagonal system for M_i or m_i is diagonally dominant and solved by an efficient inversion algorithm (see Ahlberg, Nilson, and Walsh, ref. 10 or Keller, ref. 12). Note that if M_0 and M_{N+1} are given so that all M_i $(i = 1, \ldots, N)$ are determined from equation (2), then m_0 and m_{N+1} are found from equation (5) or (6). If m_0 and m_{N+1} or $Am_0 + BM_0$ and $Cm_{N+1} + DM_{N+1}$ are prescribed, then m_{N+1} and m_0 are eliminated with equations (5) and (6) in favor of M_N and M_{N+1} and M_0 and M_1, respectively. This gives a relation of the form

$$EM_0 + FM_1 = G(u_0, u_1)$$

and

$$HM_N + JM_{N+1} = K(u_N, u_{N+1})$$

where A to F, H, and J are constants and G and K are functions of the velocity u. These two conditions with equation (2) then close the system.

If the values u_i are not prescribed but represent the solution of a quasi-linear second-order partial differential equation

$$u_t = f(u, u_x, u_{xx})$$

then an approximate solution for u_i can be obtained by considering the solution of

$$(u_t)_i = f(u_i, m_i, M_i)$$

where the time derivative is discretized in the usual finite-difference fashion:

$$\frac{u_i^{n+1} - u_i^n}{\Delta t} = (1 - \theta) f^n + \theta f^{n+1}$$

Linear Burgers' equation.- Consider the linear Burgers' equation

$$u_t + \bar{u} u_x = \nu u_{xx} \tag{7}$$

where $\bar{u} = \bar{u}(x,t)$ and $\nu = \nu(x,t)$. Therefore,

$$u_i^{n+1} = u_i^n - \Delta t\left[(1 - \theta_1)\bar{u}_i^n m_i^n + \theta_1 \bar{u}_i^{n+1} m_i^{n+1}\right] + \Delta t\left[(1 - \theta_2)\nu_i^n M_i^n + \theta_2 \nu_i^{n+1} M_i^{n+1}\right] \tag{8}$$

With equations (2) and (3) a system of $3N$ equations for $3(N + 2)$ unknowns is obtained; the system can be written as

$$A_i V_{i-1}^{n+1} + B_i V_i^{n+1} + C_i V_{i+1}^{n+1} = D_i V_i^n \tag{9a}$$

where

$$A_i = \begin{bmatrix} 0 & 0 & 0 \\ -\frac{1}{h_i} & 0 & \frac{h_i}{6} \\ \frac{3}{h_i^2} & \frac{1}{h_i} & 0 \end{bmatrix} \tag{9b}$$

$$B_i = \begin{bmatrix} \alpha_0 & \alpha_1 & \alpha_2 \\ \frac{1}{h_i} + \frac{1}{h_{i+1}} & 0 & \frac{h_i + h_{i+1}}{3} \\ \frac{3}{h_{i+1}^2} - \frac{3}{h_i^2} & \frac{2}{h_{i+1}} + \frac{2}{h_i} & 0 \end{bmatrix} \tag{9c}$$

$$C_i = \begin{bmatrix} 0 & 0 & 0 \\ -\frac{1}{h_{i+1}} & 0 & \frac{h_{i+1}}{6} \\ \frac{-3}{h_{i+1}^2} & \frac{1}{h_{i+1}} & 0 \end{bmatrix} \tag{9d}$$

$$D_i = \begin{bmatrix} \rho_0 & \rho_1 & \rho_2 \\ 0 & 0 & 0 \\ 0 & 0 & 0 \end{bmatrix} \tag{9e}$$

$$V_i = \left[u_i, m_i, M_i\right]^T \tag{9f}$$

$$\left.\begin{aligned} \alpha_0 &= 1 \\ \alpha_1 &= \theta_1 \bar{u}_i^{n+1} \Delta t \\ \alpha_2 &= -\theta_2 \nu_i^{n+1} \Delta t \\ \rho_0 &= 1 \\ \rho_1 &= -\left(1 - \theta_1\right) \bar{u}_i^{n} \Delta t \\ \rho_2 &= \left(1 - \theta_2\right) \nu_i^{n} \Delta t \end{aligned}\right\} \tag{9g}$$

Initial conditions are specified such that $u(x,0) = g(x)$. If boundary conditions are specified on $u(a,t) = r_1(t)$ and $u(b,t) = r_2(t)$, then u_0^{n+1} and u_{N+1}^{n+1} are given as $r_1(t)$ and $r_2(t)$, respectively. With derivative boundary conditions $u_x(a,t) = s_1(t)$ or $u_x(b,t) = s_2(t)$, m_0 and m_{N+1} are prescribed as $s_1(t)$ and $s_2(t)$, respectively. From equation (8), u_0^{n+1} is given as a function of M_0^{n+1} and m_0^{n+1} and u_1^{n+1} is given as a function of m_1^{n+1} and M_1^{n+1}; from equation (4), m_1^{n+1} is given as a function of M_0^{n+1}, M_1^{n+1}, and m_0^{n+1}.

With these relations for u_1^{n+1} and m_1^{n+1}, and with either u_0^{n+1} or m_0^{n+1} specified, equation (5) or (6) provides a linear relationship between M_0 and M_1. A similar result can be obtained for M_N and M_{N+1}. The system is now closed and system (9) can be solved by the tridiagonal algorithm previously noted. An analogous procedure determines the appropriate relationships between u_0 and u_1 and u_N and u_{N+1} for

m_0 and m_{N+1} specified, or m_0 and m_1 and m_N and m_{N+1} for u_0 and u_{N+1} specified.

The system (9) can be reduced by substitution of u_i and m_i as functions of M_i into a single tridiagonal system for M_i. The resulting equations for M_i ($i = 1, \ldots, N$) are, with $\theta = \theta_1 = \theta_2$,

$$a_i M_{i-1}^{n+1} + b_i M_i^{n+1} + c_i M_{i+1}^{n+1} = d_i \tag{10}$$

where

$$a_i = \frac{h_i}{6} - \theta\left(\frac{\delta_i + 2\delta_{i-1}}{3\Delta_i} + \frac{\gamma_{i-1}}{h_i\Delta_i}\right)^{n+1}$$

$$c_i = \frac{h_{i+1}}{6} + \theta\left(\frac{2\delta_{i+1} + \delta_i}{3\Delta_{i+1}} - \frac{\gamma_{i+1}}{h_{i+1}\Delta_{i+1}}\right)^{n+1}$$

$$b_i = \frac{h_i + h_{i+1}}{3} + \theta\left(\frac{\delta_{i+1} + 2\delta_i}{3\Delta_{i+1}} - \frac{2\delta_i + \delta_{i-1}}{3\Delta_i} + \frac{\gamma_i}{\Delta_{i+1}h_{i+1}} + \frac{\gamma_i}{\Delta_i h_i}\right)^{n+1}$$

$$d_i = \left(\frac{u_{i+1} - u_i}{h_{i+1}\Delta_{i+1}} - \frac{u_i - u_{i-1}}{h_i\Delta_i}\right)^n + (1 - \theta)\left(\frac{2\delta_i m_i - 2\delta_{i+1}m_{i+1}}{h_{i+1}\Delta_{i+1}} + \frac{2\delta_i m_i - 2\delta_{i-1}m_{i-1}}{h_i\Delta_i}\right.$$

$$\left. + \frac{\gamma_{i+1}M_{i+1} - \gamma_i M_i}{h_{i+1}\Delta_{i+1}} - \frac{\gamma_i M_i - \gamma_{i-1}M_{i-1}}{h_i\Delta_i}\right)^n$$

where $2\delta_i = \bar{u}_i\,\Delta t$, $\gamma_i = \nu_i\,\Delta t$, and $\Delta_i = 1 + 2h_i^{-1}(\delta_i - \delta_{i-1})\theta$.

The boundary conditions for M_0 and M_{N+1} are obtained in the same manner as outlined previously. A tridiagonal relationship similar to equation (10) can also be found for m_i^{n+1} or u_i^{n+1}, although the manipulation is somewhat more tedious.

Nonlinear Burgers' equation. - If the governing equation is nonlinear

$$u_t + uu_x = \nu u_{xx}$$

then the spline formulations gives, with $\theta = \theta_1 = \theta_2$,

$$u_i^{n+1} = u_i^n + \theta\,\Delta t\left(-u_i m_i + \nu_i M_i\right)^{n+1} + (1 - \theta)\,\Delta t\left(-u_i m_i + \nu_i M_i\right)^n \tag{11}$$

If quasi-linearization is used for $(u_i m_i)^{n+1}$, it is found that

$$(u_i m_i)^{n+1} = u_i^n m_i^{n+1} + u_i^{n+1} m_i^n - u_i^n m_i^n$$

and therefore

$$u_i^{n+1}\left(1 + \theta\ \Delta t m_i^n\right) = u_i^n - \Delta t\theta\left(u_i^n m_i^{n+1} - \nu_i^{n+1} M_i^{n+1}\right) + (1 - \theta)\nu_i^n\ \Delta t M_i^n - (1 - 2\theta)\ \Delta t u_i^n m_i^n \tag{12}$$

With equation (12) in place of equation (8), the system (9) is of the same form but with the following modifications:

$$\left.\begin{aligned} \alpha_0 &= 1 + \theta\ \Delta t m_i^n \\ \alpha_1 &= \theta u_i^n\ \Delta t \\ \rho_1 &= -(1 - 2\theta)u_i^n\ \Delta t \end{aligned}\right\} \tag{13}$$

Two-dimensional equation.- For equations with two space dimensions such that

$$u_t = f\left(u, u_x, u_y, u_{xx}, u_{yy}\right)$$

a spline-alternating-direction-implicit (SADI) formulation is developed. The two-step procedure, with quasi-linearization or some other iterative process used for nonlinear terms, is of the following form: For step 1,

$$u_{ij}^{n+\frac{1}{2}} = u_{ij}^n + \frac{\Delta t}{2} f\left(u_{ij}^{n+\frac{1}{2}}, m_{ij}^{n+\frac{1}{2}}, M_{ij}^{n+\frac{1}{2}}, \ell_{ij}^n, L_{ij}^n\right) \tag{14a}$$

and for step 2,

$$u_{ij}^{n+1} = u_{ij}^{n+\frac{1}{2}} + \frac{\Delta t}{2} f\left(u_{ij}^{n+\frac{1}{2}}, m_{ij}^{n+\frac{1}{2}}, M_{ij}^{n+\frac{1}{2}}, \ell_{ij}^{n+1}, L_{ij}^{n+1}\right) \tag{14b}$$

where ℓ_{ij} and L_{ij} are the spline approximations to $(u_y)_{ij}$ and $(u_{yy})_{ij}$, respectively. Therefore, in two dimensions with $h_{ij} = x_{ij} - x_{i-1,j}$ and $k_{ij} = y_{ij} - y_{i,j-1}$,

$$h_{ij}^{-1} m_{i-1,j} + 2\left(h_{ij}^{-1} + h_{i+1,j}^{-1}\right) m_{ij} + h_{i+1,j}^{-1} m_{i+1,j} = 3h_{i+1,j}^{-2}\left(u_{i+1,j} - u_{ij}\right) + 3h_{ij}^{-2}\left(u_{ij} - u_{i-1,j}\right) \tag{15a}$$

$$h_{ij} M_{i-1,j} + 2\left(h_{ij} + h_{i+1,j}\right) M_{ij} + h_{i+1,j} M_{i+1,j} = 6h_{i+1,j}^{-1}\left(u_{i+1,j} - u_{ij}\right) - 6h_{ij}^{-1}\left(u_{ij} - u_{i-1,j}\right) \tag{15b}$$

and

$$k_{ij}^{-1} \ell_{i,j-1} + 2\left(k_{ij}^{-1} + k_{i,j+1}^{-1}\right) \ell_{ij} + k_{i,j+1}^{-1} \ell_{i,j+1} = 3k_{i,j+1}^{-2}\left(u_{i,j+1} - u_{ij}\right) + 3k_{ij}^{-2}\left(u_{ij} - u_{i,j-1}\right) \tag{16a}$$

$$k_{ij}L_{i,j-1} + 2(k_{ij} + k_{i,j+1})L_{ij} + k_{i,j+1}L_{i,j+1} = 6k_{i,j+1}^{-1}(u_{i,j+1} - u_{ij}) - 6k_{ij}^{-1}(u_{ij} - u_{i,j-1}) \tag{16b}$$

with expressions similar to equation (4) to equation (6) relating m_{ij} to M_{ij} and ℓ_{ij} to L_{ij}.

If cross derivatives such as u_{xy} appear in the governing system, the spline approximation for these terms is found from equation (16a), with m_{ij} replacing u_{ij} and $\hat{\ell}_{ij}$ replacing ℓ_{ij}. The solutions $\hat{\ell}_{ij}$ are the necessary spline fits to u_{xy}. Alternatively one could replace u_{ij} with ℓ_{ij} and m_{ij} with $\hat{m}_{ij}$ in equation (15a). The result $\hat{\ell}_{ij} = \hat{m}_{ij}$ should be correct to third order in maximum (h_{ij}, k_{ij}).

TRUNCATION ERROR

Theory for Cubic Splines

For interior points, the spatial accuracy of the spline approximation can be directly estimated from the formulas (2) and (3) or the equivalent two-dimensional relationships (15a) and (15b). Expanding m_{ij}, M_{ij}, and u_{ij} in Taylor series and assuming the necessary continuity of derivatives for $u(x,y)$ gives

$$M_{ij} = (u_{xx})_{ij} - \left(h_{i+1,j}^3 + h_{ij}^3\right)\left(12[h_{i+1,j} + h_{ij}]\right)^{-1}(u_{xxxx})_{ij} - (u_{xxxxx})_{ij}\left[\frac{7(h_{i+1,j} - h_{ij})(h_{i+1,j}^2 - h_{ij}^2)}{90} + \frac{(h_{i+1,j} - h_{ij})(h_{i+1,j}^3 + h_{ij}^3)}{36(h_{i+1,j} + h_{ij})}\right] + 0(h_{ij}^4) \tag{17a}$$

$$m_{ij} = (u_x)_{ij} - (u_{xxxx})_{ij}(h_{i+1,j} - h_{ij})\frac{h_{ij}h_{i+1,j}}{72} + 0(h_{ij}^4) \tag{17b}$$

Fyfe (ref. 13) has presented similar relations, for constant h_i, in his collocation analysis of cubic splines for the solution of two-point boundary value problems.

Therefore, the spline approximation with nonuniform mesh is second-order accurate for M_{ij} and third-order for m_{ij}. For a uniform mesh, m_{ij} is fourth-order accurate; and with $h_{ij} = h$,

$$M_{ij} = (u_{xx})_{ij} - (u_{xxxx})_{ij}\frac{h^2}{12} + 0(h^4) \tag{18}$$

The standard three-point finite-difference approximation provides the following relationship:

$$\frac{u_{i+1,j} + u_{i-1,j} - 2u_{ij}}{h^2} = (u_{xx})_{ij} + (u_{xxxx})_{ij} \frac{h^2}{12} + 0(h^4)$$

Therefore, with a uniform mesh

$$\frac{1}{2}\left(M_{ij} + \frac{u_{i+1,j} + u_{i-1,j} - 2u_{ij}}{h^2}\right) = (u_{xx})_{ij} + 0(h^4) \tag{19}$$

and overall fourth-order accuracy is achieved. A note of warning should be included here. This approximation should not be used with a nonuniform mesh inasmuch as the finite-difference approximation introduces a first-order error. Instead, one should revert back to the second-order accurate approximation as in equation (17a).

Examples of Truncation Error Using Burgers' Equation

Second-order spatial derivative. - With equation (19) approximating u_{xx} in the model Burgers' equation (7), the system (9), with $\theta = \theta_1 = \theta_2$, takes the form

$$\tilde{A}_i V_{i-1}^{n+1} + \tilde{B}_i V_i^{n+1} + \tilde{C}_i V_{i+1}^{n+1} = \tilde{D}_i V_i^n + \tilde{E}_i\left(V_{i+1}^n + V_{i-1}^n\right) \tag{20}$$

If

$$F_i = \begin{bmatrix} \frac{\nu_i \Delta t}{2h^2} & 0 & 0 \\ 0 & 0 & 0 \\ 0 & 0 & 0 \end{bmatrix}$$

$$G_i = \begin{bmatrix} \frac{\nu_i \Delta t}{h^2} & 0 & \frac{\nu_i \Delta t}{2} \\ 0 & 0 & 0 \\ 0 & 0 & 0 \end{bmatrix}$$

then

$$\tilde{A}_i = A_i - \theta F_i^{n+1}$$

$$\tilde{B}_i = B_i + \theta G_i^{n+1}$$

$$\tilde{C}_i = C_i - \theta F_i^{n+1}$$

$$\tilde{D}_i = D_i - (1 - \theta)G_i^n$$

$$\tilde{E}_i = (1 - \theta)F_i^n$$

It should be noted that equation (19) for h_{ij} = Constant can be written as

$$\frac{1}{2}\left(M_{ij} + \frac{u_{i+1,j} + u_{i-1,j} - 2u_{ij}}{h^2}\right) = \frac{M_{i-1,j} + 10M_{ij} + M_{i+1,j}}{12} = (u_{xx})_{ij} + 0(h^4) \tag{21a}$$

or

$$(u_{xx})_{ij} = M_{ij} + \frac{M_{i-1,j} - 2M_{ij} + M_{i+1,j}}{12} + 0(h^4) \tag{21b}$$

Note that from equations (18) and (21b)

$$(u_{xxxx})_{ij} = \frac{M_{i-1,j} + M_{i+1,j} - 2M_{ij}}{h^2} + 0(h^2) \tag{22}$$

This provides a second-order accurate formula for the fourth derivative. A fourth-order finite-difference method developed by H. O. Kreiss is closely related to the present spline formulation and is outlined in the appendix.

If equation (21b) is used for u_{xx}, then the governing system is still of form given by equation (20). The matrices F_i and G_i are now

$$F_i = \begin{bmatrix} 0 & 0 & \frac{\nu_i \Delta t}{12} \\ 0 & 0 & 0 \\ 0 & 0 & 0 \end{bmatrix} \tag{23a}$$

$$G_i = \begin{bmatrix} 0 & 0 & \frac{\nu_i \Delta t}{6} \\ 0 & 0 & 0 \\ 0 & 0 & 0 \end{bmatrix} \tag{23b}$$

This paper is concerned primarily with the standard cubic spline approximation as given by equations (9).

First-order temporal derivative.- The truncation error associated with the time discretization in equation (8) or (12) is identical with that found for a typical finite-difference formulation. Consider

$$u_t = f(u_i, m_i, M_i)$$

with

$$u_i^{n+1} = u_i^n + \left[\theta f_i^{n+1} + (1 - \theta) f_i^n\right] \Delta t$$

A Taylor series expansion about $(n + \theta)\Delta t$ leads to

$$(u_t)_i = f_i + 0\left(\frac{1 - 2\theta}{2} \Delta t f_t,\ \Delta t^2 f_{tt}\right)$$

For $\theta = 1/2$, second-order temporal accuracy is achieved. For all other $0 \leq \theta \leq 1$, first-order accuracy results.

For the cases of pure convection ($\nu \equiv 0$) or pure diffusion ($\bar{u} \equiv 0$) the spline representation for the linear Burgers' equation (7) can be easily transformed into an equivalent finite-difference form.

Diffusion only.- For $\bar{u} \equiv 0$ and ν = Constant, equation (8) with equation (2) can be written in the form

$$\begin{aligned}\left(1 - 6\theta\beta_{i+1}\right) u_{i+1}^{n+1} + 2\left[1 + \sigma_i + 3\theta\left(\beta_{i+1} + \sigma_i\beta_i\right)\right] u_i^{n+1} + \sigma_i\left(1 - 6\theta\beta_i\right) u_{i-1}^{n+1} \\ = \left[1 + 6(1 - \theta)\beta_{i+1}\right] u_{i+1}^n + \sigma_i\left[1 + 6(1 - \theta)\beta_i\right] u_{i-1}^n + 2\left[1 + \sigma_i - 3(1 - \theta)\left(\beta_{i+1} + \sigma_i\beta_i\right)\right] u_i^n\end{aligned} \tag{24}$$

where $\sigma_i = h_i/h_{i+1}$ and $\beta_i = \nu\, \Delta t / h_i^2$. It can be shown directly from equation (24) or by using equations (17a) and (17b) that the truncation error e_i is given by

$$e_i = u_{tt}\left(\frac{1 - 2\theta}{2}\right)\Delta t + \nu u_{xxxx}\left[\frac{1 + \sigma_i^3}{12\left(1 + \sigma_i\right)}\right] h_{i+1}^2 + 0\left[\Delta t^2, (1 - \sigma_i) h_{i+1}^3, h_{i+1}^4\right]$$

For $\sigma_i = 1$, the difference equation (24) corresponds to a special case of a more general formulation proposed by Saul'yev (ref. 14). Papamichael and Whiteman (ref. 15) recognized this correspondence in their cubic spline analysis of the one-dimensional heat conduction equation. They considered only the case of a uniform mesh.

Convection only.- For $\nu \equiv 0$ and $\bar{u}$ = Constant, equation (8) with equation (3) can be written in the form

$$\sigma_i(1 + 3\theta c_{i+1})u_{i+1}^{n+1} + \left[2(1 + \sigma_i) - 3\theta(\sigma_i c_{i+1} - c_i)\right]u_i^{n+1} + (1 - 3\theta c_i)u_{i-1}^{n+1}$$

$$= \sigma_i\left[1 - 3(1 - \theta)c_{i+1}\right]u_{i+1}^{n} + \left[1 + 3(1 - \theta)c_i\right]u_{i-1}^{n} + \left[2(1 + \sigma_i) + 3(1 - \theta)(\sigma_i c_{i+1} - c_i)\right]u_i^{n} \tag{25}$$

where

$$c_i = \frac{\bar{u}\,\Delta t}{h_i}$$

The truncation error is

$$e_i = u_{tt}\left(\frac{1 - 2\theta}{2}\right)\Delta t - \bar{u}u_{xxxx}\left[(1 - \sigma_i)\frac{h_i h_{i+1}^2}{72}\right] + 0\left(\Delta t^2, h_i^4\right)$$

For a uniform mesh ($\sigma_i = 1$), equation (25) can be written in the form

$$\frac{u_i^{n+1} - u_i^n}{\Delta t} + \bar{u}\left[\theta\,\frac{u_{i+1}^{n+1} - u_i^{n+1}}{2h} + (1 - \theta)\frac{u_{i+1}^{n} - u_i^{n}}{2h}\right]$$

$$+ \left[\left(u_{i+1} + u_{i-1} - 2u_i\right)^{n+1} - \left(u_{i+1} + u_{i-1} - 2u_i\right)^{n}\right](6\,\Delta t)^{-1} = 0 \tag{26}$$

The fourth-order accuracy is achieved by the effective addition of a difference expression representing $h^2(u_{xxt})_i$. This cancels the $\bar{u}(u_{xxx})h^2$ error associated with a central derivative discretization for $\bar{u}u_x$. The largest error terms are now $0(h^4)$.

Fourth-order accuracy with a nonuniform mesh may be possible if a collocation procedure is used with a Hermite cubic polynomial approximation. This procedure has been analyzed for ordinary differential equations; and fourth-order accuracy can be achieved if the collocation points are appropriately located, otherwise only second-order accuracy results (see Douglas and Dupont, ref. 11, Fyfe, ref. 13, and Albasiny and Hoskins, refs. 16 and 17).

Complete equation.- For the full Burgers' equation (eq. (8)) a reduction to an equivalent finite-difference form is possible. Considerable manipulation of the system (9) is required, and the final result has not been worked out. The truncation error as obtained from equation (11) is

$$e_i = u_{tt}\left(\frac{1 - 2\theta}{\theta}\right)\Delta t + u_{xxxx}\left\{\nu\left[\frac{1 + \sigma_i^3}{12(1 + \sigma_i)}\right]h_{i+1}^2 - \hat{u}\left[\frac{(1 - \sigma_i)h_i h_{i+1}^2}{72}\right]\right\} + 0\left[\Delta t^2, (1 - \sigma_i)h_{i+1}^3, h_{i+1}^4\right]$$

STABILITY

General Development for Linearized Burgers' Equation

For the linear Burgers' equation (7) with $\bar{u}$ and ν held constant, interior point stability can be assessed with the von Neuman Fourier decomposition of the system (9). With

$$V^n = \upsilon^n \exp I\omega x$$

or

$$V^n_{i+\epsilon} = \upsilon^n_i \exp I\omega\left(x_i + \frac{\epsilon + 1}{2} h_{i+1} + \frac{\epsilon - 1}{2} h_i\right)$$

where $\epsilon = -1$, 0, or +1 and $I = \sqrt{-1}$, system (9) becomes

$$T_i \upsilon_i^{n+1} = P_i \upsilon_i^n \tag{27}$$

where

$$T_i = \begin{bmatrix} \alpha_0 & \alpha_1 & \alpha_2 \\ \pi_1 & 0 & \pi_3 \\ \tau_1 & \tau_2 & 0 \end{bmatrix}$$

$$P_i = \begin{bmatrix} \rho_0 & \rho_1 & \rho_2 \\ 0 & 0 & 0 \\ 0 & 0 & 0 \end{bmatrix}$$

and the coefficients α_j and ρ_j are defined in equations (9g). Also,

$$\pi_i = h_i^{-1}\left[1 - \exp\left(-I\varphi_i\right)\right] + h_{i+1}^{-1}\left(1 - \exp I\varphi_{i+1}\right) \tag{28a}$$

$$6\pi_3 = h_i\left[2 + \exp\left(-I\varphi_i\right)\right] + h_{i+1}\left(2 + \exp I\varphi_{i+1}\right) \tag{28b}$$

$$\tau_1 = 3h_i^{-2}\left[\exp\left(-I\varphi_i\right) - 1\right] - 3h_{i+1}^{-2}\left(\exp I\varphi_{i+1} - 1\right) \tag{28c}$$

$$\tau_2 = h_i^{-1}\left[2 + \exp\left(-I\varphi_i\right)\right] + h_{i+1}^{-1}\left(2 + \exp I\varphi_{i+1}\right) \tag{28d}$$

where $\varphi_i = \omega h_i$. Therefore,

$$v_i^{n+1} = G_i v_i^n$$

where $G_i = T_i^{-1} P_i$ is the amplification matrix. The von Neumann condition necessary for the suppression of all error growth requires that the spectral radius

$$\rho(G_i) \leq 1$$

The eigenvalues of G_i are found from

$$\det\left(T_i^{-1} P_i - \lambda_i I\right) = 0$$

where I is the identity matrix. If

$$\det T_i^{-1} = -\pi_3 \tau_2 \left(\alpha_0 - \alpha_1 \frac{\tau_1}{\tau_2} - \alpha_2 \frac{\pi_1}{\pi_3}\right) = -\pi_3 \tau_2 \Omega \neq 0$$

the three roots for λ_i are found to be

$$\lambda_i = 0,\ 0,\ \left(\rho_0 - \rho_1 \frac{\tau_1}{\tau_2} - \rho_2 \frac{\pi_1}{\pi_3}\right)\Omega^{-1} \tag{29}$$

For the one-dimensional equation (7), three numerical procedures were considered: (1) convection (m_i) and diffusion (M_i) explicit, (2) convection explicit, diffusion implicit (two steps required for inviscid stability), and (3) diffusion and convection implicit. With explicit convection, procedure (1) or (2), both divergence and nondivergence forms of the equations were evaluated.

The stability conditions imposed on these schemes are determined from

$$\left|\lambda_i\right| \leq 1$$

with λ_i given by the nonzero value in equation (29). As it is somewhat difficult to evaluate this condition with the expressions (28) for a nonuniform mesh, only the uniform mesh stability is discussed here.

Explicit convection and diffusion.- For a uniform mesh and $\theta = 0$ in equations (9g),

$$\left|\lambda_i\right|^2 = \left[1 - 6\beta(1 - \cos\varphi)(2 + \cos\varphi)^{-1}\right]^2 + (3c \sin\varphi)^2(2 + \cos\varphi)^{-2} \leq 1$$

where $\beta = \frac{\nu\,\Delta t}{h^2}$ and $c = \frac{\bar{u}\,\Delta t}{h}$. Necessary stability limits are $\beta \leq \frac{1}{6}$, $c \leq (3)^{-1/2}$, and $R_c = \frac{c}{\beta} = \frac{\bar{u}h}{\nu} \leq 2(3)^{1/2}$. These results are more restrictive than the limits found for the forward time central space explicit finite-difference method, which (from ref. 2) are

$\beta \leq \frac{1}{2}$, $c \leq 1$, and $R_c \leq 2$. In view of this result and the fact that the explicit values for m_i and M_i must still be determined by the implicit tridiagonal system (2) or (3), this explicit representation is not recommended.

Explicit convection and implicit diffusion.- For $\theta_1 = 0$ and $\theta_2 = 1$ in equations (9g),

$$|\lambda_i|^2 = \left[1 + \frac{(3c \sin \varphi)^2}{(2 + \cos \varphi)^{-2}}\right]\left[1 + 6\beta(1 - \cos \varphi)(2 + \cos \varphi)^{-1}\right]^{-2} \leq 1$$

This leads to the condition

$$c^2 \leq 2\beta$$

or

$$c \leq \frac{2}{R_c}$$

For $R_c >> 1$ this condition is quite restrictive, while for $R_c << 1$ the stability result is quite acceptable. In the inviscid limit $R_c \rightarrow \infty$, the method is unstable as the implicit and stabilizing diffusion effect vanishes. This instability can be eliminated if a second step is prescribed. This method could then be likened to the Brailovskaya finite-difference procedure (ref. 18). The spline technique remains consistent with first-order temporal accuracy and second-order spatial accuracy. If the Cheng-Allen viscous correction (ref. 19) is made on the Brailovskaya difference procedure, the explicit diffusive instability is eliminated; however, the method is no longer consistent in the transient unless $\beta << 1$ (see Rubin and Lin, ref. 20).

The spline approximation is consistent, and with two steps there is no diffusive instability. The two-step procedure is as follows: For step 1,

$$u_i^* = u_i^n - \Delta t\left(\bar{u}m_i^n + \nu M_i^*\right) \tag{30a}$$

For step 2,

$$u_i^{n+1} = u_i^n - \Delta t\left(\bar{u}m_i^* + M_i^{n+1}\right) \tag{30b}$$

Step 1 is given by system (9) with $n+1 \rightarrow *$ and

$$\left.\begin{array}{lll} \alpha_0 = 1 & \alpha_1 = 0 & \alpha_2 = -\nu\,\Delta t \\ \rho_0 = 1 & \rho_1 = -\bar{u}\,\Delta t & \rho_2 = 0 \end{array}\right\} \tag{31}$$

Step 2 is given by system (9) with $n \rightarrow *$ and

$$\left.\begin{array}{lll} \alpha_0 = 1 & \alpha_1 = 0 & \alpha_2 = -\nu\,\Delta t \\ \rho_0 = 0 & \rho_1 = -\bar{u}\,\Delta t & \rho_2 = 0 \end{array}\right\} \tag{32}$$

In addition, the term DV_i^n is added to the right-hand side of equation (9a), where

$$D = \begin{bmatrix} 1 & 0 & 0 \\ 0 & 0 & 0 \\ 0 & 0 & 0 \end{bmatrix}$$

After Fourier decomposition, step 1 becomes

$$T_i v_i^* = P_i v_i^n$$

where T_i and P_i are defined by equations (9g), (27), and (28), and step 2 becomes

$$T_i v_i^{n+1} = P_i v_i^* - D\left(v_i^* - v_i^n\right)$$

or

$$T_i v_i^{n+1} = \bar{P}_i v_i^n \tag{33a}$$

where

$$\bar{P}_i = \left(P_i - D\right)T_i^{-1}P_i + D \tag{33b}$$

Therefore,

$$\bar{P}_i = \begin{bmatrix} \bar{\rho}_0 & \bar{\rho}_1 & \bar{\rho}_2 \\ 0 & 0 & 0 \\ 0 & 0 & 0 \end{bmatrix}$$

and

$$\bar{\rho}_0 = 1 + \bar{u}\,\Delta t\,\frac{\tau_1}{\tau_2}\,\Omega^{-1}$$

$$\bar{\rho}_1 = -(\bar{u}\,\Delta t)^2\,\frac{\tau_1}{\tau_2}\,\Omega^{-1}$$

$$\bar{\rho}_2 = 0$$

$$\Omega = 1 + \frac{\pi_1}{\pi_3}\,\nu\,\Delta t$$

For a uniform mesh, with subscript i dropped, from equations (28c) and (28d),

$$\frac{\tau_1}{\tau_2} = -3I(\sin\varphi)h^{-1}(2 + \cos\varphi)^{-1} = -Ih^{-1}\Phi$$

where $I = \sqrt{-1}$ and

$$\Omega = 1 + 6\beta(1 - \cos\varphi)(2 + \cos\varphi)^{-1}$$

With $\bar{\rho}_0, \bar{\rho}_1$ replacing ρ_0, ρ_1 in equation (29)

$$|\lambda|^2 = \Omega^{-4}\left[(\Omega - c^2\Phi^2)^2 + c^2\Phi^2\right] \leqq 1$$

If $\beta = 0$ (inviscid flow), then

$$c \leqq \Phi_{min}^{-1} = \left[(2 + \cos\varphi)(3 \sin\varphi)^{-1}\right]_{min} = (3)^{-1/2}$$

This result is more restrictive than the $c \leqq 1$ CFL condition found for the Brailovskaya finite-difference method. For $\beta \neq 0$, the effect of viscosity is to improve the inviscid stability limitation; for $\bar{u} \to 0$, the method is unconditionally stable.

Implicit convection and diffusion.- For $\theta = \theta_1 = \theta_2$ and $0 < \theta \leqq 1$ in equations (9g),

$$|\lambda|^2 = \left\{\left[1 - (1 - \theta)(\Omega - 1)\right]^2 + (1 - \theta)^2c^2\Phi^2\right\}\left\{\left[1 + \theta(\Omega - 1)\right]^2 + \theta^2c^2\Phi^2\right\}^{-1} \leqq 1$$

This condition is satisfied and the spline procedure is unconditionally stable if $\theta \geqq 1/2$.

Development for SADI Procedure

For the SADI procedure, consider the linear equation

$$u_t + \bar{u}u_x + \bar{v}u_y = \nu(u_{xx} + u_{yy})$$

With the spline approximation of equations (14) and a uniform mesh $(h_{ij} = h \text{ and } k_{ij} = k)$, the amplification factors for the two steps of equations (14) are defined by

$$v_{ij}^{n+\frac{1}{2}} = G_1 v_{ij}^n$$

$$v_{ij}^{n+1} = G_2 v_{ij}^{n+\frac{1}{2}}$$

where

$$G_r = T_r^{-1}P_r \qquad (r = 1, 2)$$

and

$$T_r = \begin{bmatrix} 1 & \ell_r^1 & \ell_r^2 & \ell_r^3 & \ell_r^4 \\ -3I \sin \varphi_x & h(2 + \cos \varphi_x) & 0 & 0 & 0 \\ 6(1 - \cos \varphi_x) & 0 & h^2(2 + \cos \varphi_x) & 0 & 0 \\ -3I \sin \varphi_y & 0 & 0 & k(2 + \cos \varphi_y) & 0 \\ 6(1 - \cos \varphi_y) & 0 & 0 & 0 & k^2(2 + \cos \varphi_y) \end{bmatrix}$$

$$P_r = \begin{bmatrix} 1 & m_r^1 & m_r^2 & m_r^3 & m_r^4 \\ & & \bigcirc & & \end{bmatrix}$$

$$\upsilon_{ij} = \left[u_{ij}, m_{ij}, M_{ij}, \ell_{ij}, L_{ij}\right]^T$$

and

$$\ell_1^1 = \frac{\bar{u}\,\Delta t}{2} \qquad \ell_1^2 = \frac{-\nu\,\Delta t}{2} \qquad \ell_1^3 = \ell_1^4 = 0 \qquad m_1^1 = m_1^2 = 0$$

$$m_1^3 = \frac{-\bar{v}\,\Delta t}{2} \qquad m_1^4 = \frac{\nu\,\Delta t}{2} \qquad \ell_2^1 = \ell_2^2 = 0 \qquad \ell_2^3 = \frac{\bar{v}\,\Delta t}{2}$$

$$\ell_2^4 = \frac{-\nu\,\Delta t}{2} \qquad m_2^1 = \frac{-\bar{u}\,\Delta t}{2} \qquad m_2^2 = \frac{\nu\,\Delta t}{2} \qquad m_2^3 = m_2^4 = 0$$

$$\varphi_x = \omega_x h \qquad \varphi_y = \omega_y k$$

The only nonzero eigenvalues of G_1 and G_2 are λ_1 and λ_2, respectively; that is,

$$\lambda_1 = \frac{1 - 3\beta_y(1 - \cos \varphi_y)(2 + \cos \varphi_y)^{-1} - 3Ic_y \sin \varphi_y(4 + 2 \cos \varphi_y)^{-1}}{1 + 3\beta_x(1 - \cos \varphi_x)(2 + \cos \varphi_x)^{-1} + 3Ic_x \sin \varphi_x(4 + 2 \cos \varphi_x)^{-1}}$$

$$\lambda_2 = \frac{1 - 3\beta_x(1 - \cos \varphi_x)(2 + \cos \varphi_x)^{-1} - 3Ic_x \sin \varphi_x(4 + 2 \cos \varphi_x)^{-1}}{1 + 3\beta_y(1 - \cos \varphi_y)(2 + \cos \varphi_y)^{-1} + 3Ic_y \sin \varphi_y(4 + 2 \cos \varphi_y)^{-1}}$$

where $c_x = \frac{\bar{u}\,\Delta t}{h}$, $c_y = \frac{\bar{v}\,\Delta t}{k}$, $\beta_x = \frac{\nu\,\Delta t}{h^2}$, and $\beta_y = \frac{\nu\,\Delta t}{k^2}$. From these results it can be

seen that $|\lambda_1||\lambda_2| \leq 1$ is always satisfied so that the SADI method is unconditionally stable. Of course, boundary effects have not been considered in this interior point stability analysis.

SPLINE CURVE FITTING

In this section, the accuracy of a cubic spline fit to a given set of data points at prescribed knots is considered. Error estimates for functional interpolation and for functional derivatives are reviewed. Exact solutions of the nonlinear Burgers' equation (11) are used in a series of numerical experiments to assess the following: (1) mesh requirements and resolution in regions with locally large gradients, i.e., for $\nu << 1$ in Burgers' equation, (2) the effect of large mesh nonuniformity on overall accuracy, (3) splines under tension as a means of smoothing spurious oscillations associated with a cubic spline fit, and (4) the accuracy of a spline approximation for the nonlinear convective term $(uu_x)_i$ when this term is obtained from the nondivergence approximation $u_i m_i$ and the divergence form approximation $\tilde{m}_i$ (where $\tilde{m}_i$ is the spline derivative of the function $u^2/2$, i.e., $\tilde{m}_i$ approximates $(u^2/2)_x$). This comparison will shed light on the spline solutions of Burgers' equation in divergence and nondivergence form.

Given a set of data points u_i at the knots x_i with

$$a = x_0 < x_1 < x_2 < x_N < x_{N+1} = b$$

if the function $u(x)$, with $u(x_i) = u_i$, belongs to $C^4[a,b]$ then $S_\Delta(x)$ in equation (1) approximates $u(x)$ to $0(h_i^4)$. Moreover, $S_\Delta^p(x_i)$ approximates $(\partial^p u/\partial x^p)_i$ to $0(h_i^{4-p})$, where $S'_\Delta(x_i) = m_i$ and $S'_\Delta(x_i) = M_i$ (see Ahlberg, Nilson, and Walsh in ref. 10). The derivative results have already been inferred by equations (17a) and (17b). If the higher order spline approximation, equation (21b) is used to represent $(u_{xx})_i$, then overall fourth-order accuracy for a uniform mesh results.

Resolution

A steady-state solution to the Burgers' equation, where $\eta = x - Ut$,

$$u_t + (u - U)u_\eta = \nu u_{\eta\eta} \tag{34}$$

with boundary conditions $u \to 2U$ as $\eta \to -\infty$ and $u \to 0$ as $\eta \to \infty$ is

$$u = U\left(1 - \tanh \frac{U\eta}{2\nu}\right) \tag{35}$$

Consider the domain $-5 \leq \eta \leq 5$. At the knots $\eta = \eta_i$, $u = u_i$ is given by equation (35). The spline derivative approximations m_i and M_i are found from equations (2) and (3) or equation (4). The boundary conditions at $\eta_i = \pm 5$ are given by

$$\mp U m_i = \nu M_i$$

This represents the spline approximation of equation (34) evaluated at $\eta = \pm 5$. In several cases, less exact zero slope $(m_i = 0)$ or zero curvature $(M_i = 0)$ conditions were prescribed. These led to negligible changes in the spline curve fit.

The results of a cubic spline approximation as compared with a three-point finite-difference representation, for $U = 0.5$ and selected ν values, are presented in tables 1 to 15. Columns 4 and 8 depict the exact values of $(u_\eta)_i$ and $(u_{\eta\eta})_i$ as found from equation (35). Columns 5 and 9 contain the spline approximations, m_i and M_i, and columns 6 and 10 depict three-point finite-difference approximations as given by

$$(u_\eta)_i = \frac{\sigma_i^2 u_{i+1} - (\sigma_i^2 - 1)u_i - u_{i-1}}{\sigma_i(\sigma_i + 1)h_{i+1}} + e_i \tag{36a}$$

$$(u_{\eta\eta})_i = \frac{2\left[\sigma_i u_{i+1} - (\sigma_i + 1)u_i + u_{i-1}\right]}{\sigma_i(\sigma_i + 1)h_{i+1}^2} + e_i \tag{36b}$$

The truncation errors e_i for these derivatives are

$$u_\eta : e_i = (u_{\eta\eta\eta})_i \sigma_i \frac{h_{i+1}^2}{6} + 0(h_{i+1}^3) \tag{37a}$$

$$u_{\eta\eta} : e_i = (u_{\eta\eta\eta})_i (\sigma_i - 1)\frac{h_{i+1}}{3} - (u_{\eta\eta\eta\eta})_i (\sigma_i^3 + 1)\frac{h_{i+1}^2}{12(\sigma_i + 1)} + 0(h_{i+1}^3) \tag{37b}$$

For $\sigma_i = 0(1)$, the approximation of equation (36a) is second-order accurate; the approximation of equation (36b) is first-order accurate unless $\sigma_i = 1$, in which case second-order accuracy results. Therefore, from equations (17a), (17b), (37a), and (37b), Σ can be defined as the ratio of spline truncation error to finite-difference truncation error, so that:

$$\Sigma_{u_\eta} = (\sigma_i - 1)\frac{h_{i+1}(u_{\eta\eta\eta\eta})_i}{12(u_{\eta\eta\eta})_i} + 0\left[\frac{(u_{\eta\eta\eta\eta\eta})_i h_{i+1}^2}{(u_{\eta\eta\eta})_i}\right]$$

$$\Sigma_{u_{\eta\eta}} = \frac{(u_{\eta\eta\eta\eta})_i h_{i+1} + 0\left[(\sigma_i - 1)h_{i+1}^2, h_{i+1}^3\right]}{4(u_{\eta\eta\eta})_i (\sigma_i^2 - 1)(\sigma_i^3 + 1)^{-1} - (u_{\eta\eta\eta\eta})_i h_{i+1} + 0\left[(\sigma_i - 1)h_{i+1}^2, h_{i+1}^3\right]}$$

With derivatives of equal order of magnitude and $|\sigma_i| \leq 2$, the spline approximation to u_η should be significantly better than the equivalent finite-difference result. The spline fit for $u_{\eta\eta}$ should be somewhat better for $2 > \sigma_i > 1$; however, with a uniform mesh ($\sigma_i = 1$),

$$\Sigma_{u_{\eta\eta}} = -1 + 0(h^2)$$

so that, to lowest order, equal and opposite errors are incurred. This result has already been implied in equation (17b) where it is shown that, for a uniform mesh, a spline and finite-difference average is fourth-order accurate; this result is depicted in the last column of table 4. The exceptional accuracy of the average is apparent.

In regions of large gradients, with derivatives of increasing magnitude (e.g., boundary layers or shock waves), the local truncation errors for both spline and finite-difference approximations increase. The deterioration is magnified for the spline fit as the lowest order truncation error involves higher order derivatives. This difficulty can be circumvented with a local decrease in the mesh dimension h_i. This mesh reduction would be nonuniform so that computer storage is minimized and would be dependent on the magnitude of the local gradients. A few additional points properly located can lead to a significant improvement in the spline curve fit. The finite-difference formulas are also improved, but to a lesser degree.

For Burgers' equation (34) when $\nu \ll 1$, a region with large gradients, representative of a shock wave, develops. The tables for $\nu = 1/2$ (very weak shock), $\nu = 1/8$ (moderate shock), and $\nu = 1/24$ (strong shock) show how the spline curve fit varies with different placement of mesh points. For the strong shock ($\nu = 1/24$) and a uniform mesh ($h = 0.2$), there are few points in the shock region and the derivative approximations are poor. With fewer total points but increased density in the shock region, overall accuracy is significantly improved. Near the boundaries the derivatives may become smaller than the associated truncation errors, and large percentage differences occur. This is particularly true with few mesh points. Similar trends can be observed for $\nu = 1/8$ or $1/2$; however, the shock is weaker in these cases, and the agreement is therefore good in almost all of the examples presented. In addition to the solutions for a uniform 51-point mesh, only the 15-point curve fits are depicted. Even for this very coarse grid, the spline-derivative approximations are reasonably good for $\nu = 1/8$ and much better for $\nu = 1/2$. With 51 points the agreement is excellent.

It is significant that for all the cases presented herein, even those in which the derivative approximations are poor, the functional values between the knots as obtained from equation (1) are in excellent agreement with the exact values at the same locations. These results reflect the higher order accuracy of the interpolation formula (1).

It may be possible to further reduce the required number of knots by using a parametric cubic spline curve fit. With such a procedure, step functions can be fit with a minimum of knots; this is particularly appealing for regions with very large gradients, i.e., strong shock waves.

Splines Under Tension

A cubic spline curve fit (eq. (1)) although passing through a prescribed set of data points may exhibit spurious oscillations. These oscillations, which are generally much less severe than those found with a standard polynomial curve fit, may be suppressed by using cubic B-splines (ref. 21), which results in a more complex Galerkin or collocation procedure for the solution of differential equations, or by applying tension to the cubic spline fit described herein (see refs. 22 and 23).

In a mechanical sense, tension is used to pull taut the "thread" (curve) passing through the data. This results in more accurate interpolation between the knots. The cubic spline approximation $S_\Delta(x)$ of equation (1) is obtained from a linear distribution of the moment $S''_\Delta(x)$. If a tensile force is added, the spline function in the interval $[i-1,i]$, satisfies the following equation:

$$S''_\Delta(x) - \sigma^2 S_\Delta(x) = (M_{i-1} - \sigma^2 u_{i-1})(x_i - x)h_i^{-1} + (M_i - \sigma^2 u_i)(x - x_{i-1})h_i^{-1}$$

The coefficient σ is a tension factor; and for $\sigma = 0$, equation (1) is recovered. With $S_\Delta(x_i) = u_i$, $S'_\Delta(x_i) = m_i$, $S''_\Delta(x_i) = M_i$, and enforcing the continuity of $S'_\Delta(x_i)$ so that $S'_\Delta(x_i^+) = S'_\Delta(x_i^-)$, the following results are obtained:

$$S_\Delta(x) = \frac{M_{i-1}}{\sigma^2}\frac{\sinh \sigma(x_i - x)}{\sinh \sigma h_i} + \frac{M_i}{\sigma^2}\frac{\sinh \sigma(x - x_{i-1})}{\sinh \sigma h_i} + \left(u_{i-1} - \frac{M_{i-1}}{\sigma^2}\right)\left(\frac{x_i - x}{h_i}\right) + \left(u_i - \frac{M_i}{\sigma^2}\right)\left(\frac{x - x_{i-1}}{h_i}\right) \tag{38a}$$

$$m_i = r_i M_{i-1} + s_i M_i + (u_i - u_{i-1})h_i^{-1} \tag{38b}$$

or

$$m_i = -r_{i+1}M_{i+1} - s_{i+1}M_i + (u_{i+1} - u_i)h_{i+1}^{-1} \tag{38c}$$

$$m_{i+1} - m_i = (r_{i+1} + s_{i+1})(M_i + M_{i+1}) \tag{38d}$$

$$r_i M_{i-1} + (s_i + s_{i+1})M_i + r_{i+1}M_{i+1} = (u_{i+1} - u_i)h_{i+1}^{-1} - (u_i - u_{i-1})h_i^{-1} \tag{38e}$$

where

$$r_i = \frac{\sinh \sigma h_i - \sigma h_i}{\sigma^2 h_i \sinh \sigma h_i} \tag{38f}$$

$$s_i = \frac{\sigma h_i \cosh \sigma h_i - \sinh \sigma h_i}{\sigma^2 h_i \sinh \sigma h_i} \tag{38g}$$

From the relations (38) it can be shown that for splines under tension the coefficients of the tridiagonal system (9) become

$$a_i = r_i - \left(\frac{\theta}{h_i \Delta_i}\right)^{n+1} \left(2\delta_i r_i + 2\delta_{i-1} s_i + \gamma_i\right)^{n+1} \tag{39a}$$

$$b_i = s_i + s_{i+1} + \left(\frac{\theta}{h_{i+1}\Delta_{i+1}}\right)^{n+1} \left(2\delta_{i+1} r_{i+1} + 2\delta_i s_{i+1} + \gamma_{i+1}\right)^{n+1}$$

$$- \left(\frac{\theta}{h_i \Delta_i}\right)^{n+1} \left(2\delta_i s_i + \delta_{i-1} r_i - \gamma_i\right)^{n+1} \tag{39b}$$

$$c_i = r_{i+1} + \left(\frac{\theta}{h_{i+1}\Delta_{i+1}}\right)^{n+1} \left(2\delta_{i+1} s_{i+1} + 2\delta_i r_{i+1} - \gamma_{i+1}\right)^{n+1} \tag{39c}$$

and d_i is unchanged. For $\sigma \to 0$, $r_i \approx \frac{h_i}{6}$ and $s_i \approx \frac{h_i}{3}$ so that equations (38) reduce to equations (1) to (6) and equations (39) reduce to equations (9). For $\sigma >> 1$, there is a very large tensile force and equation (38a) becomes

$$S_\Delta(x) \approx u_{i-1}(x_i - x)h_i^{-1} + u_i(x - x_{i-1})h_i^{-1} + 0(\sigma^{-2})$$

Therefore $S_\Delta(x)$ is nearly linear between the knots. It has been found (ref. 23) that, if $\bar{h}$ represents the average mesh spacing, a dimensionless tension factor $\sigma\bar{h} = 1$ usually works rather well to eliminate oscillatory behavior.

Examples of curve fitting with tension are given in tables 16 to 24. The tension factor σ is generally chosen such that $\sigma\bar{h} = 1$. If the mesh resolution is poor (i.e., there are insufficient knots in regions of large gradients), tension will smooth the solution but accuracy of derivatives is not significantly improved. This plays an important role in the solution of differential equations where the functional values at the mesh points are unknown and where tension with a poor choice of grid points can lead to a deterioration of the solution. This is discussed further in the next two sections. With adequate mesh resolution in regions of large gradients, tension does act to reduce oscillatory behavior.

Divergence Form

It is known that for many problems in fluid mechanics accurate numerical solutions are possible only when the governing equations are expressed in integral or divergence form. For high Reynolds number flows with moderate to strong shock waves and little numerical viscosity, numerical solutions obtained with the equations in divergence form closely approximate the weak or integral solutions of the differential system (ref. 24). This allows for shock capturing by the numerical procedure. Also, for internal flows, conservation laws are generally more closely satisfied with the equations in divergence form. Bozeman and Dalton (ref. 8) have clearly demonstrated the superiority of the divergence form at large Reynolds numbers for the low speed driven cavity problem. In regions with moderate gradients or for low Reynolds number flows, there does not appear to be any advantage of the more complex divergence-form equations (refs. 1 and 8).

In order to assess the relative merits and even the necessity for divergence form when using splines, curve fits of the nonlinear term in Burgers' equation (34) were examined. In divergence form, equation (34) with $U = 0.5$ becomes

$$u_t + \left(\frac{u^2 - u}{2}\right)_\eta = \nu u_{\eta\eta}$$

If $\tilde{m}_i$ is the spline derivative of the function $\frac{u^2(\eta) - u(\eta)}{2}$ and m_i of the function $u(\eta)$, then the approximation of the nonlinear term $\left(u - \frac{1}{2}\right)u_\eta$ is given by $\tilde{m}_i$ in divergence form and by $\left(u_i - \frac{1}{2}\right)m_i$ for the nondivergence representation. These expressions are presented in tables 25 and 26. Also tabulated are the finite-difference results.

In the region of large gradients or the shock structure, it is seen that for $\nu = 1/8$ the finite-difference approximation in nondivergence form is more accurate than the divergence representation. However, for the stronger shock ($\nu = 1/24$), the reverse is true; and the behavior implies the need for divergence form in high Reynolds number finite-difference calculations if thin strong shock waves are to be accurately captured by the numerical method (ref. 24). For $\nu = 1/8$, the spline approximation provides a significantly better curve fit with nondivergence form of the data; moreover, with divergence form, symmetry is no longer maintained. For $\nu = 1/24$, this loss of symmetry is still evident, but neither of the spline curve fits is particularly good as long as the grid density in the shock region is too low; however, it will be observed that for the spline formulation the solutions in nondivergence form are generally as good as or better than those obtained with divergence form. These results agree with the conclusion of Douglas and Dupont (ref. 11) that, unlike Galerkin or finite-difference methods, there appears to be no advantage to divergence form for collocation procedures.

BURGERS' EQUATION

Numerical Procedure

The spline calculation procedure was first applied to the one-dimensional nonlinear Burgers' equation (34) with boundary conditions $u \to 2U$ as $\eta \to -\infty$ and $u \to 0$ as $\eta \to \infty$. Initial conditions were specified such that

$$u(\eta,0) = \begin{cases} 0 & (\eta > 0) \\ U & (\eta = 0) \\ 2U & (\eta < 0) \end{cases}$$

For all of the solutions presented here, $U = 0.5$, ν = Constant, and the boundary conditions are prescribed at the finite locations $\eta = \pm 5$.

The tridiagonal system (10) is used to determine M_i^{n+1}; then u_i^{n+1} and m_i^{n+1} are obtained from equations (5), (6), and (8). The predicted stability restrictions were all confirmed by the calculations. Therefore, the solutions to be discussed here were obtained either with the implicit ($\theta = 1$) procedure or the two-step method. The former is unconditionally stable; the latter has the restriction $c \leqq (3)^{-1/2}$.

Implicit method.- For the implicit method, the nonlinear coefficient $2\delta_i = \bar{u}_i \Delta t = (u_i - 0.5)\Delta t$ in system (10) was linearized by evaluation at the latest time $t = n \Delta t$. Since the steady-state solutions were obtained in a minimum of computer time, the more accurate quasi-linearization procedure of equations (11) to (13) was unnecessary. The convective derivatives as found from equations (5), (6), and (8) are given by

$$m_i^{n+1} = M_{i-1}^{n+1}\left(\frac{h_i}{6} - \frac{\delta_i + 2\delta_{i-1}}{3\Delta_i} - \frac{\gamma}{h_i\Delta_i}\right)^n + M_i^{n+1}\left(\frac{h_i}{3} - \frac{2\delta_i + \delta_{i-1}}{3\Delta_i} + \frac{\gamma}{h_i\Delta_i}\right)^n + \left(\frac{u_i - u_{i-1}}{h_i\Delta_i}\right)^n$$

The tridiagonal system (9), although unconditionally stable, is only conditionally diagonal dominant. For a uniform mesh, diagonal dominance is assured if

$$R_c = \frac{c}{\beta} = \frac{\bar{u}h}{\nu} \leqq 2$$

For $R_c > 2$, diagonal dominance requires

$$c \leqq \frac{2}{3}\left(1 - \frac{2}{R_c}\right)^{-1}$$

or for $R_c \to \infty$,

$$c \leqq \frac{2}{3}$$

A similar result is found with finite differences (see Hirsh and Rudy, ref. 25).

A correction similar to that proposed by Khosla and Rubin (ref. 26), which provides diagonal dominance of an implicit finite-difference method, can be formulated for this spline procedure. In view of the fact that the tridiagonal system (9) was inverted for c as large as 600, this correction was unnecessary for the present calculations. The final solutions were invariant for $\frac{1}{3} < \frac{\Delta t}{\Delta \eta} < 600$; this corresponds to a maximum of 431 time steps to convergence and to a minimum of 22 for the conditions: 31 points, $\nu = 1/24$, unequal spacing, $\sigma_i = 1.5$, and $\sigma = 0$.

Two-step method.- The two-step method is outlined in equations (30) to (32). The tridiagonal system (10) is obtained for each step, with $\theta = 0$ for δ_i terms and $\theta = 1$ for γ_i terms. Since the convective terms are evaluated explicitly in each step, solutions were obtained with both divergence and nondivergence forms of the convective derivative. In nondivergence form,

$$(2\delta_i m_i)^n = (u_i - 0.5)^n m_i^n \, \Delta t$$

with m_i^n obtained from equation (5) or (6). In divergence form,

$$(2\delta_i m_i)^n = \tilde{m}_i^n \, \Delta t$$

where $\tilde{m}_i^n$ is obtained from equation (3), with $m_i \rightarrow \tilde{m}_i$ and $u_i \rightarrow \frac{u_i^2 - u_i}{2}$.

The boundary conditions for both the implicit and two-step procedures, applied at $\eta_i = \pm 5$, were $u_0 = 1$, $u_{N+1} = 0$ (for $\nu = 1/2$, the exact values 0.9933 and 0.0067 were prescribed), and $\mp 0.5m = \nu M_i$. The procedure outlined previously leads to a linear relation for M_0 and M_1 and M_N and M_{N+1}, respectively. In several cases, the boundary conditions $m_i = 0$ or $M_i = 0$ were tested; these did not cause any significant variations in the solutions.

Numerical solutions were also obtained for splines under tension as described by the systems (38) and (39). The procedures for the implicit and two-step methods are identical with those of the preceding discussion.

Discussion of Numerical Results

The steady-state results of calculations for Burgers' equation are given in tables 1 to 24 and for the strong shock ($\nu = 1/24$) in figures 1 to 17. The two-step solutions are for divergence form if unspecified. In the tables, columns 3, 7, and 11 depict the calculated values of u_i, m_i, and M_i, respectively, as obtained with the implicit nondivergence-form spline procedure. The two-step results in nondivergence form were almost identical with the implicit solutions. This can be seen from several of the figures where both solutions are depicted.

In table 9, column 12, the calculated values of u_i with the two-step divergence-form procedure are presented. These are considerably less accurate than the implicit solutions and follow the pattern of the curve fits in tables 25 and 26. This loss of accuracy with divergence form is found for a nonuniform mesh as well and leads to a conclusion that is contrary to that of finite-difference procedures. For spline calculations, the nondivergence form appears to be preferable providing there is adequate grid resolution in the shock structure. This result may be significant for any shock-capturing study.

The solutions for u_i, as seen from the tables and figures, are all quite acceptable. This is true even when the agreement for m_i and M_i, with the analytic derivatives obtained form equation (35), is not very good. As the number of mesh points in the shock structure is increased, a noticeable improvement in m_i and M_i can be discerned. This behavior follows the trend found for spline curve fitting; i.e., accurate derivative representation in regions of large gradients is possible only with adequate mesh resolutions in these regions. In this respect, a nonuniform mesh requiring fewer total grid points is desirable. As few as 15 to 19 points leads to solutions for u_i that are quite good; moreover, as seen with $\sigma_i = 1.6$ and 19 total points, in the shock $(h_i)_{min} = 0.044$, while near the boundary $(h_i)_{max} = 1.905$. This represents a significant mesh variation, which is highly desirable for shock and boundary-layer problems.

Another interesting feature of the spline solution is shown in figure 1, where a nondivergence, central derivative, finite-difference calculation is also depicted. Nondivergence finite-difference solutions for a nonuniform mesh are shown in the last column of tables 5 and 6. The difference formulas are given by equations (36) and (37). Since $(R_c)_{max} = 2.4$ in this case, the finite-difference solution exhibits an oscillation typically found for $R_c > 2$. This oscillation does not occur with the spline result and may be indicative of the fourth-order accuracy of the convection derivative m_i. In addition, the interpolation formula (eq. (1)) provides intermediate $u(\eta)$ values that agree very well with the exact solution (eq. (35)) so that accurate grid realinement is possible.

In several runs, with a nonuniform mesh and few mesh points, oscillations did appear in the final solution. In most cases, tension (with $\sigma\bar{h} \approx 1$) removed or minimized this spurious behavior; $\bar{h}$ is the average mesh width (10/N+2). The primary effects of tension can be summarized as follows: First, for the 15-point calculations with boundary conditions at $\eta = \pm 5$, h_i near the boundary is extremely large, e.g., $(h_i)_{max} = 2.261$ with $\sigma_i = 1.8$, so that stable solutions are obtained only when tension is included in the spline formulation. Second, for 15 points with boundaries at $\eta = \pm 3$ or 19 points with boundaries at $\eta = \pm 5$ stable solutions are obtained, but oscillations appear near the boundaries. Tension has the effect of minimizing or eliminating the oscillations with no apparent loss of accuracy. Third, if the spline derivatives are inaccurate, as with a coarse mesh in the shock structure, tension does not improve the accuracy but appears

to have a negative effect. This is apparently due to the low mesh density in a region of large gradients; a similar effect occurred with the spline fitting under tension as previously discussed. Fourth, it does appear that tension can be used to smooth oscillations arising from large changes in mesh width when local singular regions form and increased mesh resolution is required.

DIFFUSION EQUATION

The two-dimensional diffusion equation

$$u_t = \frac{1}{R}(u_{yy} + u_{zz})$$

where $u = u(t,y,z)$, with the initial condition $u(0,y,z) = 0$ and with the boundary conditions $u(t>0,0,z\geq 0) = 1$, $u(t>0,y\geq 0,0) = 1$, and $u(t,y,z) \to 0$ as $y,z \to \infty$ has the exact solution

$$u = 1 - \text{erf } Y \text{ erf } Z$$

where $Y = \frac{y}{2}\left(\frac{R}{t}\right)^{1/2}$ and $Z = \frac{z}{2}\left(\frac{R}{t}\right)^{1/2}$ This solution describes the impulsive motion of a right-angled corner formed by two infinite flat plates and has been used by Sowerby (ref. 27) to infer the steady flow along the corner with leading edge at $t = 0$, i.e., Rayleigh's problem for a corner. This problem was used to test the accuracy of the SADI procedure previously outlined. The two-step procedure is given by

$$u_{ij}^{n+\frac{1}{2}} = u_{ij}^{n} + \frac{\Delta t}{2}\left(L_{ij}^{n+\frac{1}{2}} + P_{ij}^{n}\right)$$

and

$$u_{ij}^{n+1} = u_{ij}^{n+\frac{1}{2}} + \frac{\Delta t}{2}\left(L_{ij}^{n+\frac{1}{2}} + P_{ij}^{n+1}\right)$$

where L_{ij} and P_{ij} are the spline approximations to $(u_{yy})_{ij}$ and $(u_{zz})_{ij}$, respectively. The boundary conditions are simply $u_{ij} = 1$ on the walls and $u_{ij} \to 0$ as $y,z \to \infty$. In addition, from the governing equation, $L_{ij} = 0$ on $y = 0$ and $z > 0$ and $P_{ij} = 0$ on $z = 0$ and $y > 0$.

Some results of this SADI calculation for $R = 1000$ are given in table 27 and figure 18. A nonuniform grid was specified in order to accurately describe the boundary-layer behavior near the walls with a minimum of mesh points. The agreement with the exact solution is reasonably good so that the validity of the SADI procedure is confirmed.

INCOMPRESSIBLE FLOW IN A CAVITY

Numerical Procedure

As a final test problem the incompressible flow in a driven cavity was considered. This problem has been studied by numerous investigators, and recently Bozeman and Dalton (ref. 8) have reviewed the literature and presented some definitive results and conclusions. The governing equations in terms of a vorticity stream-function system are

$$\psi_{xx} + \psi_{yy} = \zeta \tag{40a}$$

$$\zeta_t + u\zeta_x + v\zeta_y = \frac{1}{R}(\zeta_{xx} + \zeta_{yy}) \tag{40b}$$

where ψ is the stream function, ζ is the vorticity, and $u = \psi_y$ and $v = -\psi_x$ are the velocities in the x- and y-direction, respectively. The boundary conditions and geometry are shown in figure 19. For all the calculations the initial conditions are $\psi(x,y) = 0$ and $\zeta(x,y) = 0$.

Solutions are obtained by an iterative SADI procedure. The SADI system representing equation (21) is given in two steps for both stream function and vorticity.

Stream function.- For step 1,

$$\psi_{ij}^{n+1,s+\frac{1}{2}} = \psi_{ij}^{n+1,s} + \frac{\Delta\tau}{2}\left[\left(L_{ij}^{\psi}\right)^{n+1,s+\frac{1}{2}} + \left(M_{ij}^{\psi}\right)^{n+1,s} - \zeta_{ij}^{n+1}\right] \tag{41a}$$

For step 2,

$$\psi_{ij}^{n+1,s+1} = \psi_{ij}^{n+1,s+\frac{1}{2}} + \frac{\Delta\tau}{2}\left[\left(L_{ij}^{\psi}\right)^{n+1,s+\frac{1}{2}} + \left(M_{ij}^{\psi}\right)^{n+1,s+1} - \zeta_{ij}^{n+1}\right] \tag{41b}$$

The physical time t equals $n\,\Delta t$; Δt is the time increment at each step n; $\Delta\tau$ is a fictitious time step; and $\tau = s\,\Delta\tau$. Solutions for equation (40a) are obtained as the steady-state limit ($\tau \to \infty$) of equations (41); L_{ij}^{A} and M_{ij}^{A} are the spline approximations to $\frac{\partial^2 A}{\partial y^2}$ and $\frac{\partial^2 A}{\partial x^2}$, respectively. (The superscript ψ implies that $A = \psi$.) First derivatives $\psi_y = u$ and $\psi_x = -v$ are represented by ℓ_{ij}^{ψ} and m_{ij}^{ψ}, respectively.

Vorticity.- For step 1,

$$\zeta_{ij}^{n+\frac{1}{2}} = \zeta_{ij}^{n} + \frac{\Delta t}{2}\left[-\ell_{ij}^{\overline{\psi}}\left(m_{ij}^{\zeta}\right)^{n} + m_{ij}^{\overline{\psi}}\left(\ell_{ij}^{\zeta}\right)^{n+\frac{1}{2}} + R^{-1}\left(L_{ij}^{\zeta}\right)^{n+\frac{1}{2}} + R^{-1}\left(M_{ij}^{\zeta}\right)^{n}\right] \tag{42a}$$

For step 2,

$$\zeta_{ij}^{n+1} = \zeta_{ij}^{n+\frac{1}{2}} + \frac{\Delta t}{2}\left[-\ell_{ij}^{\overline{\psi}}\left(m_{ij}^{\zeta}\right)^{n+1} + m_{ij}^{\overline{\psi}}\left(\ell_{ij}^{\zeta}\right)^{n+\frac{1}{2}} + R^{-1}\left(L_{ij}^{\zeta}\right)^{n+\frac{1}{2}} + R^{-1}\left(M_{ij}^{\zeta}\right)^{n+1}\right] \tag{42b}$$

The bar over the ψ spline derivatives denotes an average of n and n+1 values; the ζ superscript denotes ζ spline derivatives.

The iterative procedure is as follows:

(1) Given ψ_{ij}^{n} and ζ_{ij}^{n} either as initial conditions or at time $n\,\Delta t$, all the ψ spline derivatives are determined from equations (14) to (16) and (4) to (6). On the vertical surfaces, $M_{ij}^{\psi} = \zeta_{ij}$; on the horizontal boundaries, $L_{ij}^{\psi} = \zeta_{ij}$.

(2) The vorticity ζ_{ij}^{n+1} is obtained with the SADI technique as outlined in equations (42) and (9). At the boundaries, ζ_{ij} is found from an expression similar to equation (5) or (6). At the upper moving wall (w), with

$$\ell_{iw}^{\psi} = 1 = \frac{k_{iw}L_{iw}^{\psi}}{3} + \frac{k_{iw}L_{i,w-1}^{\psi}}{6} + \frac{(\psi_{iw} - \psi_{i,w-1})}{k_{iw}}$$

and with $\psi_{iw} = 0$ and $L_{iw}^{\psi} = \zeta_{iw}$, the vorticity becomes

$$\zeta_{iw} = \frac{3}{k_{iw}} - \frac{L_{i,w-1}^{\psi}}{2} + \frac{3\psi_{i,w-1}}{k_{iw}^{2}}$$

Similar relations can be derived for the three stationary walls. Boundary values for M_{ij}^{ζ} and L_{ij}^{ζ} are obtained from equations (42) evaluated at the surface. For the moving wall, equations (5) and (6) are used to eliminate m_{ij}^{ζ}. In addition, $\zeta_{iw}^{n+\frac{1}{2}}$ is evaluated with the three-point formula

$$\zeta_{iw}^{n+\frac{1}{2}} = \frac{3\zeta_{iw}^{n+1} + 6\zeta_{iw}^{n} - \zeta_{iw}^{n-1}}{8} + 0(\Delta t^2)$$

(3) The vorticity ζ_{ij}^{n+1} is used in equations (41) and the SADI procedure is applied over the fictitious time τ until a converged solution, to any specified tolerance, is obtained.

(4a) If only the steady-state solution is required, the calculation proceeds to the next time step (n+2) by returning to step (2) with $n \rightarrow n+1$. The spline derivatives for ψ have already been determined in step (3).

(4b) If an accurate transient is required, the calculation proceeds to step (2) with ψ_{ij} and all spline derivatives of ψ replaced by averages over the n and n+1 time steps. Then ζ_{ij}^{n+1} is recalculated, and this process continues until convergence.

Although accurate transient solutions have been obtained in a number of cases, only the steady-state results are presented here. The time step Δt was generally chosen such that $\Delta t \approx (h_{ij}, k_{ij})_{min}$ Larger values were used in many cases, but a careful study of optimal time integration by discrete or semidiscrete procedures must still be considered. Primary interest at this time was concerned with the applicability of the SADI procedure, as well as the accuracy, ease of handling boundary conditions, and other general characteristics of the spline approximation.

Calculations are presented for a square cavity with R = 10 and 100 and for a rectangular cavity with b/a = 2 and R = 100. Comparisons are given with finite-difference calculations in both divergence and nondivergence form. Central differences are used throughout. The vorticity equation is solved with an ADI procedure, and the solution for ψ is obtained by a direct Poisson solver or by successive overrelaxation.

Discussion of Numerical Results

The results are presented in tables 28 to 34 and figures 20 to 22. For all cases, the values of ψ_{max} and the vorticity ζ at the midpoint of the moving wall are depicted. For these values, comparisons between the spline and finite-difference solutions are possible even when the grid alinements differ. In addition, the distributions of ψ and ζ for the spline solutions, and in several cases for the finite-difference solutions, are presented. The figures depict the horizontal velocity component, u_{ij} or ℓ_{ij}^{ψ}, along a vertical line passing through the vortex center.

The results for R = 10 are given in tables 28 and 29 and figure 20. For this low Reynolds number the spline and finite-difference solutions in either divergence or nondivergence form are quite similar. For R = 100 the large disparity between the divergence and nondivergence finite-difference solutions, first noted by Bozeman and Dalton (ref. 8), is apparent. The values of ψ_{max} and ζ_{wall} are shown in table 30 for a variety of grids. Also included is a limiting solution obtained by Richardson extrapolation (ref. 12) from the two or three calculated values of each procedure. It is evident that the divergence finite-difference solution is more accurate than the nondivergence result; however, the spline solution, which is obtained in nondivergence form, appears to be even more accurate than the divergence-form finite-difference result. For example, the value of ψ_{max} as obtained from the spline calculation with 15 points (this denotes a 15×15 node mesh with h = k = 1/14) is about 1 percent higher than the extrapolated

value; the 17-point divergence-form finite-difference result is about 4 percent lower than its extrapolated value. The nondivergence 15-point finite-difference result is low by about 12 percent. These results again seem to reflect the higher order accuracy of convection terms in the spline procedure; in the vortex core region, the flow is inviscid dominated. However, near the moving wall, where diffusion is important, the vorticity results appear to show a similar trend; the spline values are always somewhat more accurate than the divergence finite-difference solutions.

Another interesting result is shown in table 30(c). The velocity at the first grid point away from the upper left boundary is depicted. With 15 points, the spline result is of an opposite sign to that obtained with the nondivergence finite-difference method. With a finer grid, the finite-difference solution changes sign so that once again the spline procedure prevails. Unfortunately, the more accurate divergence-form finite-difference solutions were obtained with a slightly different grid so that a direct comparison is not possible. However, a change in sign with mesh reduction is observed for the velocity in the corner region. An interpolation procedure is used to estimate the value at the desired location. These results are also given in table 30(c). The extrapolated limit closely approximates the solution obtained with splines. The velocity profiles through the vortex center are shown in figure 21. These values are also tabulated in table 31. The agreement is quite good.

A spline solution for $R = 100$ was also obtained with a 19-point nonuniform mesh. In the central region of the cavity $h_{ij} = k_{ij} = 1/14$ as with the 15-point mesh; however, near the boundaries there is some grid realinement to increase the mesh density in the surface boundary layers (see table 32(g)). The increased accuracy near the boundaries, where diffusion is most important, leads to a solution that appears to be almost as accurate, throughout the entire flow domain, as the 29-point results. The improved accuracy of this 19-point solution is seen in tables 30(a) and 30(b) where ψ_{max} and ζ_{wall} are indicated. These results imply the considerable advantages of the spline procedure with a nonuniform grid in regions of large gradients. In this manner, the accuracy of the second-order diffusion terms is enhanced in domains where these effects are significant. In inviscid regions the fourth-order accurate convection terms are dominant, and mesh reduction is not as important. The improved resolution of the corner vortices is seen in the ψ,ζ distributions of tables 32(g) and 32(h); the comparisons with the 65-point divergence finite-difference solutions are reasonably good.

For $R = 100$, spline solutions were also obtained for a 2×1 rectangular cavity with a 29×15 point uniform mesh; the results are presented in tables 33 and 34 and figure 22. A double vortex is observed. The flow properties are in qualitative agreement with the divergence-form finite-difference solutions obtained with a 33×17 uniform mesh.

CONCLUDING REMARKS

The use of a cubic spline approximation for the evaluation of spatial gradients provides a highly efficient and accurate procedure for numerical calculations with a uniform or nonuniform mesh. It has been shown that: (1) Second-order spatial accuracy is achieved, even with an arbitrary nonuniform mesh, for equations of the Navier-Stokes type; (2) For inviscid regions, with a nonuniform mesh, third-order accuracy results; (3) For the Navier-Stokes equations and uniform mesh, the interior point truncation error is fourth order with a combined spline finite-difference scheme; (4) Derivative boundary conditions can be treated easily and accurately so that spatial finite-difference discretization is unnecessary; (5) There appears to be no particular advantage gained with the divergence form of the equations; (6) Accurate interpolation is possible if grid realinement becomes desirable; (7) Evaluation of quadratures which are generally not of a tridiagonal form, as in finite-element or other Galerkin procedures, is unnecessary.

With a finite-difference discretization for the time-like integration, it has additionally been shown that: (1) The system of algebraic equations resulting from the spline formulation is block tridiagonal, and therefore inversion for implicit time discretization is accomplished with an efficient algorithm. Moreover, appropriate substitutions can reduce the vector system to a scalar one, thereby eliminating the necessity for any matrix inversions. (2) Explicit, implicit, and mixed time integrations have been considered. The interior point stability conditions for explicit procedures are slightly more restrictive than those found with equivalent finite-difference techniques. Implicit methods are unconditionally stable.

Solutions have been obtained for the one-dimensional nonlinear Burgers' equation, and in two dimensions for the diffusion equation and the vorticity-stream function system depicting the incompressible viscous flow in a driven cavity. Oscillations typically found with second-order accurate finite-difference methods when the cell Reynolds number exceeds 2 did not occur with the spline solutions; and this probably reflects the higher order accuracy in the convective term. Accurate solutions for Burgers' equation are obtained even with a highly nonuniform mesh if adequate mesh resolution is specified in the region of largest gradients.

For two-dimensional flows the SADI procedure appears to work quite well for both the diffusion equation and driven cavity problem. Comparisons with the analytic solution available for the former are excellent, and with finite-difference calculations for the latter are quite reasonable. The spline solutions for the cavity obtained with the nondivergence form of the equations are somewhat better than the divergence form finite-difference solutions and considerably better than the nondivergence form finite-difference results. Once again the higher-order accuracy of the convection operator may account

for the improvement with the spline formulation. The vorticity boundary condition has been treated directly and without the need of any finite-difference discretization at the boundaries.

Langley Research Center,
National Aeronautics and Space Administration,
Hampton, Va., January 30, 1975.

APPENDIX

KREISS FOURTH-ORDER FINITE-DIFFERENCE METHOD

For a uniform mesh, H. O. Kreiss has proposed a fourth-order method that is very similar to the basic spline procedure presented here, see Orszag and Israeli (ref. 28). For Burgers' equation (7), Kreiss' method reduces to the system of equations (8), (2), and (3) except that the coefficients $h/6$, $2h/3$, and $h/6$ for M_{i-1}, M_i, and M_{i+1}, respectively, in equation (2) become $h/12$, $5h/6$, and $h/12$, respectively. No longer is M_i a spline approximation but a finite-difference approximation such that

$$M_i = (u_{xx})_i + 0(h^4)$$

The system (9) describes Kreiss' method, with $h_i/6 \rightarrow h/12$ in A_i, $\frac{h_i + h_{i+1}}{3} \rightarrow \frac{5h}{6}$ in B_i and $\frac{h_{i+1}}{6} \rightarrow \frac{h}{12}$ in C_i. All other entries in equation (9c) are unchanged.

The stability of this procedure can be assessed directly from equation (29); α_i and ρ_i are given in equations (9g); τ_1, τ_2, and π_1 are given by equations (28). Due to the change of coefficients in equation (2),

$$6\pi_3 = h(5 + \cos \phi)$$

instead of the spline value

$$6\pi_3 = h(4 + 2 \cos \phi)$$

The stability condition $|\lambda_i| \leq 1$, with λ_i given by the nonzero value in equation (29), leads to the following results: (1) The implicit procedure ($\theta = 1$) is unconditionally stable; and (2) the explicit procedure ($\theta = 0$) has a stability condition

$$\left(1 - 12\beta \frac{1 - \cos \phi}{5 + \cos \phi}\right)^2 + \left(\frac{3c \sin \phi}{2 + \cos \phi}\right)^2 \leq 1$$

Therefore, necessary stability restrictions are $\beta \leq \frac{1}{3}$, $c \leq \frac{1}{\sqrt{6}}$, and $R_c \leq \frac{\sqrt{6}}{2}$.

REFERENCES

1. Moretti, Gino: Thoughts and Afterthoughts About Shock Computations. PIBAL Rep. No. 72-37 (Contract No. N00014-67-A-0438-0009), Polytechnic Inst. Brooklyn, Dec. 1972. (Available from DDC as AD 760 015.)
2. Roache, Patrick J.: Computational Fluid Dynamics. Hermosa Publ., c.1972.
3. Messiter, A. F.: Boundary-Layer Flow Near the Trailing Edge of a Flat Plate. SIAM J. App. Math., vol. 18, no. 1, Jan. 1970, pp. 241-257.
4. Anon.: Compressible Turbulent Boundary Layers. NASA SP-216, 1969.
5. Ackerberg, R. C.; and Phillips, J. H.: The Unsteady Laminar Boundary Layer on a Semi-Infinite Flat Plate Due to Small Fluctuations in the Magnitude of the Free-Stream Velocity. J. Fluid Mech., vol. 51, pt. 1, Jan. 11, 1972, pp. 137-157.
6. Rubin, Stanley G.: Incompressible Flow Along a Corner. J. Fluid Mech., vol. 26, pt. 1, Sept. 1966, pp. 97-110.
7. Briley, W. Roger: A Numerical Study of Laminar Separation Bubbles Using the Navier-Stokes Equations. J. Fluid Mech., vol. 47, pt. 4, June 1971, pp. 713-736.
8. Bozeman, James D.; and Dalton, Charles: Numerical Study of Viscous Flow in a Cavity. J. Comput. Phys., vol. 12, no. 3, July 1973, pp. 348-363.
9. Crowder, H. J.; and Dalton, C.: Errors in the Use of Nonuniform Mesh Systems. J. Comput. Phys., vol. 7, no. 1, Feb. 1971, pp. 32-45.
10. Ahlberg, J. H.; Nilson, E. N.; and Walsh, J. L.: The Theory of Splines and Their Applications. Academic Press, 1967.
11. Douglas, Jim, Jr.; and Dupont, Todd: A Finite Element Collocation Method for Quasi-linear Parabolic Equations. Math. Comput., vol. 27, no. 121, Jan. 1973, pp. 17-28.
12. Keller, Herbert B.: Numerical Methods for Two-Point Boundary-Value Problems. Blaisdell Pub. Co., c.1968.
13. Fyfe, D. J.: The Use of Cubic Splines in the Solution of Two-Point Boundary Value Problems. Computer J., vol. 12, no. 2, May 1969, pp. 188-192.
14. Saul'yev, V. K. (G. J. Tee, transl.): Integration of Equations of Parabolic Type by the Method of Nets. Macmillan Co., 1964.
15. Papamichael, N.; and Whiteman, J. R.: A Cubic Spline Technique for the One Dimensional Heat Conduction Equation. J. Inst. Math. & Its Appl., vol. 11, no. 1, Feb. 1973, pp. 111-113.

16. Albasiny, E. L.; and Hoskins, W. D.: Cubic Spline Solutions to Two-Point Boundary Value Problems. Computer J., vol. 12, no. 2, May 1969, pp. 151-153.

17. Albasiny, E. L.; and Hoskins, W. D.: Increased Accuracy Cubic Spline Solutions to Two-Point Boundary Value Problems. J. Inst. Math. & Its Appl., vol. 9, 1972, pp. 47-55.

18. Brailovskaya, I. Yu.: A Difference Scheme for Numerical Solution of the Two-Dimensional, Nonstationary Navier-Stokes Equations for a Compressible Gas. Sov. Phys. – Doklady, vol. 10, no. 2, Aug. 1965, pp. 107-110.

19. Allen J. S.; and Cheng, S. I.: Numerical Solutions of the Compressible Navier-Stokes Equations for the Laminar Near Wake. Phys. Fluids, vol. 13, no. 1, Jan. 1970. pp. 37-52.

20. Rubin, Stanley G.; and Lin, Tony C.: A Numerical Method for Three-Dimensional Viscous Flow: Application to the Hypersonic Leading Edge. J. Comput. Phys., vol. 9, no. 2, Apr. 1972, pp. 339-364.

21. De Boor, Carl: On Calculating With B-Splines. J. Approximation Theor., vol. 6, no. 1, July 1972, pp. 50-62.

22. Schweikert, Donald G.: An Interpolation Curve Using a Spline in Tension. J. Math. & Phys., vol. XLV, no. 3, Sept. 1966, pp. 312-317.

23. Cline, Alan K.: Curve Fitting Using Splines Under Tension. Atmos. Technol., Sept. 1973, pp. 60-65.

24. Lax, Peter; and Wendroff, Burton: Systems of Conservation Laws. Commun. Pure & Appl. Math., vol. XIII, no. 2, May 1960, pp. 217-237.

25. Hirsh, Richard S.; and Rudy, David H.: The Role of Diagonal Dominance and Cell Reynolds Number in Implicit Difference Methods for Fluid Mechanics Problems. J. Comput. Phys., vol. 16, no. 3, Nov. 1974, pp. 304-310.

26. Khosla, P. K.; and Rubin, S. G.: A Diagonally Dominant Second-Order Accurate Implicit Scheme. Computers & Fluids, vol. 2, no. 2, Aug. 1974, pp. 207-209.

27. Sowerby L.: The Unsteady Flow of Viscous Incompressible Fluid Inside an Infinite Channel. Phil. Mag., seventh ser., vol. 42, no. 325, Feb. 1951, pp. 176-187.

28. Orszag, Steven A.; and Israeli, Moshe: Numerical Simulation of Viscous Incompressible Flows. Annual Review of Fluid Mechanics, vol. 6, 1974, pp. 281-318.

TABLE 1.- IMPLICIT SPLINE SOLUTION TO BURGERS' EQUATION FOR $\nu = 1/2$, $\sigma = 0$, AND 51 EQUALLY SPACED POINTS

η	Exact u	Spline calculated u	Exact u_η	Spline curve fit m	Finite-difference curve fit u_η	Spline calculated m	Exact $u_{\eta\eta}$	Spline curve fit M	Finite-difference curve fit $u_{\eta\eta}$	Spline calculated M
-5.000	0.9933	0.9933	-6.648×10^{-3}	-6.647×10^{-3}	----------	-6.627×10^{-3}	-6.560×10^{-3}	-6.559×10^{-3}	----------	-6.538×10^{-3}
-4.800	.9918	.9918	-8.096×10^{-3}	-8.096×10^{-3}	-8.147×10^{-3}	-8.075×10^{-3}	-7.964×10^{-3}	-7.935×10^{-3}	-7.988×10^{-3}	-7.943×10^{-3}
-4.600	.9900	.9900	-9.853×10^{-3}	-9.853×10^{-3}	-9.915×10^{-3}	-9.833×10^{-3}	-9.657×10^{-3}	-9.630×10^{-3}	-9.685×10^{-3}	-9.637×10^{-3}
-4.400	.9879	.9879	-1.198×10^{-2}	-1.198×10^{-2}	-1.205×10^{-2}	-1.196×10^{-2}	-1.169×10^{-2}	-1.166×10^{-2}	-1.172×10^{-2}	-1.167×10^{-2}
-4.200	.9852	.9852	-1.455×10^{-2}	-1.455×10^{-2}	-1.464×10^{-2}	-1.454×10^{-2}	-1.412×10^{-2}	-1.409×10^{-2}	-1.416×10^{-2}	-1.411×10^{-2}
-4.000	.9820	.9820	-1.766×10^{-2}	-1.766×10^{-2}	-1.777×10^{-2}	-1.766×10^{-2}	-1.703×10^{-2}	-1.698×10^{-2}	-1.707×10^{-2}	-1.702×10^{-2}
-3.800	.9781	.9781	-2.140×10^{-2}	-2.140×10^{-2}	-2.153×10^{-2}	-2.140×10^{-2}	-2.046×10^{-2}	-2.041×10^{-2}	-2.051×10^{-2}	-2.047×10^{-2}
-3.600	.9734	.9734	-2.589×10^{-2}	-2.589×10^{-2}	-2.603×10^{-2}	-2.590×10^{-2}	-2.451×10^{-2}	-2.446×10^{-2}	-2.457×10^{-2}	-2.453×10^{-2}
-3.400	.9677	.9677	-3.125×10^{-2}	-3.125×10^{-2}	-3.142×10^{-2}	-3.128×10^{-2}	-2.923×10^{-2}	-2.917×10^{-2}	-2.929×10^{-2}	-2.926×10^{-2}
-3.200	.9608	.9608	-3.763×10^{-2}	-3.763×10^{-2}	-3.783×10^{-2}	-3.768×10^{-2}	-3.468×10^{-2}	-3.462×10^{-2}	-3.475×10^{-2}	-3.473×10^{-2}
-3.000	.9526	.9526	-4.517×10^{-2}	-4.518×10^{-2}	-4.539×10^{-2}	-4.525×10^{-2}	-4.089×10^{-2}	-4.083×10^{-2}	-4.095×10^{-2}	-4.096×10^{-2}
-2.800	.9427	.9426	-5.403×10^{-2}	-5.404×10^{-2}	-5.428×10^{-2}	-5.414×10^{-2}	-4.784×10^{-2}	-4.779×10^{-2}	-4.789×10^{-2}	-4.793×10^{-2}
-2.600	.9309	.9308	-6.436×10^{-2}	-6.435×10^{-2}	-6.462×10^{-2}	-6.449×10^{-2}	-5.546×10^{-2}	-5.542×10^{-2}	-5.550×10^{-2}	-5.556×10^{-2}
-2.400	.9168	.9167	-7.625×10^{-2}	-7.625×10^{-2}	-7.653×10^{-2}	-7.642×10^{-2}	-6.357×10^{-2}	-6.355×10^{-2}	-6.359×10^{-2}	-6.369×10^{-2}
-2.200	.9002	.9001	-8.980×10^{-2}	-8.980×10^{-2}	-9.007×10^{-2}	-8.998×10^{-2}	-7.188×10^{-2}	-7.190×10^{-2}	-7.187×10^{-2}	-7.201×10^{-2}
-2.000	.8808	.8806	-1.050×10^{-1}	-1.050×10^{-2}	-1.052×10^{-1}	-1.052×10^{-1}	-7.996×10^{-2}	-8.003×10^{-2}	-7.989×10^{-2}	-8.008×10^{-2}
-1.800	.8581	.8579	-1.217×10^{-1}	-1.217×10^{-1}	-1.219×10^{-1}	-1.219×10^{-1}	-8.719×10^{-2}	-8.733×10^{-2}	-8.706×10^{-2}	-8.729×10^{-2}
-1.600	.8320	.8318	-1.397×10^{-1}	-1.397×10^{-1}	-1.399×10^{-1}	-1.399×10^{-1}	-9.281×10^{-2}	-9.302×10^{-2}	-9.259×10^{-2}	-9.287×10^{-2}
-1.400	.8022	.8019	-1.587×10^{-1}	-1.587×10^{-1}	-1.587×10^{-1}	-1.588×10^{-1}	-9.590×10^{-2}	-9.619×10^{-2}	-9.561×10^{-2}	-9.590×10^{-2}
-1.200	.7685	.7682	-1.779×10^{-1}	-1.779×10^{-1}	-1.778×10^{-1}	-1.779×10^{-1}	-9.554×10^{-2}	-9.590×10^{-2}	-9.518×10^{-2}	-9.547×10^{-2}
-1.000	.7311	.7308	-1.966×10^{-1}	-1.966×10^{-1}	-1.964×10^{-1}	-1.966×10^{-1}	-9.086×10^{-2}	-9.127×10^{-2}	-9.045×10^{-2}	-9.073×10^{-2}
-8.000×10^{-1}	.6899	.6897	-2.139×10^{-1}	-2.139×10^{-1}	-2.135×10^{-1}	-2.137×10^{-1}	-8.127×10^{-2}	-8.170×10^{-2}	-8.085×10^{-2}	-8.110×10^{-2}
-6.000×10^{-1}	.6456	.6454	-2.288×10^{-1}	-2.288×10^{-1}	-2.282×10^{-1}	-2.285×10^{-1}	-6.665×10^{-2}	-6.704×10^{-2}	-6.626×10^{-2}	-6.646×10^{-2}
-4.000×10^{-1}	.5987	.5985	-2.403×10^{-1}	-2.402×10^{-1}	-2.395×10^{-1}	-2.399×10^{-1}	-4.742×10^{-2}	-4.772×10^{-2}	-4.712×10^{-2}	-4.727×10^{-2}
-2.000×10^{-1}	.5498	.5497	-2.475×10^{-1}	-2.475×10^{-1}	-2.467×10^{-1}	-2.471×10^{-1}	-2.467×10^{-2}	-2.483×10^{-2}	-2.451×10^{-2}	-2.458×10^{-2}
0	.5000	.5000	-2.500×10^{-1}	-2.500×10^{-1}	-2.492×10^{-1}	-2.495×10^{-1}	0	2.831×10^{-13}	8.882×10^{-14}	2.857×10^{-14}

TABLE 2.- IMPLICIT SPLINE SOLUTION TO BURGERS' EQUATION FOR $\nu = 1/2$, $\sigma = 0$, $\sigma_i = 1.4$, AND 15 POINTS

η	Exact u	Spline calculated u	Exact u_η	Spline curve fit m	Finite-difference curve fit u_η	Spline calculated m	Exact $u_{\eta\eta}$	Spline curve fit M	Finite-difference curve fit $u_{\eta\eta}$	Spline calculated M
-5.000	0.9933	0.9933	-6.648×10^{-3}	-5.668×10^{-3}	----------	-4.327×10^{-3}	-6.559×10^{-3}	-6.559×10^{-3}	----------	-4.268×10^{-3}
-3.419	.9683	.9712	-3.068×10^{-2}	-3.095×10^{-2}	-3.769×10^{-2}	-2.994×10^{-2}	-2.874×10^{-2}	-2.550×10^{-2}	-2.768×10^{-2}	-2.822×10^{-2}
-2.295	.9082	.9106	-8.338×10^{-2}	-8.365×10^{-2}	-8.932×10^{-2}	-8.532×10^{-2}	-6.807×10^{-2}	-6.805×10^{-2}	-6.387×10^{-2}	-7.007×10^{-2}
-1.487	.8156	.8164	-1.504×10^{-1}	-1.504×10^{-1}	-1.516×10^{-1}	-1.523×10^{-1}	-9.493×10^{-2}	-9.792×10^{-2}	-9.096×10^{-2}	-9.637×10^{-2}
-9.119×10^{-1}	.7134	.7135	-2.045×10^{-1}	-2.044×10^{-1}	-2.028×10^{-1}	-2.051×10^{-1}	-8.726×10^{-2}	-8.990×10^{-2}	-8.712×10^{-2}	-8.758×10^{-2}
-5.017×10^{-1}	.6229	.6228	-2.349×10^{-1}	-2.348×10^{-1}	-2.330×10^{-1}	-2.349×10^{-1}	-5.773×10^{-2}	-5.878×10^{-2}	-6.027×10^{-2}	-5.770×10^{-2}
-2.089×10^{-1}	.5521	.5520	-2.473×10^{-1}	-2.473×10^{-1}	-2.461×10^{-1}	-2.471×10^{-1}	-2.575×10^{-2}	-2.599×10^{-2}	-2.876×10^{-2}	-2.571×10^{-2}
0	.5000	.5000	-2.500×10^{-1}	-2.500×10^{-1}	-2.491×10^{-1}	-2.498×10^{-1}	0	1.943×10^{-14}	0	1.953×10^{-13}

TABLE 3.- IMPLICIT SPLINE SOLUTION TO BURGERS' EQUATION FOR $\nu = 1/2$, $\sigma = 0$, $\sigma = 1.8$, AND 15 POINTS

η	Exact u	Spline calculated u	Exact u_η	Spline curve fit m	Finite-difference curve fit u_η	Spline calculated m	Exact $u_{\eta\eta}$	Spline curve fit M	Finite-difference curve fit $u_{\eta\eta}$	Spline calculated M
-5.000	0.9933	0.9933	-6.648×10^{-3}	-2.496×10^{-3}	----------	3.358×10^{-4}	-6.559×10^{-3}	-6.559×10^{-3}	----------	3.313×10^{-4}
-2.739	.9393	.9496	-5.700×10^{-2}	-5.935×10^{-2}	-7.209×10^{-2}	-5.919×10^{-2}	-5.008×10^{-2}	-4.395×10^{-2}	-4.266×10^{-2}	-5.322×10^{-2}
-1.484	.8152	.8213	-1.506×10^{-1}	-1.504×10^{-1}	-1.533×10^{-1}	-1.549×10^{-1}	-9.497×10^{-2}	-1.013×10^{-1}	-8.681×10^{-2}	-9.956×10^{-2}
-7.874×10^{-1}	.6873	.6904	-2.149×10^{-1}	-2.148×10^{-1}	-2.126×10^{-1}	-2.186×10^{-1}	-8.049×10^{-2}	-8.363×10^{-2}	-8.314×10^{-2}	-8.327×10^{-2}
-4.004×10^{-1}	.5988	.6004	-2.402×10^{-1}	-2.402×10^{-1}	-2.388×10^{-1}	-2.442×10^{-1}	-4.746×10^{-2}	-4.795×10^{-2}	-5.263×10^{-2}	-4.906×10^{-2}
-1.855×10^{-1}	.5462	.5470	-2.478×10^{-1}	-2.478×10^{-1}	-2.473×10^{-1}	-2.520×10^{-1}	-2.293×10^{-2}	-2.304×10^{-2}	-2.662×10^{-2}	-2.371×10^{-2}
-6.624×10^{-2}	.5165	.5168	-2.497×10^{-1}	-2.497×10^{-1}	-2.496×10^{-1}	-2.539×10^{-1}	-8.268×10^{-3}	-8.267×10^{-3}	-1.045×10^{-2}	-8.551×10^{-3}
0	.5000	.5000	-2.500×10^{-1}	-2.500×10^{-1}	-2.499×10^{-1}	-2.542×10^{-1}	0	-1.736×10^{-12}	-8.096×10^{-13}	-2.088×10^{-13}

TABLE 4.- IMPLICIT SPLINE SOLUTION TO BURGERS' EQUATION FOR $\nu = 1/8$, $\sigma = 0$, AND 51 EQUALLY SPACE POINTS

η	Exact u	Spline calculated u	Exact u_η	Spline curve fit m	Finite-difference curve fit u_η	Spline calculated m	Exact $u_{\eta\eta}$	Spline curve fit M	Finite-difference curve fit $u_{\eta\eta}$	Spline calculated M	Average of spline curve fit M and finite-difference curve fit $u_{\eta\eta}$
-5.000	1.000	1.000	-8.245×10^{-9}	-8.128×10^{-9}	----------	-3.190×10^{-9}	-3.298×10^{-8}	-3.298×10^{-8}	----------	-1.276×10^{-8}	----------
-4.800			-1.835×10^{-8}	-1.833×10^{-8}	-2.037×10^{-8}	-7.445×10^{-9}	-7.339×10^{-8}	-6.911×10^{-8}	-7.739×10^{-8}	-2.980×10^{-8}	-7.325×10^{-8}
-4.600			-4.083×10^{-8}	-4.074×10^{-8}	-4.533×10^{-8}	-1.738×10^{-8}	-1.633×10^{-7}	-1.549×10^{-7}	-1.722×10^{-7}	-6.959×10^{-8}	-1.635×10^{-7}
-4.400			-9.088×10^{-8}	-9.069×10^{-8}	-1.009×10^{-7}	-4.059×10^{-3}	-3.635×10^{-7}	-3.445×10^{-7}	-3.833×10^{-7}	-1.624×10^{-7}	-3.639×10^{-7}
-4.200			-2.023×10^{-7}	-2.018×10^{-7}	-2.245×10^{-7}	-9.476×10^{-8}	-8.090×10^{-7}	-7.669×10^{-7}	-8.531×10^{-7}	-3.793×10^{-7}	-8.100×10^{-7}
-4.000			-4.501×10^{-7}	-4.491×10^{-7}	-4.997×10^{-7}	-2.212×10^{-6}	-1.800×10^{-6}	-1.707×10^{-6}	-1.898×10^{-6}	-8.853×10^{-7}	-1.802×10^{-6}
-3.800			-1.002×10^{-6}	-9.996×10^{-7}	-1.112×10^{-6}	-5.163×10^{-7}	-4.007×10^{-6}	-3.798×10^{-6}	-4.225×10^{-6}	-2.066×10^{-6}	-4.011×10^{-6}
-3.600			-2.229×10^{-6}	-2.225×10^{-6}	-2.475×10^{-6}	-1.205×10^{-6}	-8.918×10^{-6}	-8.453×10^{-6}	-9.404×10^{-6}	-4.822×10^{-6}	-8.928×10^{-5}
-3.400			-4.962×10^{-6}	-4.951×10^{-6}	-5.508×10^{-6}	-2.812×10^{-6}	-1.985×10^{-5}	-1.881×10^{-5}	-2.093×10^{-5}	-1.125×10^{-5}	-1.987×10^{-5}
-3.200			-1.104×10^{-5}	-1.102×10^{-5}	-1.225×10^{-5}	-6.563×10^{-6}	-4.417×10^{-5}	-4.187×10^{-5}	-4.658×10^{-5}	-2.626×10^{-5}	-4.422×10^{-5}
-3.000			-2.457×10^{-5}	-2.452×10^{-5}	-2.728×10^{-5}	-1.531×10^{-5}	-9.830×10^{-5}	-9.318×10^{-5}	-1.037×10^{-4}	-6.127×10^{-5}	-9.844×10^{-5}
-2.800			-5.469×10^{-5}	-5.458×10^{-5}	-6.072×10^{-5}	-3.574×10^{-5}	-2.188×10^{-4}	-2.074×10^{-4}	-2.307×10^{-4}	-1.429×10^{-4}	-2.190×10^{-4}
-2.600			-1.217×10^{-4}	-1.215×10^{-4}	-1.351×10^{-4}	-8.339×10^{-5}	-4.869×10^{-4}	-4.615×10^{-4}	-5.134×10^{-4}	-3.336×10^{-4}	-4.874×10^{-4}
-2.400			-2.708×10^{-4}	-2.703×10^{-4}	-3.007×10^{-4}	-1.946×10^{-4}	-1.083×10^{-3}	-1.027×10^{-3}	-1.142×10^{-3}	-7.783×10^{-4}	-1.084×10^{-3}
-2.200			-6.027×10^{-4}	-6.015×10^{-4}	-6.691×10^{-4}	-4.539×10^{-4}	-2.410×10^{-3}	-2.285×10^{-3}	-2.541×10^{-3}	-1.815×10^{-3}	-2.413×10^{-3}
-2.000	1.000	1.000	-1.341×10^{-3}	-1.338×10^{-3}	-1.488×10^{-3}	-1.058×10^{-3}	-5.630×10^{-3}	-5.082×10^{-3}	-5.651×10^{-3}	-4.233×10^{-3}	-5.366×10^{-3}
-1.800	.999	.999	-2.982×10^{-3}	-2.976×10^{-3}	-3.308×10^{-3}	-2.486×10^{-3}	-1.191×10^{-2}	-1.129×10^{-2}	-1.255×10^{-2}	-9.861×10^{-3}	-1.192×10^{-2}
-1.600	.998	.999	-6.624×10^{-3}	-6.611×10^{-3}	-7.345×10^{-3}	-5.764×10^{-3}	-2.641×10^{-2}	-2.506×10^{-2}	-2.781×10^{-2}	-2.292×10^{-2}	-2.644×10^{-2}
-1.400	.996	.997	-1.468×10^{-2}	-1.456×10^{-2}	-1.626×10^{-2}	-1.334×10^{-2}	-5.829×10^{-2}	-5.538×10^{-2}	-6.132×10^{-2}	-5.303×10^{-2}	-5.835×10^{-2}
-1.200	.992	.993	-3.238×10^{-2}	-3.233×10^{-2}	-3.575×10^{-2}	-3.077×10^{-2}	-1.274×10^{-1}	-1.214×10^{-1}	-1.336×10^{-1}	-1.213×10^{-1}	-1.275×10^{-1}
-1.000	.982	.983	-7.065×10^{-2}	-7.056×10^{-2}	-7.751×10^{-2}	-6.992×10^{-2}	-2.274×10^{-1}	-2.609×10^{-1}	-2.839×10^{-1}	-2.702×10^{-1}	-2.724×10^{-1}
-.800	.961	.962	-1.505×10^{-1}	-1.505×10^{-1}	-1.629×10^{-1}	-1.537×10^{-1}	-5.549×10^{-1}	-5.382×10^{-1}	-5.707×10^{-1}	-5.677×10^{-1}	-5.545×10^{-1}
-.600	.917	.916	-3.050×10^{-1}	-3.053×10^{-1}	-3.220×10^{-1}	-3.156×10^{-1}	-1.017	-1.010	-1.020	-1.051	-1.015
-.400	.832	.829	-5.590×10^{-1}	-5.604×10^{-1}	-5.671×10^{-1}	-5.711×10^{-1}	-1.485	-1.541	-1.431	-1.504	-1.486
-.200	.690	.686	-8.556×10^{-1}	-8.557×10^{-1}	-8.300×10^{-1}	-8.481×10^{-1}	-1.300	-1.412	-1.198	-1.265	-1.305
0	.500	.500	-1.000	-9.969×10^{-1}	-9.498×10^{-1}	-9.746×10^{-1}	0	5.276×10^{-12}	1.066×10^{-12}	-2.078×10^{-10}	3.171×10^{-12}

TABLE 5.- IMPLICIT SPLINE SOLUTION TO BURGERS' EQUATION FOR $\nu = 1/8$, $\sigma = 0$, $\sigma_i = 1.2$, AND 15 POINTS

η	Exact u	Spline calculated u	Exact u_η	Spline curve fit m	Finite-difference curve fit u_η	Spline calculated m	Exact $u_{\eta\eta}$	Spline curve fit M	Finite-difference curve fit $u_{\eta\eta}$	Spline calculated M	Nondivergence finite-difference calculated u
-5.000	1.000	1.000	-8.245×10^{-9}	-3.476×10^{-6}	----------	1.707×10^{-5}	-3.298×10^{-8}	-3.298×10^{-8}	----------	6.828×10^{-5}	1.000
-3.842	1.000	1.000	-8.473×10^{-7}	6.433×10^{-6}	-5.636×10^{-6}	-4.306×10^{-5}	-3.389×10^{-6}	1.716×10^{-5}	-9.421×10^{-6}	-1.722×10^{-4}	1.000
-2.877	1.000	1.000	-4.011×10^{-5}	-5.169×10^{-5}	-1.669×10^{-4}	1.359×10^{-4}	-1.604×10^{-4}	-1.378×10^{-4}	-3.251×10^{-4}	5.438×10^{-4}	1.000
-2.075	1.000	1.000	-9.951×10^{-5}	-7.337×10^{-4}	-2.867×10^{-3}	-5.854×10^{-4}	-3.978×10^{-3}	-1.562×10^{-3}	-6.401×10^{-3}	-2.342×10^{-3}	1.000
-1.406	.996	1.000	-1.433×10^{-2}	-1.303×10^{-2}	-3.048×10^{-3}	4.049×10^{-3}	-5.692×10^{-2}	-3.524×10^{-2}	-7.619×10^{-2}	1.621×10^{-2}	.999
-8.494×10^{-1}	.967	.978	-1.253×10^{-1}	-1.192×10^{-1}	-1.926×10^{-1}	-1.341×10^{-1}	-4.687×10^{-1}	-3.463×10^{-1}	-5.062×10^{-1}	-5.128×10^{-1}	1.003
-3.859×10^{-1}	.824	.821	-5.801×10^{-1}	-6.110×10^{-1}	-5.989×10^{-1}	-6.258×10^{-1}	-1.504	-1.776	-1.247	-1.609	.951
0	.500	.500	-1.000	-9.537×10^{-1}	-8.395×10^{-1}	-9.363×10^{-1}	0	5.862×10^{-14}	4.771×10^{-14}	1.188×10^{-11}	.500

TABLE 6.- IMPLICIT SPLINE SOLUTION TO BURGERS' EQUATION FOR $\nu = 1/8$, $\sigma = 0$, $\sigma_i = 1.4$, AND 15 POINTS

η	Exact u	Spline calculated u	Exact u_η	Spline curve fit m	Finite-difference curve fit u_η	Spline calculated m	Exact $u_{\eta\eta}$	Spline curve fit M	Finite-difference curve fit $u_{\eta\eta}$	Spline calculated M	Nondivergence finite-difference calculated u
-5.000	1.000	1.000	-8.245×10^{-9}	-2.242×10^{-5}	----------	-2.281×10^{-4}	-3.298×10^{-8}	-3.298×10^{-8}	----------	-9.126×10^{-4}	1.000
-3.419	1.000	1.000	-4.586×10^{-6}	4.276×10^{-5}	-5.373×10^{-5}	4.405×10^{-4}	-1.834×10^{-5}	8.270×10^{-5}	-6.708×10^{-5}	1.760×10^{-3}	.999
-2.295	1.000	1.000	-4.176×10^{-4}	-4.070×10^{-4}	-1.853×10^{-3}	-1.143×10^{-3}	-1.670×10^{-3}	-8.810×10^{-4}	-3.123×10^{-3}	-4.571×10^{-3}	1.000
-1.487	.997	1.000	-1.040×10^{-2}	-8.162×10^{-3}	-2.442×10^{-2}	4.891×10^{-3}	-4.140×10^{-2}	-1.839×10^{-2}	-5.295×10^{-2}	1.957×10^{-2}	.998
-9.119×10^{-1}	.975	.985	-9.897×10^{-2}	-9.731×10^{-2}	-1.489×10^{-1}	-9.048×10^{-2}	-3.758×10^{-1}	-2.919×10^{-1}	-3.803×10^{-1}	-3.516×10^{-1}	1.004
-5.017×10^{-1}	.881	.889	-4.177×10^{-1}	-4.262×10^{-1}	-4.611×10^{-1}	-4.504×10^{-1}	-1.275	-1.312	-1.142	-1.403	.956
-2.089×10^{-1}	.698	.698	-8.438×10^{-1}	-8.400×10^{-1}	-8.134×10^{-1}	-8.541×10^{-1}	-1.334	-1.515	-1.265	-1.354	.751
0	.500	.500	-1.000	-9.983×10^{-1}	-9.456×10^{-1}	-9.956×10^{-1}	0	-1.918×10^{-13}	8.135×10^{-14}	2.032×10^{-11}	.500

TABLE 7.- IMPLICIT SPLINE SOLUTION TO BURGERS' EQUATION FOR $\nu = 1/8$, $\sigma = 0$, $\sigma_i = 1.6$, AND 15 POINTS

η	Exact u	Spline calculated u	Exact u_η	Spline curve fit m	Finite-difference curve fit u_η	Spline calculated m	Exact $u_{\eta\eta}$	Spline curve fit M	Finite-difference curve fit M	Spline calculated M
-5.000	1.000	1.000	-8.245×10^{-9}	1.614×10^{-4}	----------	1.505×10^{-3}	-3.298×10^{-8}	-3.298×10^{-4}	----------	6.022×10^{-3}
-3.051	1.000	1.004	-2.006×10^{-5}	-3.312×10^{-4}	-3.287×10^{-4}	-2.516×10^{-3}	-8.024×10^{-5}	-5.070×10^{-4}	-3.346×10^{-4}	-1.016×10^{-2}
-1.833	.999	1.002	-2.611×10^{-3}	-6.264×10^{-4}	-1.061×10^{-2}	6.039×10^{-3}	-1.043×10^{-2}	2.138×10^{-5}	-1.655×10^{-2}	2.423×10^{-2}
-1.073	.986	1.000	-5.329×10^{-2}	-4.947×10^{-2}	-9.767×10^{-2}	-2.929×10^{-2}	-2.074×10^{-1}	-1.285×10^{-1}	-2.124×10^{-1}	-1.172×10^{-1}
-1.073×10^{-1}	.916	.934	-3.073×10^{-1}	-3.149×10^{-1}	-3.616×10^{-1}	-3.272×10^{-1}	-1.023	-9.893×10^{-1}	-8.990×10^{-1}	-1.137
-3.011×10^{-1}	.769	.779	-7.099×10^{-1}	-7.084×10^{-1}	-7.069×10^{-1}	-1.423×10^{-1}	-1.529	-1.664	-1.429	-1.661
-1.157×10^{-1}	.613	.617	-9.483×10^{-1}	-9.472×10^{-1}	-9.275×10^{-1}	-9.819×10^{-1}	-8.627×10^{-1}	-9.139×10^{-1}	-9.506×10^{-1}	-9.252×10^{-1}
0	.500	.500	-1.000	-1.000	-9.825×10^{-1}	-1.0356	0	5.471×10^{-13}	0	2.134×10^{-11}

TABLE 8.- IMPLICIT SPLINE SOLUTION TO BURGERS' EQUATION FOR $\nu = 1/8$, $\sigma = 0$, $\sigma_i = 1.8$, AND 15 POINTS

η	Exact u	Spline calculated u	Exact u_η	Spline curve fit m	Finite-difference curve fit u_η	Spline calculated m	Exact $u_{\eta\eta}$	Spline curve fit M	Finite-difference curve fit $u_{\eta\eta}$	Spline calculated M
-5.000	1.000	1.000	-8.245×10^{-9}	9.096×10^{-4}	----------	7.139×10^{-3}	-3.298×10^{-8}	-3.298×10^{-8}	----------	2.856×10^{-2}
-2.739	1.000	1.027	-6.968×10^{-5}	-1.847×10^{-3}	-1.342×10^{-3}	-1.048×10^{-2}	-2.787×10^{-4}	-2.449×10^{-3}	-1.181×10^{-3}	-4.422×10^{-2}
-1.484	.997	1.016	-1.050×10^{-2}	-1.019×10^{-3}	-3.624×10^{-2}	2.400×10^{-2}	-4.179×10^{-2}	3.769×10^{-3}	-5.443×10^{-2}	9.924×10^{-2}
-7.874×10^{-1}	.959	1.002	-1.577×10^{-1}	-1.649×10^{-1}	-2.301×10^{-1}	-1.469×10^{-1}	-5.789×10^{-1}	-4.743×10^{-1}	-5.020×10^{-1}	-5.900×10^{-1}
-4.004×10^{-1}	.832	.870	-5.584×10^{-1}	-5.602×10^{-1}	-5.800×10^{-1}	-6.117×10^{-1}	-1.484	-1.568	-1.306	-1.812
-1.855×10^{-1}	.677	.699	-8.740×10^{-1}	-8.721×10^{-1}	-8.587×10^{-1}	-9.729×10^{-1}	-1.241	-1.335	-1.288	-1.549
-6.624×10^{-2}	.566	.574	-9.826×10^{-1}	-9.827×10^{-1}	-9.732×10^{-1}	-1.104	-5.177×10^{-1}	-5.186×10^{-1}	-6.318×10^{-1}	-6.548×10^{-1}
0	.500	.500	-1.000	-1.000	-9.942×10^{-1}	-1.126	0	-1.749×10^{-12}	0	-1.486×10^{-11}

TABLE 9.- IMPLICIT SPLINE SOLUTION TO BURGERS' EQUATION FOR $\nu = 1/24$, $\sigma = 0$, AND 51 EQUALLY SPACED POINTS

η	Exact u	Spline calculated u	Exact u_η	Spline curve fit m	Finite-difference curve fit u_η	Spline calculated m	Exact $u_{\eta\eta}$	Spline curve fit M	Finite-difference curve fit $u_{\eta\eta}$	Spline calculated M	Two-step spline calculated u
-5.000	1.0000	1.0000	-1.051×10^{-25}	1.277×10^{-14}	0	-1.074×10^{-14}	-1.261×10^{-24}	-1.261×10^{-24}	0	-1.288×10^{-13}	1.0000
-4.800			-1.158×10^{-24}	2.553×10^{-14}	0	-4.504×10^{-14}	-1.389×10^{-23}	3.830×10^{-13}	0	-2.142×10^{-13}	
-4.600			$-.277 \times 10^{-23}$	-8.938×10^{-14}	0	-6.298×10^{-14}	-1.532×10^{-22}	-1.532×10^{-12}	0	3.466×10^{-14}	
-4.400			-1.407×10^{-22}	3.319×10^{-13}	0	-4.597×10^{-14}	-1.689×10^{-21}	5.746×10^{-12}	0	1.354×10^{-13}	
-4.200			-1.551×10^{-21}	-1.238×10^{-12}	0	-5.007×10^{-14}	-1.862×10^{-20}	-2.145×10^{-11}	0	-1.764×10^{-13}	
-4.000			-1.710×10^{-20}	4.622×10^{-12}	0	-6.371×10^{-14}	-2.052×10^{-19}	8.006×10^{-11}	0	4.005×10^{-14}	
-3.800			-1.885×10^{-19}	-1.725×10^{-11}	0	-4.608×10^{-14}	-2.262×10^{-18}	-2.988×10^{-10}	0	1.362×10^{-13}	
-3.600			-2.078×10^{-18}	6.438×10^{-11}	0	-5.008×10^{-14}	-2.494×10^{-17}	1.115×10^{-9}	0	-1.763×10^{-13}	
-3.400			-2.291×10^{-17}	-2.403×10^{-10}	0	-6.371×10^{-14}	-2.749×10^{-16}	-4.162×10^{-9}	0	4.004×10^{-14}	
-3.200			-2.525×10^{-16}	8.968×10^{-10}	0	-4.607×10^{-14}	-3.030×10^{-15}	1.553×10^{-8}	0	1.364×10^{-13}	
-3.000			-2.783×10^{-15}	-3.347×10^{-9}	0	-5.013×10^{-14}	-3.340×10^{-14}	-5.797×10^{-8}	0	-1.769×10^{-13}	
-2.800			-3.068×10^{-14}	1.249×10^{-8}	-5.329×10^{-14}	-6.349×10^{-14}	-3.682×10^{-13}	2.164×10^{-7}	-3.553×10^{-13}	4.337×10^{-14}	
-2.600			-3.382×10^{-13}	-4.662×10^{-8}	-7.638×10^{-13}	-4.718×10^{-14}	-4.058×10^{-12}	-8.075×10^{-7}	-6.572×10^{-12}	1.197×10^{-13}	
-2.400			-3.728×10^{-12}	1.739×10^{-7}	-8.491×10^{-12}	-4.457×10^{-14}	-4.474×10^{-11}	3.014×10^{-6}	-7.069×10^{-11}	-9.362×10^{-14}	
-2.200			-4.109×10^{-11}	-6.494×10^{-7}	-9.361×10^{-11}	-4.559×10^{-14}	-4.932×10^{-10}	-1.125×10^{-5}	-7.805×10^{-10}	8.344×10^{-14}	
-2.000			-4.530×10^{-10}	2.423×10^{-6}	-1.032×10^{-9}	-1.758×10^{-13}	-5.436×10^{-9}	4.197×10^{-5}	-8.601×10^{-9}	-1.386×10^{-12}	
-1.800			-4.994×10^{-9}	-9.049×10^{-6}	-1.137×10^{-8}	1.324×10^{-12}	-5.992×10^{-8}	-1.567×10^{-4}	-9.482×10^{-8}	1.638×10^{-11}	
-1.600			-5.505×10^{-8}	3.371×10^{-5}	-1.254×10^{-7}	-1.528×10^{-11}	-6.605×10^{-7}	5.843×10^{-4}	-1.045×10^{-6}	-1.824×10^{-10}	
-1.400			-6.068×10^{-7}	-1.265×10^{-4}	-1.382×10^{-6}	1.677×10^{-10}	-7.281×10^{-6}	-2.187×10^{-3}	-1.152×10^{-5}	2.013×10^{-8}	
-1.200			-6.689×10^{-6}	4.641×10^{-4}	-1.523×10^{-5}	-1.867×10^{-9}	-8.026×10^{-5}	8.094×10^{-3}	-1.269×10^{-4}	-2.236×10^{-8}	
-1.000	1.0000	1.0000	-7.373×10^{-5}	-1.821×10^{-3}	-1.679×10^{-4}	2.034×10^{-4}	-8.847×10^{-4}	-3.095×10^{-2}	-1.399×10^{-3}	2.445×10^{-7}	
-.800	.9999	1.0000	-8.126×10^{-4}	5.814×10^{-3}	-1.849×10^{-3}	-2.227×10^{-7}	-9.750×10^{-3}	1.073×10^{-1}	-1.542×10^{-2}	-2.675×10^{-6}	1.000
-.600	.9992	1.0000	-8.946×10^{-3}	-3.235×10^{-2}	-2.024×10^{-2}	2.523×10^{-6}	-1.072×10^{-1}	-4.908×10^{-1}	-1.684×10^{-1}	3.013×10^{-5}	.9996
-.400	.9918	1.0000	-9.715×10^{-2}	2.906×10^{-3}	-2.061×10^{-1}	-2.569×10^{-5}	-1.147	8.452×10^{-1}	-1.689	-3.123×10^{-4}	1.0037
-.200	.9168	.9167	-9.151×10^{-1}	-1.215	-1.229	-1.250	-9.154	-13.029	-8.545	-12.499	.9091
0	.5000	.5000	-3.000	-2.518	-2.084	-2.500	0	-9.440×10^{-11}	1.456×10^{-11}	-3.557×10^{-9}	.5000

TABLE 10.- IMPLICIT SPLINE SOLUTION TO BURGERS' EQUATION FOR $\nu = 1/24$, $\sigma = 0$, $\sigma_i = 1.2$, AND 31 POINTS

η	Exact u	Spline calculated u	Exact u_η	Spline curve fit m	Finite-difference curve fit u_η	Spline calculated m	Exact $u_{\eta\eta}$	Spline curve fit M	Finite-difference curve fit $u_{\eta\eta}$	Spline calculated M
-5.000	1.000	1.000	-1.051×10^{-25}	-4.084×10^{-10}	----------	-1.726×10^{-8}	-1.261×10^{-24}	-1.261×10^{-24}	----------	-2.071×10^{-7}
-4.106	1.000	1.000	-4.799×10^{-21}	8.172×10^{-10}	0	1.684×10^{-8}	-5.759×10^{-20}	2.743×10^{-9}	0	2.834×10^{-7}
-3.361	1.000	1.000	-3.639×10^{-17}	-2.656×10^{-9}	0	-4.489×10^{-8}	-4.367×10^{-16}	-1.208×10^{-8}	2.798×10^{-14}	-4.493×10^{-7}
-2.741	1.000	1.000	-6.188×10^{-14}	9.057×10^{-9}	-2.672×10^{-12}	8.011×10^{-8}	-7.426×10^{-13}	4.988×10^{-8}	-8.597×10^{-12}	8.528×10^{-7}
-2.225	1.000	1.000	-3.030×10^{-11}	-3.100×10^{-8}	-5.558×10^{-10}	-1.125×10^{-7}	-3.636×10^{-10}	-2.051×10^{-7}	-2.134×10^{-9}	-1.599×10^{-6}
-1.795	1.000	1.000	-5.262×10^{-9}	1.030×10^{-7}	-4.878×10^{-8}	3.191×10^{-7}	-6.314×10^{-8}	8.291×10^{-7}	-2.222×10^{-7}	3.608×10^{-6}
-1.437	1.000	1.000	-3.855×10^{-7}	-6.201×10^{-7}	-2.082×10^{-6}	-8.229×10^{-7}	-4.626×10^{-6}	-4.872×10^{-6}	-1.114×10^{-5}	-9.992×10^{-6}
-1.139	1.000	1.000	-1.376×10^{-5}	-9.260×10^{-6}	-4.869×10^{-5}	2.941×10^{-6}	-1.652×10^{-4}	-5.313×10^{-5}	-3.017×10^{-4}	3.526×10^{-5}
-8.918×10^{-1}	1.000	1.000	-2.701×10^{-4}	-2.333×10^{-4}	-6.887×10^{-4}	-1.497×10^{-5}	-3.242×10^{-3}	-1.753×10^{-3}	-4.858×10^{-3}	-1.797×10^{-4}
-6.852×10^{-1}	.999	1.000	-3.220×10^{-3}	-2.924×10^{-3}	-6.385×10^{-3}	1.402×10^{-4}	-3.862×10^{-2}	-2.430×10^{-2}	-5.029×10^{-2}	1.682×10^{-3}
-5.132×10^{-1}	.997	.999	-2.527×10^{-2}	-2.419×10^{-2}	-4.123×10^{-2}	-9.218×10^{-3}	-3.019×10^{-1}	-2.230×10^{-1}	-3.549×10^{-1}	-1.105×10^{-1}
-3.700×10^{-1}	.988	.993	-1.382×10^{-1}	-1.356×10^{-1}	-1.920×10^{-1}	-1.119×10^{-1}	-1.620	-1.333	-1.751	-1.325
-2.508×10^{-1}	.953	.959	-5.375×10^{-1}	-5.387×10^{-1}	-6.440×10^{-1}	-5.558×10^{-1}	-5.844	-5.427	-5.829	-6.119
-1.515×10^{-1}	.860	.862	-1.442	-1.453	-1.512	-1.511	-12.470	-13.000	-11.655	-13.126
-6.883×10^{-2}	.695	.694	-2.541	-2.537	-2.456	-2.542	-11.924	-13.216	-11.175	-11.813
0	.5	.5	-3.000	-2.992	-2.840	-2.948	0	1.421×10^{-14}	0	2.102×10^{-10}

TABLE 11.- IMPLICIT SPLINE SOLUTION TO BURGERS' EQUATION FOR $\nu = 1/24$, $\sigma = 0$, $\sigma_1 = 1.4$, AND 31 POINTS

η	Exact u	Spline calculated u	Exact u_η	Spline curve fit m	Finite-difference curve fit u_η	Spline calculated m	Exact $u_{\eta\eta}$	Spline curve fit M	Finite-difference curve fit $u_{\eta\eta}$	Spline calculated M
-5.000	1.000	1.000	-1.051×10^{-25}	-2.910×10^{-10}	----------	3.366×10^{-5}	-1.261×10^{-24}	-1.261×10^{-24}	----------	4.033×10^{-4}
-3.559	1.000	1.000	-3.369×10^{-18}	1.825×10^{-9}	-3.698×10^{-14}	-4.263×10^{-5}	-4.043×10^{-17}	-1.908×10^{-8}	-4.797×10^{-14}	-5.093×10^{-4}
-2.532	1.000	1.000	-7.678×10^{-13}	-1.517×10^{-8}	-3.393×10^{-10}	5.896×10^{-5}	-9.213×10^{-12}	9.166×10^{-8}	-6.601×10^{-10}	7.069×10^{-4}
-1.798	1.000	1.000	-5.121×10^{-9}	8.994×10^{-8}	-2.548×10^{-7}	-9.286×10^{-5}	-6.146×10^{-8}	-4.182×10^{-7}	-6.931×10^{-7}	-1.121×10^{-3}
-1.274	.999	1.000	-2.748×10^{-6}	-2.028×10^{-6}	-3.155×10^{-5}	1.818×10^{-4}	-3.297×10^{-5}	-3.114×10^{-6}	-1.188×10^{-4}	2.169×10^{-3}
-9.003×10^{-1}	.999	1.000	-2.439×10^{-4}	-1.726×10^{-4}	-1.070×10^{-2}	-4.706×10^{-4}	-2.927×10^{-3}	-3.405×10^{-4}	-5.438×10^{-3}	-5.658×10^{-3}
-6.334×10^{-1}	.999	1.000	-5.991×10^{-3}	-5.172×10^{-3}	-1.419×10^{-2}	2.039×10^{-3}	-7.182×10^{-2}	-3.513×10^{-2}	-9.295×10^{-2}	2.447×10^{-2}
-4.429×10^{-1}	.995	.998	-5.839×10^{-2}	-5.639×10^{-2}	-9.376×10^{-2}	-3.132×10^{-2}	-6.938×10^{-1}	-4.997×10^{-1}	-7.425×10^{-1}	-3.749×10^{-1}
-3.070×10^{-1}	.975	.982	-2.868×10^{-1}	2.873×10^{-1}	-.361	-2.668×10^{-1}	-3.273	-2.900	-3.183	-3.089
-2.099×10^{-1}	.925	.933	-8.271×10^{-1}	8.303×10^{-1}	-.901	-8.409×10^{-1}	-8.447	-8.301	-7.952	-3.742
-1.407×10^{-1}	.844	.850	-1.579	-1.580	-1.607	-1.613	-13.042	-13.335	-12.439	-13.553
-9.128×10^{-2}	.749	.753	-2.253	-2.253	-2.243	-2.293	-13.489	-13.859	-13.311	-13.958
-5.599×10^{-2}	.662	.665	-2.685	-2.685	-2.667	-2.723	-10.437	-10.627	-10.672	-10.788
-3.081×10^{-2}	.591	.593	-2.899	-2.899	-2.886	-2.948	-6.360	-6.425	-6.734	-6.576
-1.283×10^{-2}	.538	.539	-2.982	-2.982	-2.974	-3.033	-2.750	-2.760	-3.093	-2.844
0	.500	.500	-3.000	-3.000	-2.994	-3.051	0	-8.249×10^{-12}	2.157×10^{-11}	1.683×10^{-9}

TABLE 12.- IMPLICIT SPLINE SOLUTION TO BURGERS' EQUATION FOR $\nu = 1/24$, $\sigma = 0$, $\sigma_i = 1.6$, AND 31 POINTS

η	Exact u	Spline calculated u	Exact u_η	Spline curve fit m	Finite-difference curve fit u_η	Spline calculated m	Exact $u_{\eta\eta}$	Spline curve fit M	Finite-difference curve fit $u_{\eta\eta}$	Spline calculated M
-5.000	1.000	1.000	-1.051×10^{-25}	-4.516×10^{-8}	----------	-2.267×10^{-4}	-1.261×10^{-24}	-1.261×10^{-24}	----------	-2.721×10^{-3}
-3.121	1.000	.998	-6.482×10^{-16}	9.049×10^{-8}	-3.693×10^{-11}	2.838×10^{-4}	-7.778×10^{-15}	1.448×10^{-7}	-3.932×10^{-11}	3.266×10^{-3}
-1.948	1.000	.999	-8.448×10^{-10}	-2.663×10^{-7}	-3.902×10^{-7}	-3.495×10^{-4}	-1.014×10^{-8}	-7.536×10^{-7}	-6.650×10^{-7}	-4.347×10^{-3}
-1.215	.999	.999	-5.576×10^{-6}	-1.093×10^{-6}	-1.514×10^{-4}	5.888×10^{-4}	-6.691×10^{-5}	-1.504×10^{-6}	-4.116×10^{-4}	6.909×10^{-3}
-7.574×10^{-1}	.999	.999	-1.355×10^{-3}	-7.345×10^{-4}	-7.341×10^{-3}	-1.235×10^{-3}	-1.625×10^{-2}	-3.203×10^{-3}	-3.099×10^{-2}	-1.488×10^{-2}
-4.714×10^{-1}	.996	.999	-4.160×10^{-2}	-3.339×10^{-2}	-9.216×10^{-2}	4.731×10^{-3}	-4.958×10^{-1}	-2.252×10^{-1}	-5.623×10^{-1}	5.662×10^{-2}
-2.928×10^{-1}	.971	.981	-3.368×10^{-1}	-3.402×10^{-1}	-4.578×10^{-1}	-3.115×10^{-1}	-3.808	-3.211	-3.532	-3.598
-1.813×10^{-1}	.898	.908	-1.097	-1.105	-1.185	-1.130	-10.496	-10.498	-9.503	-11.087
-1.116×10^{-1}	.792	.800	-1.974	-1.972	-1.979	-2.025	-13.853	-14.400	-13.306	-14.584
-6.811×10^{-2}	.693	.698	-2.549	-2.549	-2.532	-2.614	-11.852	-12.114	-12.088	-12.471
-4.093×10^{-2}	.620	.623	-2.826	-2.826	-2.814	-2.900	-8.165	-8.246	-8.631	-8.606
-2.395×10^{-2}	.571	.573	-2.939	-2.939	-2.933	-3.018	-5.033	-5.053	-5.427	-5.311
-1.334×10^{-2}	.539	.541	-2.981	-2.981	-2.978	-3.062	-2.858	-2.863	-3.131	-3.017
-6.722×10^{-3}	.520	.521	-2.995	-2.995	-2.994	-3.077	-1.449	-1.449	-1.625	-1.529
-2.584×10^{-3}	.507	.508	-2.999	-2.999	-2.999	-3.082	-5.580×10^{-1}	-5.581×10^{-1}	-6.695×10^{-1}	-5.892×10^{-1}
0	.500	.500	-3.000	-3.000	-2.999	-3.083	0	-1.056×10^{-9}	-5.319×10^{-10}	1.813×10^{-9}

TABLE 13.- IMPLICIT SPLINE SOLUTION TO BURGERS' EQUATION FOR $\nu = 1/24$, $\sigma = 0$, $\sigma = 1.8$, AND 31 POINTS

η	Exact u	Spline calculated u	Exact u_η	Spline curve fit m	Finite-difference curve fit u_η	Spline calculated m	Exact $u_{\eta\eta}$	Spline curve fit M	Finite-difference curve fit $u_{\eta\eta}$	Spline calculated M
-5.000	1.000	1.000	-1.051×10^{-25}	1.411×10^{-4}	----------	1.602×10^{-2}	-1.261×10^{-24}	-1.261×10^{-24}	----------	1.923×10^{-1}
-2.776	1.000	1.172	-4.097×10^{-14}	-2.828×10^{-4}	-4.849×10^{-9}	-1.357×10^{-2}	-4.916×10^{-13}	-3.828×10^{-4}	-4.360×10^{-9}	-2.190×10^{-1}
-1.541	1.000	1.113	-1.117×10^{-7}	8.025×10^{-4}	-3.269×10^{-5}	1.842×10^{-2}	-1.341×10^{-6}	2.143×10^{-3}	-5.295×10^{-5}	2.709×10^{-1}
-8.553×10^{-1}	1.000	1.136	-4.185×10^{-4}	-2.493×10^{-3}	-5.619×10^{-3}	-2.627×10^{-2}	-5.022×10^{-3}	-1.176×10^{-2}	-1.624×10^{-2}	-4.013×10^{-1}
-4.746×10^{-1}	.997	1.127	-4.008×10^{-2}	-1.891×10^{-2}	-1.169×10^{-1}	5.504×10^{-2}	-4.778×10^{-1}	-7.451×10^{-2}	-5.684×10^{-1}	8.285×10^{-1}
-2.632×10^{-1}	.959	1.124	-4.693×10^{-1}	-4.853×10^{-1}	-6.511×10^{-1}	-2.448×10^{-1}	-5.172	-4.338	-4.485	-3.666
-1.458×10^{-1}	.852	1.026	-1.514	-1.518	-1.582	-1.781	-12.786	-13.253	-11.378	-22.504
-8.063×10^{-2}	.725	.857	-2.394	-2.391	-2.374	-3.489	-12.909	-13.554	-12.927	-29.937
-4.444×10^{-2}	.630	.713	-2.796	-2.796	-2.778	-4.442	-8.742	-8.832	-9.406	-22.725
-2.435×10^{-2}	.572	.619	-2.937	-2.937	-2.929	-4.809	-5.112	-5.150	-5.663	-13.840
-1.319×10^{-2}	.539	.565	-2.981	-2.981	-2.979	-4.930	-2.826	-2.825	-3.167	-7.750
-6.998×10^{-3}	.521	.534	-2.995	-2.995	-2.994	-4.967	-1.508	-1.510	-1.704	-4.152
-3.559×10^{-3}	.511	.517	-2.999	-2.999	-2.998	-4.978	-7.683×10^{-1}	-7.678×10^{-1}	-8.780×10^{-1}	-2.117
-1.649×10^{-3}	.505	.508	-2.999	-2.999	-2.999	-4.981	-3.562×10^{-1}	-3.563×10^{-1}	-4.173×10^{-1}	-9.819×10^{-1}
-5.888×10^{-4}	.502	.503	-3.000	-3.000	-3.000	-4.982	-1.272×10^{-1}	-1.269×10^{-1}	-1.611×10^{-1}	-3.506×10^{-1}
0	.500	.500	-3.000	-3.000	-3.000	-4.982	0	-1.964×10^{-8}	-1.025×10^{-8}	1.130×10^{-4}

TABLE 14.- IMPLICIT SPLINE SOLUTION TO BURGERS' EQUATION FOR $\nu = 1/24$, $\sigma = 0$, $\sigma_i = 1.4$, AND 19 POINTS

η	Exact u	Spline calculated u	Exact u_η	Spline curve fit m	Finite-difference curve fit u_η	Spline calculated m	Exact $u_{\eta\eta}$	Spline curve fit M	Finite-difference curve fit $u_{\eta\eta}$	Spline calculated M
-5.000	1.000	1.000	-1.051×10^{-25}	1.841×10^{-5}	----------	6.944×10^{-4}	-1.261×10^{-24}	-1.261×10^{-24}	----------	8.333×10^{-3}
-3.496	1.000	1.003	-7.188×10^{-18}	-3.686×10^{-5}	-1.241×10^{-13}	-8.646×10^{-4}	-8.626×10^{-17}	-7.367×10^{-5}	-1.645×10^{-13}	-1.041×10^{-2}
-2.423	1.000	1.001	-2.813×10^{-12}	1.133×10^{-4}	-1.752×10^{-9}	1.180×10^{-3}	-3.375×10^{-11}	3.538×10^{-4}	-3.265×10^{-9}	1.423×10^{-2}
-1.657	1.000	1.003	-2.760×10^{-8}	-3.622×10^{-4}	-1.734×10^{-6}	-1.832×10^{-3}	-3.312×10^{-7}	-1.596×10^{-3}	-4.519×10^{-6}	-2.209×10^{-2}
-1.111	1.000	1.001	-1.951×10^{-5}	1.152×10^{-3}	-2.615×10^{-4}	3.438×10^{-3}	-2.341×10^{-4}	7.136×10^{-3}	-9.457×10^{-4}	4.138×10^{-2}
-7.205×10^{-1}	1.000	1.002	-2.108×10^{-3}	-5.034×10^{-3}	-1.018×10^{-2}	-8.509×10^{-3}	-2.528×10^{-2}	-3.884×10^{-2}	-4.988×10^{-2}	-1.026×10^{-1}
-4.420×10^{-1}	.995	1.002	-5.906×10^{-2}	-3.590×10^{-2}	-1.430×10^{-1}	-3.353×10^{-2}	-7.017×10^{-1}	-1.828×10^{-1}	-9.040×10^{-1}	4.045×10^{-1}
-2.432×10^{-1}	.949	.966	-5.835×10^{-1}	-6.087×10^{-1}	-8.267×10^{-1}	-6.582×10^{-1}	-6.284	-5.579	-5.974	-7.363
-1.013×10^{-1}	.771	.774	-2.117	-2.138	-2.083	-2.216	-13.782	-15.981	-11.739	-14.588
0	.500	.500	-3.000	-2.948	-2.678	-2.954	0	-1.137×10^{-13}	0	2.432×10^{-9}

TABLE 15.- IMPLICIT SPLINE SOLUTION TO BURGERS' EQUATION FOR $\nu = 1/24$, $\sigma = 0$, $\sigma_i = 1.6$, AND 19 POINTS

η	Exact u	Spline calculated u	Exact u_η	Spline curve fit m	Finite-difference curve fit u_η	Spline calculated m	Exact $u_{\eta\eta}$	Spline curve fit M	Finite-difference curve fit $u_{\eta\eta}$	Spline calculated M
-5.000	1.000	1.000	-1.051×10^{-25}	-6.033×10^{-8}	----------	1.514×10^{-4}	-1.261×10^{-24}	-1.261×10^{-24}	----------	1.817×10^{-3}
-3.095	1.000	1.001	-8.849×10^{-16}	5.148×10^{-7}	-6.041×10^{-11}	-1.649×10^{-4}	-1.062×10^{-14}	2.876×10^{-6}	-6.344×10^{-11}	-2.150×10^{-3}
-1.906	1.000	1.000	-1.401×10^{-9}	-4.979×10^{-6}	-7.207×10^{-7}	2.496×10^{-4}	-1.681×10^{-8}	-3.049×10^{-5}	-1.211×10^{-6}	2.848×10^{-3}
-1.163	1.000	1.001	-1.044×10^{-5}	2.496×10^{-5}	-3.018×10^{-4}	-3.649×10^{-4}	-1.253×10^{-4}	1.877×10^{-4}	-8.092×10^{-4}	-4.503×10^{-3}
-6.988×10^{-1}	1.000	1.001	-2.736×10^{-3}	-1.839×10^{-3}	-1.529×10^{-2}	7.965×10^{-4}	-3.282×10^{-2}	-1.154×10^{-2}	-6.378×10^{-2}	9.509×10^{-3}
-4.089×10^{-1}	.993	1.001	-8.744×10^{-2}	-7.294×10^{-2}	-1.918×10^{-1}	-2.926×10^{-3}	-1.034	-5.620×10^{-1}	-1.154	-3.519×10^{-2}
-2.278×10^{-1}	.939	.956	-6.872×10^{-1}	-7.096×10^{-1}	-8.785×10^{-1}	-7.267×10^{-1}	-7.240	-6.944	-6.432	-7.959
-1.147×10^{-1}	.798	.808	-1.930	-1.929	-1.952	-2.023	-13.832	-15.205	-12.547	-14.975
-4.412×10^{-2}	.629	.632	-2.799	-2.793	-2.725	-2.876	-8.690	-9.484	-9.357	-9.172
0	.500	.500	-3.000	-2.932	-2.932	-3.079	0	4.533×10^{-12}	0	1.774×10^{-9}

TABLE 16.- IMPLICIT SPLINE SOLUTION TO BURGERS' EQUATION FOR $\nu = 1/8$, $\sigma = 2.0$, $\sigma_1 = 1.4$, AND 15 POINTS

η	Exact u	Spline calculated u	Exact u_η	Spline curve fit m	Finite-difference curve fit u_η	Spline calculated m	Exact $u_{\eta\eta}$	Spline curve fit M	Finite-difference curve fit $u_{\eta\eta}$	Spline calculated M
-5.000	1.000	1.000	-8.245×10^{-9}	-7.391×10^{-6}	----------	1.625×10^{-6}	-3.298×10^{-8}	-3.298×10^{-8}	----------	6.501×10^{-6}
-3.419	1.000	1.000	-4.586×10^{-6}	1.910×10^{-5}	-5.373×10^{-5}	-5.764×10^{-6}	-1.834×10^{-5}	5.771×10^{-5}	-6.708×10^{-5}	-2.258×10^{-5}
-2.295	1.000	1.000	-4.176×10^{-4}	-4.035×10^{-4}	-1.853×10^{-3}	2.276×10^{-5}	-1.670×10^{-3}	-1.101×10^{-3}	-3.123×10^{-3}	9.298×10^{-5}
-1.487	.997	1.000	-1.040×10^{-2}	-8.757×10^{-3}	-2.442×10^{-2}	-1.639×10^{-4}	-4.140×10^{-2}	-2.395×10^{-2}	-5.295×10^{-2}	-6.528×10^{-4}
-9.119×10^{-1}	.975	.980	-9.897×10^{-2}	-9.843×10^{-2}	-1.489×10^{-1}	-1.062×10^{-1}	-3.756×10^{-1}	-3.217×10^{-1}	-3.803×10^{-1}	-4.083×10^{-1}
-5.017×10^{-1}	.881	.879	-4.177×10^{-1}	-4.258×10^{-1}	-4.611×10^{-1}	-4.521×10^{-1}	-1.275	-1.363	-1.142	-1.372
-2.089×10^{-1}	.698	.691	-8.438×10^{-1}	-8.393×10^{-1}	-8.134×10^{-1}	-8.275×10^{-1}	-1.334	-1.542	-1.265	-1.265
0	.500	.500	-1.000	-9.982×10^{-1}	-9.456×10^{-1}	-9.578×10^{-1}	0	-1.901×10^{-13}	8.135×10^{-14}	1.067×10^{-11}

TABLE 17.- IMPLICIT SPLINE SOLUTION TO BURGERS' EQUATION FOR $\nu = 1/8$, $\sigma = 2.0$, $\sigma_1 = 1.6$, AND 15 POINTS

η	Exact u	Spline calculated u	Exact u_η	Spline curve fit m	Finite-difference curve fit u_η	Spline calculated m	Exact $u_{\eta\eta}$	Spline curve fit M	Finite-difference curve fit $u_{\eta\eta}$	Spline calculated M
-5.000	1.000	1.000	-8.245×10^{-9}	4.147×10^{-5}	----------	4.270×10^{-4}	-3.298×10^{-8}	-3.298×10^{-8}	----------	1.708×10^{-3}
-3.051	1.000	1.001	-2.006×10^{-5}	-1.543×10^{-4}	-3.287×10^{-4}	-1.349×10^{-3}	-8.024×10^{-5}	-4.078×10^{-4}	-3.346×10^{-4}	-5.409×10^{-3}
-1.833	.999	1.000	-2.611×10^{-3}	-1.238×10^{-3}	-1.061×10^{-2}	5.329×10^{-3}	-1.043×10^{-2}	-2.176×10^{-3}	-1.655×10^{-2}	2.133×10^{-2}
-1.013	.986	.994	-5.329×10^{-2}	-5.097×10^{-2}	-9.767×10^{-2}	-4.533×10^{-2}	-2.074×10^{-1}	-1.529×10^{-1}	-2.124×10^{-1}	-1.793×10^{-1}
-5.977×10^{-1}	.916	.922	-3.073×10^{-1}	-3.143×10^{-1}	-3.616×10^{-1}	-3.347×10^{-1}	-1.023	-1.024	-8.990×10^{-1}	-1.129
-3.011×10^{-1}	.769	.768	-7.099×10^{-1}	-7.078×10^{-1}	-7.069×10^{-1}	-7.204×10^{-1}	-1.529	-1.692	-1.429	-1.546
-1.157×10^{-1}	.613	.612	-9.483×10^{-1}	-9.471×10^{-1}	-9.275×10^{-1}	-9.395×10^{-1}	-8.627×10^{-1}	-9.196×10^{-1}	-9.506×10^{-1}	-8.456×10^{-1}
0	.500	.500	-1.000	-1.000	-9.825×10^{-1}	-9.882×10^{-1}	0	5.498×10^{-13}	0	3.188×10^{-11}

TABLE 18.- IMPLICIT SPLINE SOLUTION TO BURGERS' EQUATION FOR $\nu = 1/8$, $\sigma = 2.0$, $\sigma_1 = 1.8$, AND 15 POINTS

η	Exact u	Spline calculated u	Exact u_η	Spline curve fit m	Finite-difference curve fit u_η	Spline calculated m	Exact $u_{\eta\eta}$	Spline curve fit M	Finite-difference curve fit $u_{\eta\eta}$	Spline calculated M
-5.000	1.000	1.000	-8.245×10^{-9}	1.838×10^{-4}	----------	9.151×10^{-4}	-3.298×10^{-8}	-3.298×10^{-8}	----------	3.660×10^{-3}
-2.739	1.000	1.003	-6.968×10^{-5}	-7.559×10^{-4}	-1.342×10^{-3}	-2.796×10^{-3}	-2.787×10^{-4}	-1.921×10^{-3}	-1.181×10^{-3}	-1.124×10^{-2}
-1.484	.997	1.001	-1.050×10^{-2}	-4.239×10^{-3}	-3.624×10^{-2}	1.076×10^{-2}	-4.179×10^{-2}	-6.278×10^{-3}	-5.443×10^{-2}	4.316×10^{-2}
-7.874×10^{-1}	.959	.972	-1.577×10^{-1}	-1.647×10^{-1}	-2.301×10^{-1}	-1.725×10^{-1}	-5.789×10^{-1}	-5.266×10^{-1}	-5.020×10^{-1}	-6.518×10^{-1}
-4.004×10^{-1}	.832	.837	-5.584×10^{-1}	-5.591×10^{-1}	-5.800×10^{-1}	-5.827×10^{-1}	-1.484	-1.612	-1.306	-1.573
-1.855×10^{-1}	.677	.679	-8.740×10^{-1}	-8.720×10^{-1}	-8.587×10^{-1}	-8.827×10^{-1}	-1.241	-1.345	-1.288	-1.262
-6.624×10^{-2}	.566	.566	-9.826×10^{-1}	-9.827×10^{-1}	-9.732×10^{-1}	-9.887×10^{-1}	-5.177×10^{-1}	-5.199×10^{-1}	-6.319×10^{-1}	-5.241×10^{-1}
0	.500	.500	-1.000	-9.999×10^{-1}	-9.942×10^{-1}	-1.006	0	-1.751×10^{-12}	0	5.919×10^{-11}

TABLE 19.- IMPLICIT SPLINE SOLUTION TO BURGERS' EQUATION FOR $\nu = 1/24$, $\sigma = 5.0$, $\sigma_1 = 1.4$, AND 31 POINTS

η	Exact u	Spline calculated u	Exact u_η	Spline curve fit m	Finite-difference curve fit u_η	Spline calculated m	Exact $u_{\eta\eta}$	Spline curve fit M	Finite-difference curve fit $u_{\eta\eta}$	Spline calculated M
-5.000	1.000	1.000	-1.051×10^{-25}	-2.911×10^{-10}	----------	1.151×10^{-6}	-1.261×10^{-24}	----------	-5.040×10^{-14}	1.382×10^{-5}
-3.559	1.000	1.000	-3.369×10^{-18}	1.825×10^{-9}	-3.698×10^{-14}	-3.118×10^{-6}	-4.043×10^{-17}	1.059×10^{-8}	-4.797×10^{-14}	-3.519×10^{-5}
-2.532	1.000	1.000	-7.678×10^{-13}	-1.517×10^{-8}	-3.393×10^{-10}	6.007×10^{-6}	-9.213×10^{-12}	-9.658×10^{-8}	-6.601×10^{-10}	8.136×10^{-5}
-1.798	1.000	1.000	-5.121×10^{-9}	3.944×10^{-8}	-2.548×10^{-7}	-1.843×10^{-5}	-6.145×10^{-8}	6.470×10^{-7}	-6.931×10^{-7}	-2.099×10^{-4}
-1.274	.999	1.000	-2.748×10^{-6}	-2.028×10^{-6}	-3.155×10^{-5}	4.970×10^{-5}	-3.297×10^{-5}	-1.290×10^{-5}	-1.188×10^{-4}	6.042×10^{-4}
-9.003×10^{-1}	.999	1.000	-2.439×10^{-4}	-1.726×10^{-4}	-1.070×10^{-2}	-1.827×10^{-4}	-2.927×10^{-3}	-1.151×10^{-3}	-5.438×10^{-3}	-2.190×10^{-3}
-6.334×10^{-1}	.999	1.000	-5.991×10^{-3}	-5.172×10^{-3}	-1.419×10^{-2}	1.097×10^{-3}	-7.183×10^{-2}	-4.172×10^{-2}	-9.295×10^{-2}	1.317×10^{-2}
-4.429×10^{-1}	.995	.998	-5.839×10^{-2}	-5.639×10^{-2}	-9.376×10^{-2}	-3.829×10^{-2}	-.694	-.536	-.742	-.457
-3.070×10^{-1}	.975	.980	-2.868×10^{-1}	-.287	-.361	-2.787×10^{-1}	-3.273	-2.990	-3.183	-3.215
-2.099×10^{-1}	.925	.930	-8.271×10^{-1}	-.830	-.901	-8.488×10^{-1}	-8.447	-8.420	-7.951	-8.763
-1.407×10^{-1}	.844	.847	-1.579	-1.580	-1.607	-1.608	-13.043	-13.444	-12.439	-13.393
-9.128×10^{-2}	.749	.751	-2.253	-2.253	-2.243	-2.275	-13.489	-13.908	-13.311	-13.704
-5.599×10^{-2}	.662	.663	-2.685	-2.684	-2.667	-2.702	-10.437	-10.645	-10.672	-10.561
-3.081×10^{-2}	.591	.592	-2.899	-2.899	-2.886	-2.916	-6.360	-6.431	-6.734	-6.430
-1.283×10^{-2}	.538	.539	-2.982	-2.982	-2.974	-2.998	-2.750	-2.765	-3.093	-2.779
0	.500	.500	-3.000	-3.000	-2.994	-3.0163	0	-8.253×10^{-12}	2.157×10^{-11}	4.667×10^{-10}

TABLE 20.- IMPLICIT SPLINE SOLUTION TO BURGERS' EQUATION FOR $\nu = 1/24$, $\sigma = 5.0$, $\sigma_i = 1.6$, AND 31 POINTS

η	Exact u	Spline calculated u	Exact u_η	Spline curve fit m	Finite-difference curve fit u_η	Spline calculated m	Exact $u_{\eta\eta}$	Spline curve fit M	Finite-difference curve fit $u_{\eta\eta}$	Spline calculated M
-5.000	1.000	1.000	-1.051×10^{-25}	9.752×10^{-9}	----------	1.952×10^{-5}	-1.261×10^{-24}	-1.261×10^{-24}	----------	2.343×10^{-4}
-3.121	1.000	1.000	-6.482×10^{-16}	-8.197×10^{-8}	-3.693×10^{-11}	-7.599×10^{-5}	-7.778×10^{-15}	-4.587×10^{-7}	-3.931×10^{-11}	-7.120×10^{-4}
-1.948	1.000	1.000	-8.448×10^{-10}	7.803×10^{-7}	-3.902×10^{-7}	1.170×10^{-4}	-1.014×10^{-8}	4.795×10^{-6}	-6.650×10^{-7}	1.683×10^{-3}
-1.215	1.000	1.000	-5.576×10^{-6}	-7.365×10^{-6}	-1.514×10^{-4}	-3.764×10^{-4}	-6.691×10^{-5}	-4.767×10^{-5}	-4.116×10^{-4}	-4.279×10^{-3}
-7.574×10^{-1}	1.000	1.000	-1.355×10^{-3}	-8.335×10^{-4}	-7.341×10^{-3}	1.096×10^{-3}	-1.625×10^{-2}	-5.015×10^{-3}	-3.099×10^{-2}	1.330×10^{-2}
-4.714×10^{-1}	.996	1.000	-4.160×10^{-2}	-3.513×10^{-2}	-9.216×10^{-2}	-5.797×10^{-3}	-4.958×10^{-1}	-2.744×10^{-1}	5.623×10^{-1}	-6.946×10^{-2}
-2.928×10^{-1}	.971	.979	-3.368×10^{-1}	-3.405×10^{-1}	-4.578×10^{-1}	-3.291×10^{-1}	-3.808	-3.370	-3.532	-3.789
-1.813×10^{-1}	.898	.905	-1.099	-1.041	-1.184	-1.136	-10.496	-10.672	-9.503	-11.056
-1.116×10^{-1}	.792	.797	-1.974	-1.972	-1.979	-2.012	-13.853	-14.488	-13.306	-14.347
-6.811×10^{-2}	.694	.697	-2.549	-2.549	-2.532	-2.588	-11.852	-12.143	-12.088	-12.212
-4.093×10^{-2}	.620	.622	-2.826	-2.826	-2.814	-2.868	-8.165	-8.254	-8.631	-8.412
-2.395×10^{-2}	.571	.572	-2.939	-2.939	-2.933	-2.983	-5.033	-5.055	-5.427	-5.188
-1.335×10^{-2}	.540	.540	-2.981	-2.981	-2.978	-3.026	-2.858	-2.863	-3.131	-2.947
-6.722×10^{-3}	.520	.520	-2.995	-2.995	-2.994	-3.041	-1.449	-1.450	-1.625	-1.494
-2.584×10^{-3}	.508	.508	-2.999	-2.999	-2.999	-3.045	-5.580×10^{-1}	-5.582×10^{-1}	-6.695×10^{-1}	-5.754×10^{-1}
0	.500	.500	-3.000	-3.000	-2.999	-3.046	0	-1.057×10^{-9}	-5.319×10^{-10}	8.488×10^{-10}

TABLE 21.- IMPLICIT SPLINE SOLUTION TO BURGERS' EQUATION FOR $\nu = 1/24$, $\sigma = 5.0$, $\sigma_i = 1.8$, AND 31 POINTS

η	Exact u	Spline calculated u	Exact u_η	Spline curve fit m	Finite-difference curve fit u_η	Spline calculated m	Exact $u_{\eta\eta}$	Spline curve fit M	Finite-difference curve fit $u_{\eta\eta}$	Spline calculated M
-5.000	1.000	1.000	-1.051×10^{-25}	2.080×10^{-6}	----------	4.136×10^{-4}	-1.261×10^{-24}	-1.261×10^{-24}	----------	4.964×10^{-3}
-2.776	1.000	1.002	-4.097×10^{-14}	-2.106×10^{-5}	-4.849×10^{-9}	-9.968×10^{-4}	-4.916×10^{-13}	-1.157×10^{-4}	-4.360×10^{-9}	-1.202×10^{-2}
-1.541	1.000	1.000	-1.117×10^{-7}	2.111×10^{-4}	-3.270×10^{-5}	2.439×10^{-3}	-1.341×10^{-6}	1.282×10^{-3}	-5.295×10^{-5}	2.927×10^{-2}
-8.553×10^{-1}	1.000	1.002	-4.185×10^{-4}	-1.384×10^{-3}	-5.619×10^{-3}	-6.299×10^{-3}	-5.022×10^{-3}	-9.794×10^{-3}	-1.624×10^{-2}	-7.589×10^{-2}
-4.746×10^{-1}	.997	1.001	-4.008×10^{-2}	-2.402×10^{-2}	-1.169×10^{-1}	2.244×10^{-2}	-4.778×10^{-1}	-1.431×10^{-1}	-5.684×10^{-1}	2.699×10^{-1}
-2.632×10^{-1}	.959	.974	-4.693×10^{-1}	-4.846×10^{-1}	-6.511×10^{-1}	-4.818×10^{-1}	-5.172	-4.613	-4.485	-5.476
-1.458×10^{-1}	.852	.862	-1.514	-1.516	-1.582	-1.576	-12.786	-13.467	-11.378	-13.370
-8.063×10^{-2}	.725	.731	-2.394	-2.391	-2.374	-2.458	-12.909	-13.614	-12.927	-13.614
-4.444×10^{-2}	.630	.634	-2.796	-2.796	-2.778	-2.870	-8.742	-8.845	-9.406	-9.219
-2.435×10^{-2}	.572	.574	-2.937	-2.937	-2.929	-3.017	-5.112	-5.152	-5.663	-5.398
-1.319×10^{-2}	.539	.541	-2.981	-2.981	-2.979	-3.064	-2.826	-2.826	-3.167	-2.985
-6.998×10^{-3}	.521	.521	-2.995	-2.995	-2.994	-3.078	-1.508	-1.510	-1.704	-1.593
-3.559×10^{-3}	.511	.511	-2.999	-2.999	-2.998	-3.082	-7.683×10^{-1}	-7.677×10^{-1}	-8.780×10^{-1}	-8.118×10^{-1}
-1.649×10^{-3}	.505	.505	-2.999	-2.999	-2.999	-3.083	-3.562×10^{-1}	-3.564×10^{-1}	-4.173×10^{-1}	-3.763×10^{-1}
-5.888×10^{-4}	.502	.502	-2.999	-2.999	-3.000	-3.084	-1.272×10^{-1}	-1.271×10^{-1}	-1.611×10^{-1}	-1.344×10^{-1}
0	.500	.500	-3.000	-3.000	-3.000	-3.084	0	-2.023×10^{-8}	-1.025×10^{-8}	1.596×10^{-8}

TABLE 22.- IMPLICIT SPLINE SOLUTION TO BURGERS' EQUATION FOR $\nu = 1/24$, $\sigma = 5.0$, $\sigma_1 = 1.4$, AND 19 POINTS

η	Exact u	Spline calculated u	Exact u_η	Spline curve fit m	Finite-difference curve fit u_η	Spline calculated m	Exact $u_{\eta\eta}$	Spline curve fit M	Finite-difference curve fit $u_{\eta\eta}$	Spline calculated M
-5.000	1.000	1.000	-1.051×10^{-25}	3.848×10^{-7}	----------	2.383×10^{-6}	-1.261×10^{-24}	-1.261×10^{-24}	----------	2.859×10^{-5}
-3.496	1.000	1.000	-7.188×10^{-18}	-2.529×10^{-6}	-1.241×10^{-13}	-2.497×10^{-6}	-8.626×10^{-17}	-1.458×10^{-5}	-1.645×10^{-13}	-5.302×10^{-5}
-2.423	1.000	1.000	-2.813×10^{-12}	2.201×10^{-5}	-1.752×10^{-9}	1.731×10^{-5}	-3.375×10^{-11}	1.384×10^{-4}	-3.265×10^{-9}	1.530×10^{-4}
-1.657	1.000	1.000	-2.760×10^{-8}	-1.384×10^{-4}	-1.734×10^{-5}	-2.620×10^{-5}	-3.312×10^{-7}	-9.764×10^{-4}	-4.519×10^{-6}	-3.803×10^{-4}
-1.111	1.000	1.000	-1.951×10^{-5}	6.639×10^{-4}	-2.615×10^{-4}	9.329×10^{-5}	-2.341×10^{-4}	5.546×10^{-3}	-9.451×10^{-4}	1.061×10^{-3}
-7.205×10^{-1}	1.000	1.000	-2.108×10^{-3}	-4.231×10^{-3}	-1.018×10^{-2}	-3.071×10^{-4}	-2.528×10^{-2}	-3.813×10^{-2}	-4.988×10^{-2}	-3.726×10^{-3}
-4.420×10^{-1}	.995	1.000	-5.906×10^{-2}	-3.993×10^{-2}	-1.430×10^{-1}	1.703×10^{-3}	-7.017×10^{-1}	-2.583×10^{-1}	-9.040×10^{-1}	2.042×10^{-2}
-2.432×10^{-1}	.949	.955	-5.835×10^{-1}	-6.118×10^{-1}	-8.267×10^{-1}	-7.014×10^{-1}	-6.284	-5.960	-5.974	-7.666
-1.013×10^{-1}	.771	.763	-2.117	-2.134	-2.083	-2.147	-13.728	-15.387	-11.739	-13.559
0	.500	.500	-3.000	-2.947	-2.678	-2.819	0	-1.421×10^{-13}	0	5.907×10^{-10}

TABLE 23.- IMPLICIT SPLINE SOLUTION TO BURGERS' EQUATION FOR $\nu = 1/24$, $\sigma = 5.0$, $\sigma_1 = 1.6$, AND 19 POINTS

η	Exact u	Spline calculated u	Exact u_η	Spline curve fit m	Finite-difference curve fit u_η	Spline calculated m	Exact $u_{\eta\eta}$	Spline curve fit M	Finite-difference curve fit $u_{\eta\eta}$	Spline calculated M
-5.000	1.000	1.000	-1.051×10^{-25}	-6.033×10^{-8}	----------	1.353×10^{-4}	-1.261×10^{-24}	-1.261×10^{-24}	----------	1.623×10^{-3}
-3.095	1.000	1.000	-8.849×10^{-16}	5.148×10^{-7}	-6.041×10^{-11}	-3.271×10^{-4}	-1.062×10^{-14}	2.876×10^{-6}	-6.344×10^{-11}	-3.936×10^{-3}
-1.096	1.000	1.000	-1.401×10^{-9}	-4.979×10^{-6}	-7.207×10^{-7}	8.011×10^{-4}	-1.681×10^{-8}	-3.049×10^{-5}	-1.211×10^{-6}	9.607×10^{-3}
-1.163	1.000	1.001	-1.044×10^{-5}	2.496×10^{-5}	-3.018×10^{-4}	-2.041×10^{-3}	-1.253×10^{-4}	1.877×10^{-4}	-8.092×10^{-4}	-2.453×10^{-2}
-6.988×10^{-1}	1.000	1.000	-2.736×10^{-3}	-1.839×10^{-3}	-1.529×10^{-2}	6.251×10^{-3}	-3.282×10^{-2}	-1.154×10^{-2}	-6.378×10^{-2}	7.502×10^{-2}
-4.089×10^{-1}	.993	.999	-8.744×10^{-2}	-7.294×10^{-2}	-1.918×10^{-1}	-3.201×10^{-2}	-1.034	-5.620×10^{-1}	-1.154	-3.837×10^{-1}
-2.278×10^{-1}	.939	.949	-6.872×10^{-1}	-7.096×10^{-1}	-8.785×10^{-1}	-7.532×10^{-1}	-7.240	-6.944	-6.432	-8.120
-1.147×10^{-1}	.798	.800	-1.930	-1.929	-1.952	-1.992	-13.832	-15.205	-12.547	-14.369
-4.412×10^{-2}	.629	.629	-2.799	-2.793	-2.725	-2.797	-8.690	-9.484	-9.357	-8.661
0	.500	.500	-3.000	-3.001	-2.932	-2.987	0	4.533×10^{-12}	0	4.864×10^{-9}

TABLE 24.- IMPLICIT SPLINE SOLUTION TO BURGERS' EQUATION FOR $\nu = 1/24$, $\sigma = 5.0$, $\sigma_1 = 1.8$, AND 19 POINTS

η	Exact u	Spline calculated u	Exact u_η	Spline curve fit m	Finite-difference curve fit u_η	Spline calculated m	Exact $u_{\eta\eta}$	Spline curve fit M	Finite-difference curve fit $u_{\eta\eta}$	Spline calculated M
-5.000	1.000	1.000	-1.051×10^{-25}	2.791×10^{-6}	----------	4.393×10^{-4}	-1.261×10^{-24}	-1.261×10^{-24}	----------	5.212×10^{-3}
-2.765	1.000	1.003	-4.668×10^{-14}	-2.840×10^{-5}	-5.912×10^{-9}	-1.058×10^{-3}	-5.602×10^{-13}	-1.559×10^{-4}	-5.291×10^{-9}	-1.216×10^{-2}
-1.524	1.000	1.000	-1.369×10^{-7}	2.864×10^{-4}	-4.151×10^{-5}	2.589×10^{-3}	-1.643×10^{-6}	1.736×10^{-3}	-6.688×10^{-5}	3.107×10^{-2}
-8.350×10^{-1}	1.000	1.002	-5.338×10^{-4}	-1.866×10^{-3}	-7.288×10^{-3}	-6.676×10^{-3}	-6.405×10^{-3}	-1.321×10^{-2}	-2.097×10^{-2}	-8.046×10^{-2}
-4.524×10^{-1}	.996	1.001	-5.218×10^{-2}	-3.091×10^{-2}	-1.517×10^{-1}	2.367×10^{-2}	-6.207×10^{-1}	-1.823×10^{-1}	-7.339×10^{-1}	2.848×10^{-1}
-2.400×10^{-1}	.947	.962	-6.039×10^{-1}	-6.297×10^{-1}	-8.158×10^{-1}	-6.518×10^{-1}	-6.477	-5.976	-5.519	-7.232
-1.220×10^{-1}	.812	.819	-1.830	-1.828	-1.868	-1.905	-13.714	-14.922	-12.326	-14.630
-5.655×10^{-2}	.663	.667	-2.679	-2.675	-2.635	-2.735	-10.510	-11.199	-11.095	-10.944
-2.019×10^{-2}	.560	.561	-2.956	-2.956	-2.932	-3.014	-4.277	-4.298	-5.252	-4.446
0	.500	.500	-3.000	-2.999	-2.985	-3.059	0	1.856×10^{-11}	0	2.415×10^{-8}

TABLE 25.- COMPARISON OF SPLINE AND FINITE-DIFFERENCE CURVE FITS OF THE EXACT SOLUTION TO BURGERS' EQUATION FOR $\nu = 1/8$, $\sigma = 0$, AND 51 EQUALLY SPACED POINTS

η	Exact u	Spline curve fit $\left(u - \frac{1}{2}\right)m$	Spline curve fit $\tilde{m}$	Exact $\left(u - \frac{1}{2}\right)u_\eta$	Finite-difference curve fit $\left(u - \frac{1}{2}\right)u_\eta$	Finite-difference curve fit $\frac{d}{d\eta}\frac{u^2}{2} - \frac{1}{2}u_\eta$
-5.0	0.9999999980	0	0	-4.12231×10^{-9}	----------	----------
-4.8	.9999999950	-8.91817×10^{-9}	-1.07708×10^{-8}	-9.17436×10^{-9}	-1.01850×10^{-8}	-1.01850×10^{-8}
-4.6	.9999999900	-2.04316×10^{-8}	-2.59096×10^{-8}	-2.04179×10^{-8}	-2.26687×10^{-8}	-2.26688×10^{-8}
-4.4	.9999999770	-4.53333×10^{-8}	-5.76708×10^{-8}	-4.54409×10^{-8}	-5.04462×10^{-8}	-5.04463×10^{-8}
-4.2	.9999999490	-1.00921×10^{-7}	-1.28429×10^{-7}	-1.01131×10^{-7}	-1.12267×10^{-7}	-1.12268×10^{-7}
-4.0	.9999998870	-2.24592×10^{-7}	-2.85815×10^{-7}	-2.25070×10^{-7}	-2.49856×10^{-7}	-2.49856×10^{-7}
-3.8	.9999997500	-4.99854×10^{-7}	-6.36108×10^{-7}	-5.00903×10^{-7}	-5.56073×10^{-7}	-5.56074×10^{-7}
-3.6	.9999994430	-1.11242×10^{-6}	-1.41567×10^{-6}	-1.11478×10^{-6}	-1.23755×10^{-6}	-1.23755×10^{-6}
-3.4	.9999987600	-2.47574×10^{-6}	-3.15061×10^{-6}	-2.48098×10^{-6}	-2.75421×10^{-6}	-2.75420×10^{-6}
-3.2	.9999972390	-5.50985×10^{-6}	-7.01175×10^{-6}	-5.52148×10^{-6}	-6.12957×10^{-6}	-6.12956×10^{-6}
-3.0	.9999938560	-1.22623×10^{-5}	-1.56046×10^{-5}	-1.22881×10^{-5}	-1.36414×10^{-5}	-1.36413×10^{-5}
-2.8	.9999863260	-2.72893×10^{-5}	-3.47272×10^{-5}	-2.73469×10^{-5}	-3.03584×10^{-5}	-3.03581×10^{-5}
-2.6	.9999695680	-6.07295×10^{-5}	-7.72793×10^{-5}	-6.08576×10^{-5}	-6.75586×10^{-5}	-6.75572×10^{-5}
-2.4	.9999322760	-1.35136×10^{-4}	-1.71951×10^{-4}	-1.35421×10^{-4}	-1.50328×10^{-4}	-1.50321×10^{-4}
-2.2	.9998492900	-3.00652×10^{-4}	-3.82503×10^{-4}	-3.01284×10^{-4}	-3.34432×10^{-4}	-3.34398×10^{-4}
-2.0	.9996646500	-6.68627×10^{-4}	-8.50373×10^{-4}	-6.70026×10^{-4}	-7.43649×10^{-4}	-7.43481×10^{-4}
-1.8	.9992539710	-1.48564×10^{-3}	-1.88809×10^{-3}	-1.48872×10^{-3}	-1.65185×10^{-3}	-1.65101×10^{-3}
-1.6	.9983411990	-3.29445×10^{-3}	-4.18002×10^{-3}	-3.30111×10^{-3}	-3.66058×10^{-3}	-3.65649×10^{-3}
-1.4	.9963157600	-7.27317×10^{-3}	-9.19513×10^{-3}	-7.28724×10^{-3}	-8.06981×10^{-3}	-8.04987×10^{-3}
-1.2	.9918374290	-.0159005100	-.0199423470	-.0159275520	-.0175856100	-.0174900500
-1.0	.9820137900	-.0340113120	-.0419268740	-.0340546720	-.0373498670	-.0369197820
-.8	.9608342770	-.0693448020	-.0823970730	-.0693680360	-.0751004190	-.0732403660
-.6	.9168273040	-.1272710330	-.1404670520	-.1271406630	-.1342349520	-.1276650290
-.4	.8320183850	-.1860746010	-.1786129160	-.1856165940	-.1882982690	-.1720683720
-.2	.6899744810	-.1625654640	-.1168326780	-.1625495349	-.1576875510	-.1377952600
0	.5	0	.0555355540	0	0	0
.2	.3100255190	.1625654640	.1980830400	.1625495340	.1576875510	.1377952600
.4	.1679816150	.1860746010	.2041741100	.1856165940	.1882982690	.1720683720
.6	.0831726960	.1272710330	.1350634280	.1271406630	.1342349520	.1276650290
.8	.0391657230	.0693448020	.0725351440	.0693680360	.0751004190	.0732403660
1.0	.0179862100	.0340113120	.0353506390	.0340546720	.0373598670	.0369197820
1.2	8.16257×10^{-3}	.0159005100	.0164784110	.0159275520	.0175856100	.0174900500
1.4	3.68424×10^{-3}	7.27317×10^{-3}	7.52787×10^{-3}	7.28724×10^{-3}	8.06981×10^{-3}	8.04987×10^{-3}
1.6	1.65880×10^{-3}	3.29445×10^{-3}	3.40778×10^{-3}	3.30111×10^{-3}	3.66058×10^{-3}	3.65649×10^{-3}
1.8	7.46029×10^{-4}	1.48564×10^{-3}	1.53635×10^{-3}	1.48872×10^{-3}	1.65185×10^{-3}	1.65101×10^{-3}
2.0	3.35350×10^{-4}	6.68627×10^{-4}	6.91368×10^{-4}	6.70026×10^{-4}	7.43649×10^{-4}	7.43481×10^{-4}
2.2	1.50710×10^{-4}	3.00652×10^{-4}	3.10862×10^{-4}	3.01284×10^{-4}	3.34432×10^{-4}	3.34398×10^{-4}
2.4	6.77241×10^{-5}	1.35136×10^{-4}	1.39722×10^{-4}	1.35421×10^{-4}	1.50328×10^{-4}	1.50321×10^{-4}
2.6	3.04316×10^{-5}	6.07295×10^{-5}	6.27896×10^{-5}	6.08576×10^{-5}	6.75586×10^{-5}	6.75572×10^{-5}
2.8	1.36740×10^{-5}	2.72894×10^{-5}	2.82149×10^{-5}	2.73469×10^{-5}	3.03584×10^{-5}	3.03581×10^{-5}
3.0	6.14417×10^{-6}	1.22623×10^{-5}	1.26781×10^{-5}	1.22881×10^{-5}	1.36414×10^{-5}	1.36413×10^{-5}
3.2	2.76076×10^{-6}	5.50987×10^{-6}	5.69672×10^{-6}	5.52148×10^{-6}	6.12957×10^{-6}	6.12956×10^{-6}
3.4	1.24049×10^{-6}	2.47575×10^{-6}	2.55971×10^{-6}	2.48098×10^{-6}	2.75421×10^{-6}	2.75420×10^{-6}
3.6	5.57393×10^{-7}	1.11243×10^{-6}	1.15016×10^{-6}	1.11478×10^{-6}	1.23755×10^{-6}	1.23755×10^{-6}
3.8	2.50451×10^{-7}	4.99858×10^{-7}	5.16809×10^{-7}	5.00903×10^{-7}	5.56073×10^{-7}	5.56073×10^{-7}
4.0	1.12534×10^{-7}	2.24591×10^{-7}	2.32207×10^{-7}	2.25070×10^{-7}	2.49856×10^{-7}	2.49856×10^{-7}
4.2	5.05660×10^{-8}	1.00922×10^{-7}	1.04344×10^{-7}	1.01131×10^{-7}	1.12267×10^{-7}	1.12267×10^{-7}
4.4	2.27200×10^{-8}	4.53286×10^{-8}	4.68685×10^{-8}	4.54409×10^{-8}	5.04462×10^{-8}	5.04462×10^{-8}
4.6	1.02090×10^{-8}	2.04423×10^{-8}	2.11259×10^{-8}	2.04179×10^{-8}	2.26687×10^{-8}	2.26687×10^{-8}
4.8	4.58500×10^{-9}	8.91511×10^{-9}	9.07434×10^{-9}	9.17436×10^{-9}	1.01850×10^{-8}	1.01850×10^{-8}
5.0	2.06100×10^{-9}	0	0	4.12231×10^{-9}	----------	----------

TABLE 26.- COMPARISON OF SPLINE AND FINITE-DIFFERENCE CURVE FITS OF THE EXACT SOLUTION TO BURGERS' EQUATION FOR $\nu = 1/24$, $\sigma = 0$, AND 51 EQUALLY SPACED POINTS

η	Exact u	Spline curve fit $\left(u - \frac{1}{2}\right)m$	Spline curve fit $\tilde{m}$	Exact $\left(u - \frac{1}{2}\right)u_\eta$	Finite-difference curve fit $\left(u - \frac{1}{2}\right)u_\eta$	Finite-difference curve fit $\frac{d}{d\eta}\frac{u^2}{2} - \frac{1}{2}u_\eta$
-5.0	1.0	0	0	-5.25391×10^{-26}	----------	----------
-4.8	1.0	1.27547×10^{-14}	-1.12666×10^{-14}	-5.79147×10^{-25}	0	0
-4.6	1.0	-4.46447×10^{-14}	3.94928×10^{-14}	-6.38404×10^{-24}	0	0
-4.4	1.0	1.65835×10^{-13}	-1.46687×10^{-13}	-7.03724×10^{-23}	0	0
-4.2	1.0	-6.18734×10^{-13}	5.47288×10^{-13}	-7.75728×10^{-22}	0	0
-4.0	1.0	2.30925×10^{-12}	-2.04260×10^{-12}	-8.55098×10^{-21}	0	0
-3.8	1.0	-8.61880×10^{-12}	7.62358×10^{-12}	-9.42590×10^{-20}	0	0
-3.6	1.0	3.21680×10^{-11}	-2.84535×10^{-11}	-1.03903×10^{-18}	0	0
-3.4	1.0	-1.20061×10^{-10}	1.06197×10^{-10}	-1.14535×10^{-17}	0	0
-3.2	1.0	4.48104×10^{-10}	-3.96361×10^{-10}	-1.26253×10^{-16}	0	0
-3.0	1.0	-1.672460×10^{-9}	1.479340×10^{-9}	-1.39171×10^{-15}	0	0
-2.8	1.0	6.242140×10^{-9}	-5.521350×10^{-9}	-1.53411×10^{-14}	0	0
-2.6	1.0	-2.329760×10^{-8}	2.060740×10^{-8}	-1.69108×10^{-13}	0	0
-2.4	1.0	8.695370×10^{-8}	-7.691310×10^{-8}	-1.86410×10^{-12}	0	-1.00000×10^{-11}
-2.2	1.0	-3.245380×10^{-7}	2.869740×10^{-7}	-2.05483×10^{-11}	-5.00000×10^{-11}	-4.25000×10^{-11}
-2.0	1.0	1.211040×10^{-6}	-1.072200×10^{-6}	-2.26508×10^{-10}	-5.15000×10^{-10}	-5.15000×10^{-10}
-1.8	1.0	-4.523020×10^{-6}	3.989670×10^{-6}	-2.496840×10^{-9}	-5.685000×10^{-9}	-5.685000×10^{-9}
-1.6	.9999999950	1.684800×10^{-5}	-1.502460×10^{-5}	-2.752310×10^{-8}	-6.268750×10^{-8}	-6.268750×10^{-8}
-1.4	.9999999490	-6.324910×10^{-5}	5.460020×10^{-5}	-3.033920×10^{-7}	-6.910100×10^{-7}	-6.910100×10^{-7}
-1.2	.9999994430	2.320170×10^{-4}	-2.200570×10^{-4}	-3.344330×10^{-6}	-7.617000×10^{-6}	-7.616960×10^{-6}
-1.0	.9999938560	-9.105680×10^{-4}	6.419600×10^{-4}	-3.686440×10^{-5}	-8.395740×10^{-5}	-8.395270×10^{-5}
-.8	.9999322760	2.906350×10^{-3}	-4.371200×10^{-3}	-4.062620×10^{-4}	-9.247310×10^{-4}	-9.241600×10^{-4}
-.6	.9992539710	-.01624217000	-5.226220×10^{-3}	-4.466160×10^{-3}	-.01010346100	-.01003528000
-.4	.9918374290	1.425470×10^{-3}	-.19277486800	-.04778265700	-.10135130100	-.09438690800
-.2	.9168273040	-.50665763800	-.33255690200	-.38142198800	-.51252817300	-.30238007100
0	.5	0	.16384511900	0	0	0
.2	.0831726960	.50665763800	.46984169900	.38142198800	.51252817300	.30238007100
.4	8.16257×10^{-3}	-1.425470×10^{-3}	.02632517100	.04778265700	.10135130100	.09438690800
.6	7.46029×10^{-4}	.01624217000	9.038650×10^{-3}	4.466160×10^{-3}	.01010346100	.01003528000
.8	6.77241×10^{-5}	-2.906350×10^{-3}	-9.405780×10^{-4}	4.062620×10^{-4}	9.247310×10^{-4}	9.241600×10^{-4}
1.0	6.14417×10^{-6}	9.105680×10^{-4}	3.865550×10^{-4}	3.686440×10^{-5}	8.395740×10^{-5}	8.395270×10^{-5}
1.2	5.57393×10^{-7}	-2.320170×10^{-4}	-9.136280×10^{-5}	3.344330×10^{-6}	7.617000×10^{-6}	7.616960×10^{-6}
1.4	5.05660×10^{-8}	6.324910×10^{-5}	2.558630×10^{-5}	3.033920×10^{-7}	6.910100×10^{-7}	6.910100×10^{-7}
1.6	4.58500×10^{-9}	-1.684800×10^{-5}	-6.754910×10^{-6}	2.752310×10^{-8}	6.268750×10^{-8}	6.268750×10^{-8}
1.8	4.1600×10^{-10}	4.523020×10^{-6}	1.818960×10^{-6}	2.496840×10^{-9}	5.685000×10^{-9}	5.685000×10^{-9}
2.0	3.7000×10^{-11}	-1.211050×10^{-6}	-4.865290×10^{-7}	2.26508×10^{-10}	5.15000×10^{-10}	5.15000×10^{-10}
2.2	4.0000×10^{-12}	3.245490×10^{-7}	1.304300×10^{-7}	2.05483×10^{-11}	4.62500×10^{-11}	4.62500×10^{-11}
2.4	0	-8.694880×10^{-8}	-3.493800×10^{-8}	1.86410×10^{-12}	5.00000×10^{-12}	5.00000×10^{-12}
2.6	0	2.329630×10^{-8}	9.360980×10^{-9}	1.69108×10^{-13}	0	0
2.8	0	-6.241790×10^{-9}	-2.508100×10^{-9}	1.53411×10^{-14}	0	0
3.0	0	1.672370×10^{-9}	6.71996×10^{-10}	1.39171×10^{-15}	0	0
3.2	0	-4.48079×10^{-10}	-1.80048×10^{-10}	1.26253×10^{-16}	0	0
3.4	0	1.20054×10^{-10}	4.82405×10^{-11}	1.14535×10^{-17}	0	0
3.6	0	-3.21662×10^{-11}	-1.29251×10^{-11}	1.03903×10^{-18}	0	0
3.8	0	8.61832×10^{-12}	3.46304×10^{-12}	9.42590×10^{-20}	0	0
4.0	0	-2.30912×10^{-12}	-9.27859×10^{-13}	8.55098×10^{-21}	0	0
4.2	0	6.18699×10^{-13}	2.48616×10^{-13}	7.75728×10^{-22}	0	0
4.4	0	-1.65825×10^{-13}	-6.66621×10^{-14}	7.03724×10^{-23}	0	0
4.6	0	4.46422×10^{-14}	1.80488×10^{-14}	6.38404×10^{-24}	0	0
4.8	0	-1.27539×10^{-14}	-5.76497×10^{-15}	5.79147×10^{-25}	0	0
5.0	0	0	0	5.25391×10^{-26}	----------	----------

TABLE 27.- COMPARISON OF SADI SOLUTION WITH EXACT SOLUTION TO THE TWO-DIMENSIONAL DIFFUSION EQUATION

t	1 - u	Exact 1 - u	1 - u	Exact 1 - u	1 - u	Exact 1 - u	1 - u	Exact 1 - u
	$Z = 2.437 \times 10^{-2}$;	$Y = 2.437 \times 10^{-2}$	$Z = 9.651 \times 10^{-2}$;	$Y = 7.500 \times 10^{-3}$	$Z = 9.651 \times 10^{-2}$;	$Y = 3.956 \times 10^{-2}$	$Z = 2.245 \times 10^{-1}$;	$Y = 2.245 \times 10^{-1}$
0	1.000	1.000	1.000	1.000	1.000	1.000	1.000	1.000
.900	1.898×10^{-1}	1.887×10^{-1}	1.390×10^{-1}	1.371×10^{-1}	6.443×10^{-1}	6.340×10^{-1}	9.992×10^{-1}	1.000
1.800	1.001×10^{-1}	9.950×10^{-2}	8.987×10^{-2}	8.876×10^{-2}	4.433×10^{-1}	4.375×10^{-1}	1.002	9.996×10^{-1}
2.700	6.797×10^{-2}	6.754×10^{-2}	6.661×10^{-2}	6.592×10^{-2}	3.357×10^{-1}	3.322×10^{-1}	1.006	9.955×10^{-1}
3.600	5.144×10^{-2}	5.111×10^{-2}	5.293×10^{-2}	5.245×10^{-2}	2.698×10^{-1}	2.673×10^{-1}	1.000	9.832×10^{-1}
5.400	3.462×10^{-2}	3.439×10^{-2}	3.752×10^{-2}	3.722×10^{-2}	1.934×10^{-1}	1.919×10^{-1}	9.602×10^{-1}	9.397×10^{-1}
7.200	2.608×10^{-2}	2.591×10^{-2}	2.906×10^{-2}	2.884×10^{-2}	1.507×10^{-1}	1.495×10^{-1}	8.999×10^{-1}	8.813×10^{-1}
9.000	2.092×10^{-2}	2.078×10^{-2}	2.371×10^{-2}	2.354×10^{-2}	1.234×10^{-1}	1.225×10^{-1}	8.364×10^{-1}	8.208×10^{-1}
10.800	1.747×10^{-2}	1.735×10^{-2}	2.003×10^{-2}	1.989×10^{-2}	1.044×10^{-1}	1.037×10^{-1}	7.762×10^{-1}	7.632×10^{-1}
12.600	1.499×10^{-2}	1.489×10^{-2}	1.734×10^{-2}	1.721×10^{-2}	9.025×10^{-2}	8.990×10^{-2}	7.215×10^{-1}	7.106×10^{-1}
14.400	1.313×10^{-2}	1.304×10^{-2}	1.528×10^{-2}	1.517×10^{-2}	7.991×10^{-2}	7.935×10^{-2}	6.723×10^{-1}	6.633×10^{-1}
16.200	1.168×10^{-2}	1.160×10^{-2}	1.366×10^{-2}	1.357×10^{-2}	7.151×10^{-2}	7.101×10^{-2}	6.290×10^{-1}	6.209×10^{-1}
18.000	1.052×10^{-2}	1.045×10^{-2}	1.235×10^{-2}	1.227×10^{-2}	6.470×10^{-2}	6.426×10^{-2}	5.902×10^{-1}	5.831×10^{-1}
19.800	9.569×10^{-3}	9.504×10^{-3}	1.127×10^{-2}	1.119×10^{-2}	5.908×10^{-2}	5.867×10^{-2}	5.555×10^{-1}	5.492×10^{-1}
21.600	8.775×10^{-3}	8.715×10^{-3}	1.036×10^{-2}	1.029×10^{-2}	5.436×10^{-2}	5.398×10^{-2}	5.245×10^{-1}	5.188×10^{-1}
23.400	8.103×10^{-3}	8.048×10^{-3}	9.594×10^{-3}	9.523×10^{-3}	5.034×10^{-2}	4.999×10^{-2}	4.965×10^{-1}	4.913×10^{-1}
25.200	7.527×10^{-3}	7.475×10^{-3}	8.929×10^{-3}	8.868×10^{-3}	4.687×10^{-2}	4.654×10^{-2}	4.713×10^{-1}	4.665×10^{-1}
27.000	7.027×10^{-3}	6.979×10^{-3}	8.351×10^{-3}	8.293×10^{-3}	4.384×10^{-2}	4.354×10^{-2}	4.483×10^{-1}	4.440×10^{-1}
28.800	6.589×10^{-3}	6.544×10^{-3}	7.843×10^{-3}	7.789×10^{-3}	4.119×10^{-2}	4.090×10^{-2}	4.275×10^{-1}	4.235×10^{-1}
30.600	6.203×10^{-3}	6.160×10^{-3}	7.393×10^{-3}	7.342×10^{-3}	3.884×10^{-2}	3.857×10^{-2}	4.085×10^{-1}	4.047×10^{-1}
32.400	5.859×10^{-3}	5.819×10^{-3}	6.992×10^{-3}	6.944×10^{-3}	3.674×10^{-2}	3.698×10^{-2}	3.910×10^{-1}	3.875×10^{-1}
34.200	5.519×10^{-3}	5.514×10^{-3}	6.632×10^{-3}	6.586×10^{-3}	3.485×10^{-2}	3.462×10^{-2}	3.749×10^{-1}	3.717×10^{-1}
36.000	5.273×10^{-3}	5.239×10^{-3}	6.307×10^{-3}	6.264×10^{-3}	3.316×10^{-2}	3.293×10^{-2}	3.601×10^{-1}	3.571×10^{-1}

TABLE 28. - COMPARISON OF RESULTS FOR THE SQUARE CAVITY FOR R = 10

(a) Vorticity at center of moving wall

Calculation method	Points	Vorticity at center of moving wall
Spline	15 × 15	5.8884
Finite difference	15 × 15	5.9264
Finite difference, divergence form	15 × 15	5.9129

(b) Maximum stream function

Calculation method	Points	Maximum stream function
Spline	15 × 15	-0.10027
Finite difference	15 × 15	-.09790
Finite difference, divergence form	15 × 15	-.09805

TABLE 29.- CALCULATED VORTICITY AND STREAM FUNCTION FOR THE SQUARE CAVITY FOR R = 10

(a) SADI calculated stream function, 15 × 15 points equally spaced

x / y	0	0.0714	0.1428	0.2143	0.2857	0.3571	0.4286	0.5000	0.5714	0.6428	0.7143	0.7857	0.8571	0.9286	1.0
1.0000	0	0	0	0	0	0	0	0	0	0	0	0	0	0	0
.9286	0	-2.097×10^{-2}	-3.893×10^{-2}	-4.752×10^{-2}	-5.224×10^{-2}	-5.498×10^{-2}	-5.649×10^{-2}	-5.710×10^{-2}	-5.690×10^{-2}	-5.583×10^{-2}	-5.358×10^{-2}	-4.936×10^{-2}	-4.104×10^{-2}	-2.236×10^{-2}	0
.8571	0	-1.543×10^{-2}	-4.108×10^{-2}	-6.079×10^{-2}	-7.373×10^{-2}	-8.192×10^{-2}	-8.665×10^{-2}	-8.860×10^{-2}	-8.797×10^{-2}	-8.455×10^{-2}	-7.756×10^{-2}	-6.537×10^{-2}	-4.526×10^{-2}	-1.744×10^{-2}	0
.7857	0	-1.145×10^{-2}	-3.493×10^{-2}	-5.831×10^{-2}	-7.661×10^{-2}	-8.932×10^{-2}	-9.704×10^{-2}	-1.003×10^{-1}	-9.913×10^{-2}	-9.330×10^{-2}	-8.196×10^{-2}	-6.396×10^{-2}	-3.925×10^{-2}	-1.312×10^{-2}	0
.7143	0	-8.794×10^{-3}	-2.854×10^{-2}	-5.079×10^{-2}	-7.036×10^{-2}	-8.508×10^{-2}	-9.442×10^{-2}	-9.833×10^{-2}	-9.672×10^{-2}	-8.928×10^{-2}	-7.562×10^{-2}	-5.583×10^{-2}	-3.195×10^{-2}	-9.959×10^{-3}	0
.6428	0	-6.808×10^{-3}	-2.288×10^{-2}	-4.222×10^{-2}	-6.043×10^{-2}	-7.430×10^{-2}	-8.438×10^{-2}	-8.830×10^{-2}	-8.637×10^{-2}	-7.841×10^{-2}	-6.458×10^{-2}	-4.589×10^{-2}	-2.155×10^{-2}	-7.517×10^{-3}	0
.5714	0	-5.224×10^{-3}	-1.794×10^{-2}	-3.387×10^{-2}	-4.949×10^{-2}	-6.234×10^{-2}	-7.091×10^{-2}	-7.438×10^{-2}	-7.235×10^{-2}	-6.479×10^{-2}	-5.225×10^{-2}	-3.615×10^{-2}	-1.924×10^{-2}	-5.591×10^{-3}	0
.5000	0	-3.916×10^{-3}	-1.366×10^{-2}	-2.621×10^{-2}	-3.884×10^{-2}	-4.945×10^{-2}	-5.659×10^{-2}	-5.940×10^{-2}	-5.748×10^{-2}	-5.092×10^{-2}	-4.041×10^{-2}	-2.741×10^{-2}	-1.428×10^{-2}	-4.062×10^{-3}	0
.4286	0	-2.826×10^{-3}	-1.000×10^{-2}	-1.944×10^{-2}	-2.912×10^{-2}	-3.736×10^{-2}	-4.294×10^{-2}	-4.056×10^{-2}	-4.340×10^{-2}	-3.811×10^{-2}	-2.986×10^{-2}	-1.994×10^{-2}	-1.021×10^{-2}	-2.851×10^{-3}	0
.3571	0	-1.925×10^{-3}	-6.924×10^{-3}	-1.364×10^{-3}	-2.064×10^{-2}	-2.667×10^{-2}	-3.075×10^{-2}	-3.226×10^{-2}	-3.095×10^{-2}	-2.697×10^{-2}	-2.090×10^{-2}	-1.376×10^{-2}	-6.926×10^{-3}	-1.897×10^{-3}	0
.2857	0	-1.196×10^{-3}	-4.406×10^{-3}	-8.831×10^{-3}	-1.353×10^{-2}	-1.762×10^{-2}	-2.039×10^{-2}	-2.140×10^{-2}	-2.046×10^{-2}	-1.769×10^{-2}	-1.356×10^{-2}	-8.799×10^{-3}	-4.339×10^{-3}	-1.157×10^{-3}	0
.2143	0	-6.329×10^{-4}	-2.440×10^{-3}	-5.030×10^{-3}	-7.842×10^{-3}	-1.032×10^{-2}	-1.200×10^{-2}	-1.260×10^{-2}	-1.201×10^{-2}	-1.031×10^{-2}	-7.808×10^{-3}	-4.965×10^{-3}	-2.374×10^{-3}	-6.028×10^{-4}	0
.1428	0	-2.422×10^{-4}	-1.039×10^{-3}	-2.257×10^{-3}	-3.617×10^{-3}	-4.828×10^{-3}	-5.656×10^{-3}	-5.950×10^{-3}	-5.654×10^{-3}	-4.814×10^{-3}	-3.585×10^{-3}	-2.213×10^{-3}	-9.996×10^{-4}	-2.260×10^{-4}	0
.0714	0	-3.892×10^{-5}	-2.336×10^{-4}	-5.648×10^{-4}	-9.455×10^{-4}	-1.288×10^{-3}	-1.523×10^{-3}	-1.607×10^{-3}	-1.522×10^{-3}	-1.283×10^{-3}	-9.347×10^{-4}	-5.503×10^{-4}	-2.215×10^{-4}	-3.426×10^{-5}	0
0	0	0	0	0	0	0	0	0	0	0	0	0	0	0	0

TABLE 29.- CALCULATED VORTICITY AND STREAM FUNCTION FOR THE SQUARE CAVITY FOR R = 10 – Continued

(b) SADI calculated vorticity, 15 × 15 points equally spaced

y \ x	0	0.0714	0.1428	0.2143	0.2857	0.3571	0.4286	0.5000	0.5714	0.6428	0.7143	0.7857	0.8571	0.9286	1.0
1.0000	----------	2.937×10	1.577×10	1.071×10	8.234	6.883	6.167	5.888	5.892	6.484	7.562	9.680	1.441×10	2.833×10	----------
.9286	-1.438×10	4.681	8.237	7.356	6.457	5.804	5.402	5.229	5.282	5.590	6.218	7.265	8.670	5.523	-1.539×10
.8571	-8.403	-1.892	2.538	4.097	4.440	4.456	4.408	4.393	4.450	4.589	4.764	4.742	3.425	-1.568	-9.662
.7857	-5.631	-2.423	2.091×10^{-1}	1.897	2.758	3.169	3.373	3.481	3.536	3.519	3.318	2.597	7.311×10^{-1}	-2.548	-6.546
.7143	-4.121	-2.222	-5.226×10^{-1}	7.694	1.630	2.156	2.461	2.616	2.644	2.509	2.098	1.207	-3.419×10^{-1}	-2.443	-4.703
.6428	-3.102	-1.876	-7.277×10^{-1}	2.236×10^{-1}	9.326×10^{-1}	1.419	1.419	1.867	1.859	1.663	1.209	4.156×10^{-1}	-7.265×10^{-1}	-2.078	-3.430
.5714	-2.337	-1.520	-7.315×10^{-1}	-4.417×10^{-2}	5.002×10^{-1}	8.947×10^{-1}	1.146	1.259	1.225	1.022	6.175×10^{-1}	-3.204×10^{-3}	-8.022×10^{-1}	-1.669	-2.491
.5000	-1.728	-1.190	-6.563×10^{-1}	-1.726×10^{-1}	2.254×10^{-1}	5.224×10^{-1}	7.122×10^{-1}	7.896×10^{-1}	7.455×10^{-1}	5.675×10^{-1}	2.478×10^{-1}	-2.027×10^{-1}	-7.401×10^{-1}	-1.286	-1.776
.4286	-1.231	-8.981×10^{-1}	-5.534×10^{-1}	-2.284×10^{-1}	4.726×10^{-2}	2.567×10^{-1}	3.899×10^{-1}	4.390×10^{-1}	3.968×10^{-1}	2.586×10^{-1}	2.732×10^{-2}	-2.792×10^{-1}	-6.234×10^{-1}	-9.513×10^{-1}	-1.226
.3571	-8.250×10^{-1}	-6.469×10^{-1}	-4.468×10^{-1}	-2.467×10^{-1}	-7.083×10^{-2}	6.506×10^{-2}	1.509×10^{-1}	1.799×10^{-1}	1.471×10^{-1}	5.160×10^{-2}	-1.005×10^{-1}	-2.924×10^{-1}	-4.953×10^{-1}	-6.719×10^{-1}	-8.002×10^{-1}
.2857	-4.997×10^{-1}	-4.390×10^{-1}	-3.497×10^{-1}	-2.475×10^{-1}	-1.528×10^{-1}	-7.809×10^{-2}	-3.096×10^{-2}	-1.613×10^{-2}	-3.637×10^{-2}	-9.145×10^{-2}	-1.765×10^{-1}	-2.787×10^{-1}	-3.781×10^{-1}	-4.480×10^{-1}	-4.743×10^{-1}
.2143	-2.508×10^{-1}	-2.760×10^{-1}	-2.689×10^{-1}	-2.431×10^{-1}	-2.154×10^{-1}	-1.934×10^{-1}	-1.798×10^{-1}	-1.760×10^{-1}	-1.829×10^{-1}	-2.009×10^{-1}	-2.285×10^{-1}	-2.596×10^{-1}	-2.823×10^{-1}	-2.773×10^{-1}	-2.329×10^{-1}
.1428	-8.210×10^{-2}	-1.579×10^{-1}	-2.050×10^{-1}	-2.390×10^{-1}	-2.706×10^{-1}	-2.987×10^{-1}	-3.181×10^{-1}	-3.250×10^{-1}	-3.183×10^{-1}	-3.001×10^{-1}	-2.743×10^{-1}	-2.443×10^{-1}	-2.090×10^{-1}	-1.566×10^{-1}	-7.297×10^{-2}
.0714	-4.032×10^{-3}	-7.576×10^{-2}	-1.474×10^{-1}	-2.331×10^{-1}	-3.268×10^{-1}	-4.109×10^{-1}	-4.686×10^{-1}	-4.888×10^{-1}	-4.675×10^{-1}	-4.089×10^{-1}	-3.247×10^{-1}	-2.313×10^{-1}	-1.458×10^{-1}	-7.384×10^{-2}	-1.562×10^{-3}
0	0	3.865×10^{-3}	-7.784×10^{-2}	-2.203×10^{-1}	-3.885×10^{-1}	-5.410×10^{-1}	-6.460×10^{-1}	-6.834×10^{-1}	-6.456×10^{-1}	-5.387×10^{-1}	-3.834×10^{-1}	-2.134×10^{-1}	-7.214×10^{-2}	-1.813×10^{-3}	0

TABLE 29.- CALCULATED VORTICITY AND STREAM FUNCTION FOR THE SQUARE CAVITY FOR R = 10 – Continued

(c) Divergence-form finite-difference calculated stream function, 15 × 15 points equally spaced

y \ x	0	0.0714	0.1428	0.2143	0.2857	0.3571	0.4286	0.5000	0.5714	0.6428	0.7143	0.7857	0.8571	0.9286	1.0
1.0000	0	0	0	0	0	0	0	0	0	0	0	0	0	0	0
.9286	0	-1.907×10^{-2}	-3.481×10^{-2}	-4.461×10^{-2}	-5.042×10^{-2}	-5.380×10^{-2}	-5.563×10^{-2}	-5.610×10^{-2}	-5.610×10^{-2}	-5.480×10^{-2}	-5.201×10^{-2}	-4.677×10^{-2}	-3.714×10^{-2}	-2.056×10^{-2}	0
.8571	0	-1.750×10^{-2}	-3.987×10^{-2}	-5.811×10^{-2}	-7.112×10^{-2}	-7.971×10^{-2}	-8.478×10^{-2}	-8.690×10^{-2}	-8.626×10^{-2}	-8.263×10^{-2}	-7.529×10^{-2}	-6.299×10^{-2}	-4.430×10^{-2}	-1.990×10^{-2}	0
.7857	0	-1.358×10^{-2}	-3.586×10^{-2}	-5.734×10^{-2}	-7.462×10^{-2}	-8.703×10^{-2}	-9.476×10^{-2}	-9.805×10^{-2}	-9.697×10^{-2}	-9.122×10^{-2}	-8.020×10^{-2}	-6.326×10^{-2}	-4.060×10^{-2}	-1.575×10^{-2}	0
.7143	0	-1.031×10^{-2}	-2.991×10^{-2}	-5.095×10^{-2}	-6.934×10^{-2}	-8.334×10^{-2}	-9.236×10^{-2}	-9.621×10^{-2}	-9.473×10^{-2}	-8.768×10^{-2}	-7.482×10^{-2}	-5.639×10^{-2}	-3.380×10^{-2}	-1.185×10^{-2}	0
.6428	0	-7.830×10^{-3}	-2.409×10^{-2}	-4.231×10^{-2}	-6.011×10^{-2}	-7.384×10^{-2}	-8.288×10^{-2}	-8.668×10^{-2}	-8.494×10^{-2}	-7.752×10^{-2}	-6.455×10^{-2}	-4.689×10^{-2}	-2.678×10^{-2}	-8.760×10^{-3}	0
.5714	0	-5.900×10^{-3}	-1.888×10^{-2}	-3.453×10^{-2}	-4.957×10^{-2}	-6.185×10^{-2}	-7.004×10^{-2}	-7.341×10^{-2}	-7.159×10^{-2}	-6.454×10^{-2}	-5.269×10^{-2}	-3.723×10^{-2}	-2.050×10^{-2}	-6.380×10^{-3}	0
.5000	0	-4.360×10^{-3}	-1.436×10^{-2}	-2.681×10^{-2}	-3.912×10^{-2}	-4.937×10^{-2}	-5.626×10^{-2}	-5.902×10^{-2}	-5.729×10^{-2}	-5.112×10^{-2}	-4.107×10^{-2}	-2.839×10^{-2}	-1.520×10^{-2}	-4.560×10^{-3}	0
.4286	0	-3.110×10^{-3}	-1.050×10^{-2}	-1.995×10^{-2}	-2.949×10^{-2}	-3.754×10^{-2}	-4.299×10^{-2}	-4.511×10^{-2}	-4.361×10^{-2}	-3.857×10^{-2}	-3.057×10^{-2}	-2.075×10^{-2}	-1.086×10^{-2}	-3.160×10^{-3}	0
.3571	0	-2.100×10^{-3}	-7.260×10^{-3}	-1.405×10^{-2}	-2.102×10^{-2}	-2.698×10^{-2}	-3.102×10^{-2}	-3.256×10^{-2}	-3.136×10^{-2}	-2.753×10^{-2}	-2.156×10^{-2}	-1.440×10^{-2}	-7.270×10^{-3}	-2.080×10^{-3}	0
.2857	0	-1.280×10^{-3}	-4.620×10^{-3}	-9.140×10^{-3}	-1.388×10^{-2}	-1.797×10^{-2}	-2.075×10^{-2}	-2.180×10^{-2}	-2.093×10^{-2}	-1.824×10^{-2}	-1.412×10^{-2}	-9.270×10^{-3}	-4.630×10^{-3}	-1.250×10^{-3}	0
.2143	0	-6.600×10^{-4}	-2.560×10^{-3}	-5.250×10^{-3}	-8.130×10^{-3}	-1.063×10^{-2}	-1.235×10^{-2}	-1.299×10^{-2}	-1.244×10^{-2}	-1.076×10^{-2}	-8.220×10^{-3}	-5.280×10^{-3}	-2.540×10^{-3}	-6.300×10^{-4}	0
.1428	0	-2.300×10^{-4}	-1.080×10^{-3}	-2.380×10^{-3}	-3.800×10^{-3}	-5.060×10^{-3}	-5.930×10^{-3}	-6.250×10^{-2}	-5.970×10^{-3}	-5.120×10^{-3}	-3.840×10^{-3}	-2.380×10^{-3}	-1.070×10^{-3}	-2.100×10^{-4}	0
.0714	0	-1.000×10^{-5}	-2.300×10^{-4}	-6.000×10^{-4}	-1.030×10^{-3}	-1.410×10^{-3}	-1.680×10^{-3}	-1.780×10^{-2}	-1.690×10^{-3}	-1.430×10^{-3}	-1.040×10^{-3}	-6.000×10^{-4}	-2.200×10^{-4}	-1.000×10^{-6}	0
0	0	0	0	0	0	0	0	0	0	0	0	0	.0	0	0

TABLE 29.- CALCULATED VORTICITY AND STREAM FUNCTION FOR THE SQUARE CAVITY FOR R = 10 – Concluded

(d) Divergence-form finite-difference calculated vorticity, 15 × 15 points equally spaced

y \ x	0	0.0714	0.1428	0.2143	0.2857	0.3571	0.4286	0.5000	0.5714	0.6428	0.7143	0.7857	0.8571	0.9286	1.0
1.0000	----------	2.052 × 10	1.435 × 10	1.051 × 10	8.237	6.912	6.194	5.913	6.009	6.520	7.610	9.665	1.344 × 10	1.994 × 10	----------
.9286	-7.477	4.700	6.997	6.878	6.299	5.768	5.407	5.244	5.291	5.573	6.114	6.851	7.239	4.937	-8.059
.8571	-6.859	-4.962	2.589	3.824	4.237	4.333	4.335	4.343	4.398	4.499	4.575	4.375	3.246	-1.949×10^{-1}	-7.801
.7857	-5.322	-1.835	5.356×10^{-1}	1.922	2.678	3.079	3.293	3.407	3.454	3.412	3.180	2.528	1.037	-1.834	-6.173
.7143	-4.042	-1.974	-3.068×10^{-1}	8.648×10^{-1}	1.632	2.114	2.402	2.549	2.570	2.435	2.058	1.289	-7.012×10^{-1}	-2.139	-4.644
.6428	-3.069	-1.761	-6.022×10^{-1}	3.026×10^{-1}	9.584×10^{-1}	1.406	1.686	1.821	1.814	1.636	1.232	5.233×10^{-1}	-5.529×10^{-1}	-1.957	-3.432
.5714	-2.314	-1.461	-6.591×10^{-1}	9.880×10^{-3}	5.257×10^{-1}	8.950×10^{-1}	1.130	1.237	1.209	1.028	6.638×10^{-1}	8.612×10^{-2}	-7.025×10^{-1}	-1.624	-2.502
.5000	-1.711	-1.159	-6.142×10^{-1}	-1.375×10^{-1}	2.457×10^{-1}	5.282×10^{-1}	7.087×10^{-1}	7.849×10^{-1}	7.494×10^{-1}	5.901×10^{-1}	2.947×10^{-1}	-1.392×10^{-1}	-6.858×10^{-1}	-1.273	-1.788
.4286	-1.220	-8.824×10^{-1}	-5.291×10^{-1}	-2.060×10^{-1}	6.255×10^{-2}	2.646×10^{-1}	3.937×10^{-1}	4.444×10^{-1}	4.102×10^{-1}	2.847×10^{-1}	6.572×10^{-2}	-2.377×10^{-1}	-5.959×10^{-1}	-9.532×10^{-1}	-1.238
.3571	-8.215×10^{-1}	-6.418×10^{-1}	-4.338×10^{-1}	-2.326×10^{-1}	-5.969×10^{-2}	7.282×10^{-2}	1.576×10^{-1}	1.889×10^{-1}	1.622×10^{-1}	7.426×10^{-2}	-7.277×10^{-2}	-2.672×10^{-1}	-4.833×10^{-1}	-6.809×10^{-1}	-8.141×10^{-1}
.2857	-5.024×10^{-1}	-4.411×10^{-1}	-3.438×10^{-1}	-2.393×10^{-1}	-1.454×10^{-1}	-7.205×10^{-2}	-2.495×10^{-2}	-8.000×10^{-3}	-2.043×10^{-2}	-7.546×10^{-2}	-1.589×10^{-1}	-2.650×10^{-1}	-3.748×10^{-1}	-4.601×10^{-1}	-4.887×10^{-1}
.2143	-2.579×10^{-1}	-2.822×10^{-1}	-2.674×10^{-1}	-2.394×10^{-1}	-2.118×10^{-1}	-1.904×10^{-1}	-1.766×10^{-1}	-1.714×10^{-1}	-1.763×10^{-1}	-1.926×10^{-1}	-2.199×10^{-1}	-2.540×10^{-1}	-2.837×10^{-1}	-2.899×10^{-1}	-2.466×10^{-1}
.1428	-8.930×10^{-2}	-1.648×10^{-1}	-2.066×10^{-1}	-2.398×10^{-1}	-2.715×10^{-1}	-2.994×10^{-1}	-3.184×10^{-1}	-3.247×10^{-1}	-3.178×10^{-1}	-2.998×10^{-1}	-2.747×10^{-1}	-2.460×10^{-1}	-2.132×10^{-1}	-1.670×10^{-1}	-8.293×10^{-2}
.0714	-3.680×10^{-3}	-8.168×10^{-2}	-1.546×10^{-1}	-2.410×10^{-1}	-3.332×10^{-1}	-4.150×10^{-1}	-4.712×10^{-1}	-4.914×10^{-1}	-4.719×10^{-1}	-4.164×10^{-1}	-3.348×10^{-1}	-2.427×10^{-1}	-1.557×10^{-1}	-8.142×10^{-2}	-1.460×10^{-3}
0	0	-3.68×10^{-3}	-8.879×10^{-2}	-2.354×10^{-1}	-4.032×10^{-1}	-5.541×10^{-1}	-6.586×10^{-1}	-6.977×10^{-1}	-6.637×10^{-1}	5.611×10^{-1}	-4.078×10^{-1}	-2.354×10^{-1}	-8.576×10^{-1}	-1.460×10^{-3}	0

TABLE 30.- COMPARISON OF RESULTS FOR THE SQUARE CAVITY FOR R = 100

(a) Vorticity at center of moving wall

Calculation method	Points	Vorticity at center of moving wall
Spline	15 × 15	7.1376
Spline	29 × 29	6.6876
Extrapolated spline	------	6.5376
Spline (unequal spacing)	19 × 19	6.2970
Finite difference	15 × 15	8.9160
Finite difference	57 × 57	6.6960
Extrapolated finite difference	------	6.5480
Finite difference[a]	17 × 17	7.3755
Finite difference[a]	33 × 33	6.7653
Finite difference[a]	65 × 65	6.6091
Extrapolated finite difference[a]	------	6.5567

[a]Divergence form.

(b) Maximum stream function

Calculation method	Points	Maximum stream function
Spline	15 × 15	-0.10529
Spline	29 × 29	-.10432
Extrapolated spline	------	-.10399
Spline (unequal spacing)	19 × 19	-.10472
Finite difference	15 × 15	-.08742
Finite difference	57 × 57	-.10128
Extrapolated finite difference	------	-.10220
Finite difference[a]	17 × 17	-.09867
Finite difference[a]	33 × 33	-.10213
Finite difference[a]	65 × 65	-.10318
Extrapolated finite difference[a]	------	-.10355
Reference 8	51 × 51	-.10316

[a]Divergence form.

(c) Corner point velocity u

Calculation method	Points	Velocity u at corner (a)
Spline	15 × 15	-0.13230
Spline	29 × 29	-.10036
Extrapolated spline	------	-.08971
Finite difference	15 × 15	.05730
Finite difference	57 × 57	-.06615
Extrapolated finite difference	------	-.07438
Interpolated finite difference[b]	17 × 17	.02079
Interpolated finite difference[b]	33 × 33	-.05189
Interpolated finite difference[b]	65 × 65	-.07560
Extrapolated finite difference[b]	------	-.08399

[a]Locations: 0.07143 down from moving surface; 0.07143 in from left surface.

[b]Divergence form.

TABLE 31.- COMPARISON OF RESULTS FOR THE VELOCITY u THROUGH POINT OF MAXIMUM STREAM FUNCTION FOR R = 100

y	Spline (15 × 15)	Spline (29 × 29)	Finite difference (15 × 15)	Finite difference (57 × 57)	y	Finite difference, divergence form (17 × 17)	Finite difference, divergence form (33 × 33)	Finite difference, divergence form (65 × 65)
0	0	0	0	0	0	0	0	0
.0714	-3.837×10^{-2}	-4.160×10^{-2}	-2.612×10^{-2}	-3.556×10^{-2}	.0625	-3.509×10^{-2}	-3.455×10^{-2}	-3.440×10^{-2}
.1428	-7.364×10^{-2}	-7.807×10^{-2}	-5.018×10^{-2}	-6.774×10^{-2}	.1250	-6.513×10^{-2}	-6.479×10^{-2}	-6.471×10^{-2}
.2143	-1.111×10^{-1}	-1.155×10^{-1}	-7.583×10^{-2}	-1.019×10^{-1}	.1875	-9.419×10^{-2}	-9.494×10^{-2}	-9.518×10^{-2}
.2857	-1.532×10^{-1}	-1.566×10^{-1}	-1.054×10^{-1}	-1.409×10^{-1}	.2500	-1.245×10^{-1}	-1.275×10^{-1}	-1.284×10^{-1}
.3571	-1.975×10^{-1}	-1.986×10^{-1}	-1.388×10^{-1}	-1.834×10^{-1}	.3125	-1.563×10^{-1}	-1.627×10^{-1}	-1.647×10^{-1}
.4286	-2.347×10^{-1}	-2.321×10^{-1}	-1.724×10^{-1}	-2.215×10^{-1}	.3750	-1.868×10^{-1}	-1.977×10^{-1}	-2.009×10^{-1}
.5000	-2.491×10^{-1}	-2.424×10^{-1}	-1.968×10^{-1}	-2.404×10^{-1}	.4375	-2.107×10^{-1}	-2.254×10^{-1}	-2.297×10^{-1}
.5714	-2.250×10^{-1}	-2.151×10^{-1}	-1.980×10^{-1}	-2.233×10^{-1}	.5000	-2.198×10^{-1}	-2.360×10^{-1}	-2.407×10^{-1}
.6429	-1.553×10^{-1}	-1.450×10^{-1}	-1.616×10^{-1}	-1.606×10^{-1}	.5625	-2.057×10^{-1}	-2.197×10^{-1}	-2.235×10^{-1}
.7143	-4.382×10^{-2}	-3.739×10^{-2}	-7.891×10^{-2}	-5.416×10^{-2}	.6250	-1.622×10^{-1}	-1.708×10^{-1}	-1.885×10^{-1}
.7857	1.062×10^{-1}	1.046×10^{-1}	5.022×10^{-2}	9.200×10^{-1}	.6875	-8.745×10^{-2}	-8.966×10^{-2}	-8.951×10^{-2}
.8571	3.110×10^{-1}	3.006×10^{-1}	2.445×10^{-1}	2.929×10^{-1}	.7500	1.782×10^{-2}	2.032×10^{-2}	2.182×10^{-2}
.9286	6.049×10^{-1}	5.973×10^{-1}	5.470×10^{-1}	5.905×10^{-1}	.8125	1.578×10^{-1}	1.625×10^{-1}	1.645×10^{-1}
1.0	1.0	1.0	1.0	1.0	.8750	3.519×10^{-1}	3.574×10^{-1}	3.593×10^{-1}
-----	----------	----------	----------	----------	.9375	6.315×10^{-1}	6.370×10^{-1}	6.385×10^{-1}
-----	----------	----------	----------	----------	1.0	1.0	1.0	1.0

TABLE 32. - CALCULATED VORTICITY AND STREAM FUNCTION FOR THE SQUARE CAVITY FOR R = 100

(a) SADI calculated stream function, 15 × 15 points equally spaced

y \ x	0	0.0714	0.1428	0.2143	0.2857	0.3571	0.4286	0.5000	0.5714	0.6428	0.7143	0.7857	0.8571	0.9286	1.0
1.0000	0	0	0	0	0	0	0	0	0	0	0	0	0	0	0
.9286	0	-1.647×10^{-2}	-3.110×10^{-2}	-3.939×10^{-2}	-4.507×10^{-2}	-4.928×10^{-2}	-5.249×10^{-2}	-5.485×10^{-2}	-5.632×10^{-2}	-5.676×10^{-2}	-5.588×10^{-2}	-5.322×10^{-2}	-4.701×10^{-2}	-2.821×10^{-2}	0
.8571	0	-9.847×10^{-3}	-2.815×10^{-2}	-4.447×10^{-2}	-5.761×10^{-2}	-6.827×10^{-2}	-7.683×10^{-2}	-8.333×10^{-2}	-8.751×10^{-2}	-8.882×10^{-2}	-8.634×10^{-2}	-7.839×10^{-2}	-6.054×10^{-2}	-2.715×10^{-2}	0
.7857	0	-7.413×10^{-3}	-2.368×10^{-2}	-4.196×10^{-2}	-5.895×10^{-2}	-7.377×10^{-2}	-8.615×10^{-2}	-9.572×10^{-2}	-1.018×10^{-1}	-1.033×10^{-1}	-9.865×10^{-2}	-8.515×10^{-2}	-5.905×10^{-2}	-2.246×10^{-2}	0
.7143	0	-6.355×10^{-3}	-2.110×10^{-2}	-3.904×10^{-2}	-5.703×10^{-2}	-7.349×10^{-2}	-8.753×10^{-2}	-9.831×10^{-2}	-1.047×10^{-1}	-1.053×10^{-1}	-9.795×10^{-2}	-8.016×10^{-2}	-5.091×10^{-2}	-1.729×10^{-2}	0
.6428	0	-5.649×10^{-3}	-1.902×10^{-2}	-3.579×10^{-2}	-5.317×10^{-2}	-6.942×10^{-2}	-8.333×10^{-2}	-9.372×10^{-2}	-9.917×10^{-2}	-9.796×10^{-2}	-8.813×10^{-2}	-6.828×10^{-2}	-4.021×10^{-2}	-1.254×10^{-2}	0
.5714	0	-4.956×10^{-3}	-1.675×10^{-2}	-3.172×10^{-2}	-4.741×10^{-2}	-6.217×10^{-2}	-7.466×10^{-2}	-8.352×10^{-2}	-8.721×10^{-2}	-8.410×10^{-2}	-7.285×10^{-2}	-5.351×10^{-2}	-2.951×10^{-2}	-8.584×10^{-3}	0
.5000	0	-4.163×10^{-3}	-1.410×10^{-2}	-2.678×10^{-2}	-4.010×10^{-2}	-5.256×10^{-2}	-6.283×10^{-2}	-6.955×10^{-2}	-7.133×10^{-2}	-6.690×10^{-2}	-5.573×10^{-2}	-3.895×10^{-2}	-2.030×10^{-2}	-5.569×10^{-3}	0
.4286	0	-3.284×10^{-3}	-1.117×10^{-2}	-2.128×10^{-2}	-3.189×10^{-2}	-4.168×10^{-2}	-4.946×10^{-2}	-5.403×10^{-2}	-5.427×10^{-2}	-4.944×10^{-2}	-3.965×10^{-2}	-2.650×10^{-2}	-1.314×10^{-2}	-3.424×10^{-3}	0
.3571	0	-2.383×10^{-3}	-8.189×10^{-3}	-1.569×10^{-2}	-2.356×10^{-2}	-3.071×10^{-2}	-3.615×10^{-2}	-3.894×10^{-2}	-3.830×10^{-2}	-3.392×10^{-2}	-2.627×10^{-2}	-1.685×10^{-2}	-7.988×10^{-3}	-1.975×10^{-3}	0
.2857	0	-1.542×10^{-3}	-5.405×10^{-3}	-1.048×10^{-2}	-1.583×10^{-2}	-2.063×10^{-2}	-2.414×10^{-2}	-2.568×10^{-2}	-2.478×10^{-2}	-2.139×10^{-2}	-1.603×10^{-2}	-9.890×10^{-3}	-4.465×10^{-3}	-1.034×10^{-3}	0
.2143	0	-8.371×10^{-4}	-3.053×10^{-3}	-6.066×10^{-3}	-9.276×10^{-3}	-1.214×10^{-2}	-1.417×10^{-2}	-1.495×10^{-2}	-1.420×10^{-2}	-1.198×10^{-2}	-8.701×10^{-3}	-5.135×10^{-3}	-2.169×10^{-3}	-4.473×10^{-4}	0
.1428	0	-3.277×10^{-4}	-1.312×10^{-3}	-2.731×10^{-3}	-4.276×10^{-3}	-5.661×10^{-3}	-6.629×10^{-3}	-6.965×10^{-3}	-6.544×10^{-3}	-5.408×10^{-3}	-3.795×10^{-3}	-2.109×10^{-3}	-7.909×10^{-4}	-1.180×10^{-4}	0
.0714	0	-5.630×10^{-5}	-2.974×10^{-4}	-6.803×10^{-4}	-1.108×10^{-3}	-1.495×10^{-3}	-1.767×10^{-3}	-1.860×10^{-3}	-1.736×10^{-3}	-1.407×10^{-3}	-9.465×10^{-4}	-4.790×10^{-4}	-1.361×10^{-4}	3.981×10^{-6}	0
0	0	0	0	0	0	0	0	0	0	0	0	0	0	0	0

TABLE 32.- CALCULATED VORTICITY AND STREAM FUNCTION FOR THE SQUARE CAVITY FOR R = 100 – Continued

(b) SADI calculated vorticity, 15 × 15 points equally spaced

y \ x	0	0.0714	0.1428	0.2143	0.2857	0.3571	0.4286	0.5000	0.5714	0.6428	0.7143	0.7857	0.8571	0.9286	1.0
1.0000	----------	3.292 × 10	2.128 × 10	1.588 × 10	1.249 × 10	1.015 × 10	8.374	7.137	6.390	6.192	6.673	8.026	1.114 × 10	2.419 × 10	----------
.9286	-1.124 × 10	1.892	5.839	6.381	6.285	5.999	5.678	5.392	5.187	5.125	5.267	5.894	8.143	9.865	-2.030 × 10
.8571	-5.087	-2.293	9.294×10^{-2}	1.402	2.155	2.675	3.078	3.424	3.750	4.085	4.477	5.216	6.305	1.823	-1.666 × 10
.7857	-3.529	-1.826	-6.207×10^{-1}	2.357×10^{-1}	8.790×10^{-1}	1.425	1.942	2.460	2.995	3.555	4.168	4.811	4.109	-1.749	-1.231 × 10
.7143	-2.939	-1.658	-6.205×10^{-1}	1.204×10^{-1}	6.871×10^{-1}	1.191	1.696	2.225	2.782	3.351	3.854	3.834	1.856	-3.065	-8.683
.6428	-2.586	-1.464	-5.610×10^{-1}	1.012×10^{-1}	6.184×10^{-1}	1.091	1.574	2.076	2.573	2.994	3.123	2.404	1.338×10^{-1}	-3.194	-5.858
.5714	-2.264	-1.277	-4.969×10^{-1}	6.595×10^{-2}	5.082×10^{-1}	9.192×10^{-1}	1.339	1.756	2.115	2.290	2.032	9.989×10^{-1}	-8.585×10^{-1}	-2.742	-3.772
.5000	-1.899	-1.079	-4.436×10^{-1}	6.369×10^{-3}	3.554×10^{-1}	6.758×10^{-1}	9.909×10^{-1}	1.274	1.452	1.397	9.413×10^{-1}	-3.486×10^{-3}	-1.210	-2.091	-2.316
.4286	-1.491	-8.744×10^{-1}	-3.989×10^{-1}	-6.750×10^{-2}	1.834×10^{-1}	4.046×10^{-1}	6.043×10^{-1}	7.498×10^{-1}	7.756×10^{-1}	5.969×10^{-1}	1.517×10^{-1}	-5.101×10^{-1}	-1.154	-1.462	-1.351
.3571	-1.072	-6.710×10^{-1}	-3.584×10^{-1}	-1.418×10^{-1}	1.737×10^{-2}	1.497×10^{-1}	2.544×10^{-1}	3.021×10^{-1}	2.494×10^{-1}	5.931×10^{-2}	-2.649×10^{-1}	-6.425×10^{-1}	-9.199×10^{-1}	-9.520×10^{-1}	-7.345×10^{-1}
.2857	-6.799×10^{-1}	-4.811×10^{-1}	-3.185×10^{-1}	-2.055×10^{-1}	-1.259×10^{-1}	-6.339×10^{-2}	-2.085×10^{-2}	-1.917×10^{-2}	-8.235×10^{-2}	-2.192×10^{-1}	-4.059×10^{-1}	-5.799×10^{-1}	-6.581×10^{-1}	-5.786×10^{-1}	-3.525×10^{-1}
.2143	-3.531×10^{-1}	-3.170×10^{-1}	-2.772×10^{-1}	-2.521×10^{-1}	-2.406×10^{-1}	-2.324×10^{-1}	-2.269×10^{-1}	-2.355×10^{-1}	-2.713×10^{-1}	-3.357×10^{-1}	-4.101×10^{-1}	-4.583×10^{-1}	-4.399×10^{-1}	-3.263×10^{-1}	-1.242×10^{-1}
.1428	-1.224×10^{-1}	-1.880×10^{-1}	-2.330×10^{-1}	-2.783×10^{-1}	-3.282×10^{-1}	-3.698×10^{-1}	-3.940×10^{-1}	-4.019×10^{-1}	-4.004×10^{-1}	-3.943×10^{-1}	-3.798×10^{-1}	-3.463×10^{-1}	-2.802×10^{-1}	-1.679×10^{-1}	-5.912×10^{-3}
.0714	-1.086×10^{-2}	-9.361×10^{-2}	-1.777×10^{-1}	-2.815×10^{-1}	-3.948×10^{-1}	-4.939×10^{-1}	-5.579×10^{-1}	-5.744×10^{-1}	-5.415×10^{-1}	-4.667×10^{-1}	-3.652×10^{-2}	-2.556×10^{-1}	-1.551×10^{-1}	-6.777×10^{-2}	2.058×10^{-2}
0	0	-8.545×10^{-3}	-1.003×10^{-1}	-2.633×10^{-1}	-4.500×10^{-1}	-6.209×10^{-1}	-7.424×10^{-1}	-7.846×10^{-1}	-7.290×10^{-1}	-5.801×10^{-1}	-3.731×10^{-1}	-1.669×10^{-1}	-2.446×10^{-2}	1.798×10^{-2}	0

TABLE 32. - CALCULATED VORTICITY AND STREAM FUNCTION FOR THE SQUARE CAVITY FOR R = 100 – Continued

(c) Nondivergence-form finite-difference calculated stream function, 57 × 57 points equally spaced

y \ x	0	0.0714	0.1428	0.2143	0.2857	0.3571	0.4286	0.5000	0.5714	0.6428	0.7143	0.7857	0.8571	0.9286	1.0
1.0000	0	0	0	0	0	0	0	0	0	0	0	0	0	0	0
.9286	0	-1.555×10^{-2}	-2.985×10^{-2}	-3.863×10^{-2}	-4.455×10^{-2}	-4.888×10^{-2}	-5.213×10^{-2}	-5.448×10^{-2}	-5.589×10^{-2}	-5.619×10^{-2}	-5.506×10^{-2}	-5.189×10^{-2}	-4.512×10^{-2}	-2.856×10^{-2}	0
.8571	0	-1.037×10^{-2}	-2.759×10^{-2}	-4.316×10^{-2}	-5.604×10^{-2}	-6.659×10^{-2}	-7.509×10^{-2}	-8.156×10^{-2}	-8.571×10^{-2}	-8.695×10^{-2}	-8.429×10^{-2}	-7.604×10^{-2}	-5.876×10^{-2}	-2.713×10^{-2}	0
.7857	0	-7.670×10^{-3}	-2.361×10^{-2}	-4.101×10^{-2}	-5.726×10^{-2}	-7.156×10^{-2}	-8.358×10^{-2}	-9.290×10^{-2}	-9.880×10^{-2}	-1.002×10^{-1}	-9.549×10^{-2}	-8.223×10^{-2}	-5.724×10^{-2}	-2.180×10^{-2}	0
.7143	0	-6.410×10^{-3}	-2.088×10^{-2}	-3.810×10^{-2}	-5.553×10^{-2}	-7.097×10^{-2}	-8.442×10^{-2}	-9.476×10^{-2}	-1.009×10^{-1}	-1.013×10^{-1}	-9.402×10^{-2}	-7.683×10^{-2}	-4.876×10^{-2}	-1.634×10^{-2}	0
.6428	0	-5.600×10^{-3}	-1.860×10^{-2}	-3.465×10^{-2}	-5.115×10^{-2}	-6.656×10^{-2}	-7.976×10^{-2}	-8.959×10^{-2}	-9.467×10^{-2}	-9.334×10^{-2}	-8.378×10^{-2}	-6.476×10^{-2}	-3.789×10^{-2}	-1.156×10^{-2}	0
.5714	0	-4.850×10^{-3}	-1.618×10^{-2}	-3.041×10^{-2}	-4.522×10^{-2}	-5.911×10^{-2}	-7.083×10^{-2}	-7.908×10^{-2}	-8.243×10^{-2}	-7.932×10^{-2}	-6.853×10^{-2}	-5.014×10^{-2}	-2.737×10^{-2}	-7.770×10^{-3}	0
.5000	0	-4.020×10^{-3}	-1.348×10^{-2}	-2.542×10^{-2}	-3.790×10^{-2}	-4.952×10^{-2}	-5.905×10^{-2}	-6.524×10^{-2}	-6.676×10^{-2}	-6.247×10^{-2}	-5.189×10^{-2}	-3.608×10^{-2}	-1.859×10^{-2}	-4.970×10^{-3}	0
.4286	0	-3.130×10^{-3}	-1.057×10^{-2}	-2.002×10^{-2}	-2.988×10^{-2}	-3.894×10^{-2}	-4.610×10^{-2}	-5.025×10^{-2}	-5.037×10^{-2}	-4.579×10^{-2}	-3.662×10^{-2}	-2.434×10^{-2}	-1.194×10^{-2}	-3.030×10^{-3}	0
.3571	0	-2.250×10^{-3}	-7.680×10^{-3}	-1.464×10^{-2}	-2.191×10^{-2}	-2.849×10^{-2}	-3.347×10^{-2}	-3.599×10^{-2}	-3.535×10^{-2}	-3.126×10^{-2}	-2.415×10^{-2}	-1.542×10^{-2}	-7.230×10^{-3}	-1.740×10^{-3}	0
.2857	0	-1.440×10^{-3}	-5.030×10^{-3}	-9.720×10^{-3}	-1.464×10^{-2}	-1.905×10^{-2}	-2.225×10^{-2}	-2.365×10^{-2}	-2.281×10^{-2}	-1.968×10^{-2}	-1.473×10^{-2}	-9.050×10^{-3}	-4.050×10^{-3}	-9.100×10^{-4}	0
.2143	0	-7.700×10^{-4}	-2.820×10^{-3}	-5.600×10^{-3}	-8.550×10^{-3}	-1.117×10^{-2}	-1.304×10^{-2}	-1.375×10^{-2}	-1.308×10^{-2}	-1.104×10^{-2}	-8.020×10^{-3}	-4.720×10^{-3}	-1.980×10^{-3}	-3.900×10^{-4}	0
.1428	0	-3.000×10^{-4}	-1.210×10^{-3}	-2.510×10^{-3}	-3.930×10^{-3}	-5.200×10^{-3}	-6.100×10^{-3}	-6.420×10^{-3}	-6.040×10^{-3}	-5.010×10^{-3}	-3.520×10^{-3}	-1.950×10^{-3}	-7.200×10^{-4}	-1.000×10^{-4}	0
.0714	0	-4.000×10^{-5}	-2.700×10^{-4}	-6.200×10^{-4}	-1.020×10^{-3}	-1.380×10^{-3}	-1.630×10^{-3}	-1.730×10^{-3}	-1.620×10^{-3}	-1.310×10^{-3}	-8.900×10^{-4}	-4.400×10^{-4}	-1.200×10^{-4}	-1.000×10^{-5}	0
0	0	0	0	0	0	0	0	0	0	0	0	0	0	0	0

TABLE 32.- CALCULATED VORTICITY AND STREAM FUNCTION FOR THE SQUARE CAVITY FOR R = 100 - Continued

(d) Nondivergence-form finite-difference calculated vorticity, 57 × 57 points equally spaced

y \ x	0	0.0714	0.1428	0.2143	0.2857	0.3571	0.4286	0.5000	0.5714	0.6428	0.7143	0.7857	0.8571	0.9286	1.0
1.0000	----------		2.099 × 10	1.495 × 10	1.159 × 10	9.338	7.749	6.696	6.187	6.317	7.254	9.314	1.345 × 10	2.537 × 10	----------
.9286	-1.291 × 10	3.805 × 10	6.096	6.718	6.603	6.287	5.937	5.624	5.393	5.296	5.418	5.969	7.587	9.314	-1.784 × 10
.8571	-5.622	-1.630	4.408×10^{-1}	1.520	2.198	2.683	3.072	3.421	3.764	4.128	4.561	5.184	5.861	1.160	-1.650 × 10
.7857	-3.662	-1.808	-4.909×10^{-1}	3.429×10^{-1}	9.494×10^{-1}	1.466	1.960	2.463	2.989	3.544	4.118	4.574	3.743	-2.257	-1.176 × 10
.7143	-2.955	-1.625	-5.830×10^{-1}	1.401×10^{-1}	6.891×10^{-1}	1.180	1.673	2.191	2.729	3.262	3.674	3.538	1.563	-3.278	-7.588
.6428	-2.565	-1.429	-5.405×10^{-1}	9.230×10^{-2}	5.837×10^{-1}	1.036	1.499	1.981	2.448	2.817	2.876	2.133	-7.014×10^{-2}	-3.180	-4.996
.5714	-2.218	-1.235	-4.834×10^{-1}	4.798×10^{-2}	4.615×10^{-1}	8.450 × 10	1.235	1.620	1.941	2.074	1.795	7.996×10^{-1}	-9.464×10^{-1}	-2.610	-3.164
.5000	-1.836	-1.035	-4.318×10^{-1}	-1.229×10^{-2}	3.092×10^{-1}	6.012×10^{-1}	8.847×10^{-1}	1.134	1.281	1.209	7.721×10^{-1}	-1.050×10^{-1}	-1.199	-1.931	-1.921
.4286	-1.421	-8.311×10^{-1}	-3.863×10^{-1}	-8.093×10^{-2}	1.470×10^{-1}	3.443×10^{-1}	5.184×10^{-1}	6.401×10^{-1}	6.515×10^{-1}	4.793×10^{-1}	7.067×10^{-2}	-5.260×10^{-1}	-1.091	-1.325	-1.112
.3571	-1.004	-6.322×10^{-1}	-3.435×10^{-1}	-1.462×10^{-1}	-3.540×10^{-3}	1.126×10^{-1}	2.018×10^{-1}	2.388×10^{-1}	1.865×10^{-1}	1.356×10^{-2}	-2.761×10^{-1}	-6.029×10^{-1}	-8.463×10^{-1}	-8.533×10^{-1}	-6.003×10^{-1}
.2857	-6.233×10^{-1}	-4.492×10^{-1}	-3.008×10^{-1}	-1.995×10^{-1}	-1.298×10^{-1}	-7.603×10^{-1}	-4.025×10^{-2}	-4.022×10^{-2}	-9.653×10^{-2}	-2.169×10^{-1}	-3.807×10^{-1}	-5.323×10^{-1}	-5.961×10^{-1}	-5.159×10^{-1}	-2.831×10^{-1}
.2143	-3.115×10^{-1}	-2.927×10^{-1}	-2.572×10^{-1}	-2.367×10^{-1}	-2.292×10^{-1}	-2.241×10^{-1}	-2.203×10^{-1}	-2.275×10^{-1}	-2.572×10^{-1}	-3.114×10^{-1}	-3.745×10^{-1}	-4.146×10^{-1}	-3.950×10^{-1}	-2.900×10^{-1}	-9.135×10^{-2}
.1428	-9.455×10^{-2}	-1.711×10^{-1}	-2.124×10^{-1}	-2.567×10^{-1}	-3.051×10^{-1}	-3.453×10^{-1}	-3.685×10^{-1}	-3.755×10^{-1}	-3.722×10^{-1}	-3.632×10^{-1}	-3.464×10^{-1}	-3.127×10^{-1}	-2.504×10^{-1}	-1.481×10^{-1}	1.013×10^{-2}
.0714	-6.710×10^{-3}	-8.313×10^{-2}	-1.608×10^{-1}	-2.579×10^{-1}	-3.635×10^{-1}	-4.559×10^{-1}	-5.163×10^{-1}	-5.328×10^{-1}	-5.029×10^{-1}	-4.331×10^{-1}	-3.375×10^{-1}	-2.339×10^{-1}	-1.393×10^{-1}	-5.867×10^{-2}	2.978×10^{-2}
0	0	6.610×10^{-3}	-8.180×10^{-2}	-2.378×10^{-1}	-4.141×10^{-1}	-5.763×10^{-1}	-6.946×10^{-1}	-7.403×10^{-1}	-6.929×10^{-1}	-5.532×10^{-1}	-3.528×10^{-1}	-1.498×10^{-1}	-8.960×10^{-3}	2.866×10^{-2}	0

TABLE 32.- CALCULATED VORTICITY AND STREAM FUNCTION FOR THE SQUARE CAVITY FOR R = 100 – Continued

(e) Divergence-form finite-difference calculated stream function, 65 × 65 points equally spaced

y \ x	0	0.0625	0.1250	0.1815	0.2500	0.3125	0.3570	0.4375	0.5000	0.5625	0.6250	0.6875	0.7500	0.8125	0.8750	0.9375	1.0
1.0000	0	0	0	0	0	0	0	0	0	0	0	0	0	0	0	0	0
.9375	0	-1.449×10^{-2}	-2.717×10^{-2}	-3.465×10^{-2}	-3.958×10^{-2}	-4.316×10^{-2}	-4.590×10^{-2}	-4.802×10^{-2}	-4.957×10^{-2}	-5.055×10^{-2}	-5.085×10^{-2}	-5.035×10^{-2}	-4.876×10^{-2}	-4.559×10^{-2}	-3.932×10^{-2}	-2.429×10^{-2}	0
.8750	0	-9.562×10^{-3}	-2.509×10^{-2}	-3.878×10^{-2}	-4.990×10^{-2}	-5.897×10^{-2}	-6.641×10^{-2}	-7.244×10^{-2}	-7.709×10^{-2}	-8.020×10^{-2}	-8.148×10^{-2}	-8.044×10^{-2}	-7.629×10^{-2}	-6.765×10^{-2}	-5.138×10^{-2}	-2.322×10^{-2}	0
.8125	0	-6.834×10^{-3}	-2.097×10^{-2}	-3.633×10^{-2}	-5.062×10^{-2}	-6.330×10^{-2}	-7.426×10^{-2}	-8.344×10^{-2}	-9.065×10^{-2}	-9.551×10^{-2}	-9.745×10^{-2}	-9.559×10^{-2}	-8.867×10^{-2}	-7.471×10^{-2}	-5.108×10^{-2}	-1.924×10^{-2}	0
.7500	0	-5.554×10^{-3}	-1.825×10^{-2}	-3.353×10^{-2}	-4.891×10^{-2}	-6.329×10^{-2}	-7.614×10^{-2}	-8.708×10^{-2}	-9.567×10^{-2}	-1.013×10^{-1}	-1.030×10^{-1}	-9.984×10^{-2}	-9.013×10^{-2}	-7.215×10^{-2}	-4.521×10^{-2}	-1.514×10^{-2}	0
.6875	0	-4.848×10^{-3}	-1.636×10^{-2}	-3.089×10^{-2}	-4.617×10^{-2}	-6.088×10^{-2}	-7.426×10^{-2}	-8.571×10^{-2}	-9.453×10^{-2}	-9.989×10^{-2}	-1.008×10^{-1}	-9.588×10^{-2}	-8.385×10^{-2}	-6.375×10^{-2}	-3.710×10^{-2}	-1.142×10^{-2}	0
.6250	0	-4.312×10^{-3}	-1.468×10^{-2}	-2.807×10^{-2}	-4.244×10^{-2}	-5.649×10^{-2}	-6.937×10^{-2}	-8.029×10^{-2}	-8.844×10^{-2}	-9.285×10^{-2}	-9.240×10^{-2}	-8.595×10^{-2}	-7.258×10^{-2}	-5.249×10^{-2}	-2.869×10^{-2}	-8.273×10^{-3}	0
.5625	0	-3.780×10^{-3}	-1.292×10^{-2}	-2.483×10^{-2}	-3.773×10^{-2}	-5.043×10^{-2}	-6.204×10^{-2}	-7.171×10^{-2}	-7.856×10^{-2}	-8.160×10^{-2}	-7.982×10^{-2}	-7.236×10^{-2}	-5.894×10^{-2}	-4.070×10^{-2}	$-2.1.0 \times 10^{-2}$	-5.771×10^{-3}	0
.5000	0	-3.203×10^{-3}	-1.097×10^{-2}	-2.116×10^{-2}	-3.224×10^{-2}	-4.314×10^{-2}	-5.300×10^{-2}	-6.099×10^{-2}	-6.626×10^{-2}	-6.791×10^{-2}	-6.513×10^{-2}	-5.746×10^{-2}	-4.520×10^{-2}	-2.994×10^{-2}	-1.484×10^{-2}	-3.883×10^{-3}	0
.4375	0	-2.587×10^{-3}	-8.906×10^{-3}	-1.723×10^{-2}	-2.630×10^{-2}	-3.519×10^{-2}	-4.312×10^{-2}	-4.932×10^{-2}	-5.303×10^{-2}	-5.353×10^{-2}	-5.029×10^{-2}	-4.320×10^{-2}	-3.290×10^{-2}	-2.100×10^{-2}	-1.002×10^{-2}	-2.517×10^{-3}	0
.3750	0	-1.965×10^{-3}	-6.822×10^{-3}	-1.327×10^{-2}	-2.032×10^{-2}	-2.720×10^{-2}	-3.323×10^{-2}	-3.776×10^{-2}	-4.017×10^{-2}	-3.993×10^{-2}	-3.676×10^{-2}	-3.079×10^{-2}	-2.276×10^{-2}	-1.406×10^{-2}	-6.473×10^{-3}	-1.562×10^{-3}	0
.3125	0	-1.376×10^{-3}	-4.853×10^{-3}	-9.537×10^{-3}	-1.469×10^{-2}	-1.969×10^{-2}	-2.402×10^{-2}	-2.714×10^{-2}	-2.859×10^{-2}	-2.802×10^{-2}	-2.532×10^{-2}	-2.072×10^{-2}	-1.491×10^{-2}	-8.924×10^{-3}	-3.957×10^{-3}	-9.094×10^{-4}	0
.2500	0	-8.596×10^{-4}	-3.117×10^{-3}	-6.233×10^{-3}	-9.699×10^{-3}	-1.307×10^{-2}	-1.595×10^{-2}	-1.797×10^{-2}	-1.879×10^{-2}	-1.819×10^{-2}	-1.617×10^{-2}	-1.296×10^{-2}	-9.074×10^{-3}	-5.248×10^{-3}	-2.219×10^{-3}	-4.722×10^{-4}	0
.1875	0	-4.467×10^{-4}	-1.712×10^{-3}	-3.531×10^{-3}	-5.594×10^{-3}	-7.614×10^{-3}	-9.333×10^{-3}	-1.051×10^{-2}	-1.094×10^{-2}	-1.051×10^{-2}	-9.208×10^{-3}	-7.226×10^{-3}	-4.912×10^{-3}	-2.716×10^{-3}	-1.063×10^{-3}	-1.913×10^{-4}	0
.1250	0	-1.615×10^{-4}	-7.092×10^{-4}	-1.553×10^{-3}	-2.535×10^{-3}	-3.509×10^{-3}	-4.341×10^{-3}	-4.909×10^{-3}	-5.109×10^{-3}	-4.878×10^{-3}	-4.222×10^{-3}	-3.241×10^{-3}	-2.121×10^{-3}	-1.093×10^{-3}	-3.642×10^{-4}	-3.438×10^{-5}	0
.0625	0	-1.956×10^{-5}	-1.491×10^{-4}	-3.737×10^{-4}	-6.433×10^{-4}	-9.139×10^{-4}	-1.148×10^{-3}	-1.309×10^{-3}	-1.368×10^{-3}	-1.303×10^{-3}	-1.115×10^{-3}	-8.335×10^{-4}	-5.158×10^{-4}	-2.326×10^{-4}	-4.674×10^{-5}	-1.459×10^{-5}	0
0		0	0	0	0	0	0	0	0	0	0	0	0	0	0	0	0

TABLE 32.- CALCULATED VORTICITY AND STREAM FUNCTION FOR THE SQUARE CAVITY FOR R = 100 - Continued

(f) Divergence-form finite-difference calculated vorticity, 65 × 65 points equally spaced

y \ x	0	0.0625	0.1250	0.1815	0.2500	0.3125	0.3750	0.4375	0.5000	0.5625	0.6250	0.6875	0.7500	0.8125	0.8750	0.9375	1.0
1.0000	----------	4.086 × 10	2.280 × 10	1.639 × 10	1.286 × 10	1.048 × 10	8.753	7.479	6.609	6.115	6.182	6.788	8.140	1.059 × 10	1.537 × 10	2.985	----------
.9375	-1.598 × 10	3.667	7.571	8.004	7.694	7.216	6.725	6.274	5.891	5.548	5.439	5.455	5.754	6.591	8.676	9.828	-2.996
.8750	-6.836	-1.847	7.319×10^{-1}	1.986	2.692	3.134	3.440	3.676	3.882	4.083	4.303	4.574	4.971	5.664	6.317	7.905×10^{-1}	-1.827×10
.8125	-4.256	-2.136	-6.314×10^{-1}	3.006×10^{-1}	9.452×10^{-1}	1.452	1.893	2.309	2.719	3.139	3.577	4.043	4.548	4.953	3.889	-2.755	-1.289×10
.7500	-3.303	-1.934	-8.273×10^{-1}	-5.295×10^{-2}	5.156×10^{-1}	9.865×10^{-1}	1.424	1.861	2.313	2.785	3.271	3.748	4.109	3.887	1.649	-3.868	-9.290
.6875	-2.847	-1.725	-7.959×10^{-1}	-1.121×10^{-1}	4.055×10^{-1}	8.458×10^{-1}	1.267	1.699	2.147	2.602	3.035	3.369	3.383	2.521	-3.220×10^{-2}	-3.873	-6.579
.6250	-2.527	-1.533	-7.225×10^{-1}	-1.207×10^{-1}	3.396×10^{-1}	7.380×10^{-1}	1.127	1.527	1.934	2.320	2.626	2.727	2.369	1.167	-1.037	-3.369	-4.531
.5625	-2.216	-1.343	-6.446×10^{-1}	-1.313×10^{-1}	2.602×10^{-1}	6.000×10^{-1}	9.321×10^{-1}	1.269	1.594	1.866	2.004	1.877	1.296	1.201×10^{-1}	-1.448	-2.683	-3.026
.5000	-1.875	-1.146	-5.698×10^{-1}	-1.518×10^{-1}	1.633×10^{-1}	4.336×10^{-1}	6.923×10^{-1}	9.431×10^{-1}	1.163	1.304	1.291	1.024	4.174×10^{-1}	-4.999×10^{-1}	-1.453	-2.003	-1.955
.4375	-1.507	-9.437×10^{-1}	-4.989×10^{-1}	-1.788×10^{-1}	5.882×10^{-2}	2.577×10^{-1}	4.401×10^{-1}	6.031×10^{-1}	7.225×10^{-1}	7.562×10^{-1}	6.500×10^{-1}	3.529×10^{-1}	-1.433×10^{-1}	-7.464×10^{-1}	-1.246	-1.420	-1.218
.3750	-1.132	-7.439×10^{-1}	-4.312×10^{-1}	-2.062×10^{-1}	-4.185×10^{-2}	9.139×10^{-2}	2.069×10^{-1}	2.984×10^{-1}	3.446×10^{-1}	3.159×10^{-1}	1.827×10^{-1}	-6.782×10^{-2}	-4.082×10^{-1}	-7.511×10^{-1}	-9.687×10^{-1}	-9.615×10^{-1}	-7.214×10^{-1}
.3125	-7.776×10^{-1}	-5.552×10^{-1}	-3.659×10^{-1}	-2.286×10^{-1}	-1.304×10^{-1}	-5.332×10^{-2}	1.013×10^{-2}	5.351×10^{-2}	6.066×10^{-2}	1.333×10^{-2}	-1.000×10^{-1}	-2.736×10^{-1}	-4.741×10^{-1}	-6.404×10^{-1}	-7.036×10^{-1}	-6.206×10^{-1}	-3.930×10^{-1}
.2500	-4.678×10^{-1}	-3.869×10^{-1}	-3.038×10^{-1}	-2.429×10^{-1}	-2.026×10^{-1}	-1.729×10^{-1}	-1.488×10^{-1}	-1.338×10^{-1}	-1.393×10^{-1}	-1.763×10^{-1}	-2.481×10^{-1}	-3.449×10^{-1}	-4.411×10^{-1}	-4.998×10^{-1}	-4.857×10^{-1}	-3.786×10^{-1}	-1.787×10
.1875	-2.228×10^{-1}	-2.472×10^{-1}	-2.457×10^{-1}	-2.475×10^{-1}	-2.578×10^{-1}	-2.701×10^{-1}	-2.782×10^{-1}	-2.821×10^{-1}	-2.876×10^{-1}	-3.018×10^{-1}	-3.270×10^{-1}	-3.577×10^{-1}	-3.795×10^{-1}	-3.736×10^{-1}	-3.224×10^{-1}	-2.148×10^{-1}	-4.481×10^{-2}
.1250	-5.867×10^{-2}	-1.414×10^{-2}	-1.913×10^{-1}	-2.411×10^{-1}	-2.966×10^{-1}	-3.501×10^{-1}	-3.914×10^{-1}	-4.148×10^{-1}	-4.202×10^{-1}	-4.112×10^{-1}	-3.917×10^{-1}	-3.636×10^{-1}	-3.255×10^{-1}	-2.738×10^{-1}	-2.041×10^{-1}	-1.098×10^{-1}	2.319×10^{-2}
.0625	1.102×10^{-2}	-6.582×10^{-2}	-1.337×10^{-1}	-2.202×10^{-1}	-3.205×10^{-1}	-4.195×10^{-1}	-5.017×10^{-1}	-5.540×10^{-1}	-5.683×10^{-1}	-5.421×10^{-1}	-4.792×10^{-1}	-3.897×10^{-1}	-2.878×10^{-1}	-1.895×10^{-1}	-1.070×10^{-1}	-4.139×10^{-2}	2.746×10^{-2}
0	0	1.082×10^{-2}	-5.194×10^{-2}	-1.782×10^{-1}	-3.326×10^{-1}	-4.887×10^{-1}	-6.253×10^{-1}	-7.221×10^{-1}	-7.594×10^{-1}	-7.233×10^{-1}	-6.125×10^{-1}	-4.444×10^{-1}	-2.548×10^{-1}	-8.932×10^{-1}	1.093×10^{-2}	2.689×10^{-2}	0

TABLE 32.- CALCULATED VORTICITY AND STREAM FUNCTION FOR THE SQUARE CAVITY FOR R = 100 – Continued

(g) SADI calculated stream function, 19 × 19 points unequally spaced

x / y	0	0.0201	0.0482	0.0877	0.1428	0.2143	0.2857	0.3571	0.4286	0.5000	0.5714	0.6428	0.7143	0.7857	0.8571	0.9123	0.9517	0.9799	1.0
0	0	0	0	0	0	0	0	0	0	0	0	0	0	0	0	0	0	0	0
.9799	0	-5.558×10^{-3}	-1.167×10^{-2}	-1.461×10^{-2}	-1.627×10^{-2}	-1.729×10^{-2}	-1.790×10^{-2}	-1.832×10^{-2}	-1.862×10^{-2}	-1.883×10^{-2}	-1.892×10^{-2}	-1.890×10^{-2}	-1.874×10^{-2}	-1.838×10^{-2}	-1.764×10^{-2}	-1.636×10^{-2}	-1.368×10^{-2}	-6.871×10^{-3}	0
.9517	0	-3.149×10^{-3}	-1.204×10^{-2}	-2.126×10^{-2}	-2.814×10^{-2}	-3.298×10^{-2}	-3.602×10^{-2}	-3.818×10^{-2}	-3.977×10^{-2}	-4.087×10^{-2}	-4.146×10^{-2}	-4.148×10^{-2}	-4.076×10^{-2}	-3.905×10^{-2}	-3.551×10^{-2}	-2.924×10^{-2}	-1.824×10^{-2}	-5.278×10^{-3}	0
.9123	0	-1.762×10^{-3}	-8.216×10^{-3}	-1.926×10^{-2}	-3.118×10^{-2}	-4.286×10^{-2}	-5.057×10^{-2}	-5.634×10^{-2}	-6.073×10^{-2}	-6.390×10^{-2}	-6.576×10^{-2}	-6.608×10^{-2}	-6.442×10^{-2}	-6.003×10^{-2}	-5.068×10^{-2}	-3.534×10^{-2}	-1.688×10^{-2}	-3.852×10^{-3}	0
.8571	0	-1.026×10^{-3}	-5.254×10^{-3}	-1.433×10^{-2}	-2.857×10^{-2}	-4.498×10^{-2}	-5.830×10^{-2}	-6.906×10^{-2}	-7.763×10^{-2}	-8.403×10^{-2}	-8.799×10^{-2}	-8.891×10^{-2}	-8.585×10^{-2}	-7.715×10^{-2}	-5.896×10^{-2}	-3.465×10^{-2}	-1.399×10^{-2}	-2.888×10^{-3}	0
.7857	0	-6.970×10^{-4}	-3.727×10^{-3}	-1.091×10^{-2}	-2.411×10^{-2}	-4.245×10^{-2}	-5.954×10^{-2}	-7.443×10^{-2}	-8.680×10^{-2}	-9.624×10^{-2}	-1.021×10^{-1}	-1.031×10^{-1}	-9.784×10^{-2}	-8.363×10^{-2}	-5.726×10^{-2}	-2.942×10^{-2}	-1.075×10^{-2}	-2.084×10^{-3}	0
.7143	0	-5.796×10^{-4}	-3.126×10^{-3}	-9.343×10^{-3}	-2.138×10^{-2}	-3.943×10^{-2}	-5.747×10^{-2}	-7.393×10^{-2}	-8.791×10^{-2}	-9.852×10^{-2}	-1.046×10^{-1}	-1.047×10^{-1}	-9.675×10^{-2}	-7.837×10^{-2}	-4.902×10^{-2}	-2.310×10^{-2}	-7.949×10^{-3}	-1.485×10^{-3}	0
.6428	0	-5.115×10^{-4}	-2.762×10^{-3}	-8.297×10^{-3}	-1.920×10^{-2}	-3.604×10^{-2}	-5.342×10^{-2}	-6.962×10^{-2}	-8.341×10^{-2}	-9.358×10^{-2}	-9.869×10^{-2}	-9.699×10^{-2}	-8.663×10^{-2}	-6.642×10^{-2}	-3.852×10^{-2}	-1.702×10^{-2}	-5.606×10^{-3}	-1.017×10^{-3}	0
.5714	0	-4.473×10^{-4}	-2.415×10^{-3}	-7.259×10^{-3}	-1.686×10^{-2}	-3.184×10^{-2}	-4.750×10^{-2}	-6.216×10^{-2}	-7.448×10^{-2}	-8.308×10^{-2}	-8.642×10^{-2}	-8.291×10^{-2}	-7.129×10^{-2}	-5.185×10^{-2}	-2.821×10^{-2}	-1.183×10^{-2}	-3.763×10^{-3}	-6.667×10^{-4}	0
.5000	0	-3.743×10^{-4}	-2.021×10^{-3}	-6.082×10^{-3}	-1.415×10^{-2}	-2.680×10^{-2}	-4.005×10^{-2}	-5.239×10^{-2}	-6.247×10^{-2}	-6.894×10^{-2}	-7.042×10^{-2}	-6.570×10^{-2}	-5.436×10^{-2}	-3.767×10^{-2}	-1.941×10^{-2}	-7.902×10^{-3}	-2.406×10^{-3}	-4.170×10^{-4}	0
.4286	0	-2.929×10^{-4}	-1.586×10^{-3}	-4.788×10^{-3}	-1.118×10^{-2}	-2.124×10^{-2}	-3.177×10^{-2}	-4.143×10^{-2}	-4.903×10^{-2}	-5.339×10^{-2}	-5.341×10^{-2}	-4.842×10^{-2}	-3.861×10^{-2}	-2.562×10^{-2}	-1.259×10^{-2}	-4.874×10^{-3}	-1.461×10^{-3}	-2.477×10^{-4}	0
.3571	0	-2.096×10^{-4}	-1.142×10^{-3}	-3.473×10^{-3}	-8.174×10^{-3}	-1.563×10^{-2}	-2.431×10^{-2}	-3.045×10^{-2}	-3.575×10^{-2}	-3.838×10^{-2}	-3.761×10^{-2}	-3.316×10^{-2}	-2.556×10^{-2}	-1.631×10^{-2}	-7.677×10^{-3}	-2.861×10^{-3}	-8.311×10^{-4}	-1.373×10^{-4}	0
.2857	0	-1.323×10^{-4}	-7.299×10^{-4}	-2.252×10^{-3}	-5.384×10^{-3}	-1.042×10^{-2}	-1.571×10^{-2}	-2.042×10^{-2}	-2.383×10^{-2}	-2.527×10^{-2}	-2.431×10^{-2}	-2.090×10^{-2}	-1.561×10^{-2}	-9.591×10^{-2}	-4.307×10^{-3}	-1.530×10^{-3}	-4.246×10^{-4}	-6.721×10^{-5}	0
.2143	0	-6.803×10^{-5}	-3.865×10^{-4}	-1.231×10^{-3}	-3.035×10^{-3}	-6.021×10^{-3}	-9.189×10^{-3}	-1.200×10^{-2}	-1.397×10^{-2}	-1.469×10^{-2}	-1.392×10^{-2}	-1.170×10^{-2}	-8.478×10^{-3}	-4.992×10^{-3}	-2.100×10^{-3}	-6.858×10^{-4}	-1.721×10^{-4}	-2.428×10^{-5}	0
.1428	0	-2.264×10^{-5}	-1.414×10^{-4}	-4.914×10^{-4}	-1.301×10^{-3}	-2.708×10^{-3}	-4.233×10^{-3}	-5.591×10^{-3}	-6.532×10^{-3}	-6.846×10^{-3}	-6.417×10^{-3}	-5.389×10^{-3}	-3.703×10^{-3}	-2.055×10^{-3}	-7.668×10^{-4}	-2.004×10^{-4}	-3.252×10^{-5}	-1.245×10^{-6}	0
.0877	0	-3.407×10^{-6}	-3.354×10^{-5}	-1.496×10^{-4}	-4.553×10^{-4}	-1.017×10^{-3}	-1.638×10^{-3}	-2.197×10^{-3}	-2.585×10^{-3}	-2.713×10^{-3}	-2.530×10^{-3}	-2.054×10^{-3}	-1.393×10^{-3}	-7.208×10^{-4}	-2.204×10^{-4}	-2.741×10^{-5}	9.607×10^{-6}	4.551×10^{-6}	0
.0482	0	1.168×10^{-6}	-2.216×10^{-6}	-3.194×10^{-5}	-1.252×10^{-4}	-3.053×10^{-4}	-5.068×10^{-4}	-6.892×10^{-4}	-8.173×10^{-4}	-8.606×10^{-4}	-8.007×10^{-4}	-6.431×10^{-4}	-4.240×10^{-4}	-2.037×10^{-4}	-4.564×10^{-5}	7.514×10^{-6}	1.034×10^{-5}	3.087×10^{-6}	0
.0201	0	6.493×10^{-7}	1.172×10^{-6}	-3.106×10^{-6}	-1.956×10^{-5}	-5.240×10^{-5}	-8.938×10^{-5}	-1.230×10^{-4}	-1.468×10^{-4}	-1.552×10^{-4}	-1.442×10^{-4}	-1.149×10^{-4}	-7.398×10^{-5}	-3.305×10^{-5}	-4.464×10^{-6}	3.991×10^{-6}	3.045×10^{-6}	7.754×10^{-7}	0
0	0	0	0	0	0	0	0	0	0	0	0	0	0	0	0	0	0	0	0

TABLE 32.- CALCULATED VORTICITY AND STREAM FUNCTION FOR THE SQUARE CAVITY FOR R = 100 – Concluded

(h) SADI calculated vorticity, 19 × 19 points unequally spaced

y \ x	0	0.0201	0.0482	0.0877	0.1428	0.2143	0.2857	0.3571	0.4286	0.5000	0.5714	0.6428	0.7143	0.7857	0.8571	0.9123	0.9517	0.9799	1.0
1.0000	----------	1.076×10^{2}	5.022×10^{2}	2.991×10	2.006×10	1.435×10	1.109×10	8.870	7.310	6.297	5.848	6.045	7.056	9.086	1.323×10	2.017×10	3.591×10	9.549×10	----------
.9799	-4.751×10	1.332×10	2.832×10	2.242×10	1.711×10	1.311×10	1.057×10	8.762	7.418	6.464	5.904	5.808	6.276	7.582	1.030×10	1.580×10	2.748×10	2.295×10	-5.973×10
.9517	-1.985×10	-9.382	4.485	1.061×10	1.101×10	9.884	8.694	7.675	6.831	6.166	5.701	5.491	5.619	6.318	8.225	1.255×10	1.256×10	-9.458	-3.542×10
.9123	-9.916	-6.472	-2.682	1.370	4.007	5.093	5.342	5.314	5.195	5.062	4.963	4.944	5.073	5.566	7.220	8.397	6.179×10^{-1}	-1.259×10	-2.235×10
.8571	-5.466	-4.459	-2.964	-1.364	1.835×10^{-1}	1.418	2.188	2.725	3.142	3.502	3.839	4.177	4.559	5.206	6.061	3.252	4.297	-1.116×10	-1.590×10
.7857	-3.616	-3.128	-2.457	-1.567	-6.139×10^{-1}	2.502×10^{-1}	8.973×10^{-1}	1.453	1.982	2.514	3.063	3.628	4.217	4.748	3.799	-4.883×10^{-1}	-5.409	-8.867	-1.104×10
.7143	-2.996	-2.617	-2.088	-1.410	-6.214×10^{-1}	1.307×10^{-1}	7.021×10^{-1}	1.211	1.722	2.259	2.821	3.383	3.839	3.693	1.552	-2.094	-4.979	-6.681	-7.688
.6428	-2.643	-2.301	-1.838	-1.245	-5.588×10^{-1}	1.082×10^{-1}	6.275×10^{-1}	1.102	1.586	2.088	2.579	2.977	3.047	2.233	-7.392×10^{-2}	-2.542	-4.037	-4.783	-5.166
.5714	-2.314	-2.008	-1.598	-1.084	-4.957×10^{-1}	6.985×10^{-2}	5.119×10^{-1}	9.214×10^{-1}	1.338	1.748	2.092	2.237	1.933	8.638×10^{-1}	-9.533×10^{-1}	-2.356	-3.016	-3.252	-3.330
.5000	-1.935	-1.681	-1.342	-9.188×10^{-1}	-4.425×10^{-1}	7.976×10^{-3}	3.554×10^{-1}	6.723×10^{-1}	9.812×10^{-1}	1.254	1.415	1.337	8.617×10^{-1}	-7.653×10^{-2}	-1.226	-1.892	-2.100	-2.103	-2.050
.4286	-1.512	-1.322	-1.069	-7.523×10^{-1}	-3.977×10^{-1}	-6.692×10^{-2}	1.818×10^{-1}	3.989×10^{-1}	5.923×10^{-1}	7.285×10^{-1}	7.428×10^{-1}	5.539×10^{-1}	1.086×10^{-1}	-5.322×10^{-1}	-1.134	-1.377	-1.377	-1.291	-1.198
.3571	-1.077	-9.577×10^{-1}	-7.954×10^{-1}	-5.896×10^{-1}	-3.568×10^{-1}	-1.412×10^{-1}	1.608×10^{-2}	1.452×10^{-2}	2.452×10^{-1}	2.873×10^{-1}	2.296×10^{-1}	3.853×10^{-2}	-2.780×10^{-1}	-6.375×10^{-1}	-8.921×10^{-1}	-9.277×10^{-1}	-8.498×10^{-1}	-7.446×10^{-1}	-6.499×10^{-1}
.2857	-6.731×10^{-1}	-6.191×10^{-1}	-5.417×10^{-1}	-4.379×10^{-1}	-3.163×10^{-1}	-2.041×10^{-1}	-1.258×10^{-1}	-8.514×10^{-2}	-2.511×10^{-2}	-2.578×10^{-2}	-8.971×10^{-2}	-2.238×10^{-1}	-4.032×10^{-1}	-5.663×10^{-1}	-6.345×10^{-1}	-5.843×10^{-1}	-4.875×10^{-1}	-3.889×10^{-1}	-3.066×10^{-1}
.2143	-3.383×10^{-1}	-3.364×10^{-1}	-3.268×10^{-1}	-3.049×10^{-1}	-2.744×10^{-1}	-2.496×10^{-1}	-2.386×10^{-1}	-2.311×10^{-1}	-2.265×10^{-1}	-2.355×10^{-1}	-2.705×10^{-1}	-3.322×10^{-1}	-4.019×10^{-1}	-4.450×10^{-1}	-4.233×10^{-1}	-3.448×10^{-1}	-2.521×10^{-1}	-1.672×10^{-1}	-9.843×10^{-2}
.1428	-1.033×10^{-1}	-1.338×10^{-1}	-1.663×10^{-1}	-1.969×10^{-1}	-2.296×10^{-1}	-2.751×10^{-1}	-3.248×10^{-1}	-3.661×10^{-1}	-3.899×10^{-1}	-3.974×10^{-1}	-3.951×10^{-1}	-3.875×10^{-1}	-3.711×10^{-1}	-3.359×10^{-1}	-2.695×10^{-1}	-1.889×10^{-1}	-1.116×10^{-1}	-4.379×10^{-2}	1.096×10^{-2}
.0877	-6.433×10^{-2}	-4.279×10^{-2}	-8.363×10^{-2}	-1.286×10^{-1}	-1.889×10^{-1}	-2.795×10^{-1}	-3.769×10^{-1}	-4.607×10^{-1}	-5.129×10^{-1}	-5.250×10^{-1}	-4.977×10^{-1}	-4.385×10^{-1}	-3.580×10^{-1}	-2.676×10^{-1}	-1.761×10^{-1}	-1.049×10^{-1}	-4.951×10^{-2}	-3.511×10^{-3}	3.392×10^{-2}
.0482	1.256×10^{-2}	-1.213×10^{-2}	-4.120×10^{-2}	-8.067×10^{-2}	-1.515×10^{-1}	-2.737×10^{-1}	-4.090×10^{-1}	-5.290×10^{-1}	-6.088×10^{-1}	-6.311×10^{-1}	-5.895×10^{-1}	-4.915×10^{-1}	-3.585×10^{-1}	-2.212×10^{-1}	-1.095×10^{-1}	-5.029×10^{-2}	-1.843×10^{-2}	3.581×10^{-3}	2.035×10^{-2}
.0201	5.165×10^{-3}	-1.364×10^{-3}	-1.183×10^{-2}	-4.005×10^{-2}	-1.171×10^{-1}	-2.649×10^{-1}	-4.311×10^{-1}	-5.811×10^{-1}	-6.855×10^{-1}	-7.194×10^{-1}	-6.692×10^{-1}	-5.406×10^{-1}	-3.630×10^{-1}	-1.842×10^{-1}	-5.403×10^{-2}	-6.096×10^{-3}	3.196×10^{-3}	4.346×10^{-3}	4.668×10^{-3}
0	0	5.152×10^{-3}	1.249×10^{-2}	-5.197×10^{-3}	-8.790×10^{-2}	-2.567×10^{-1}	-4.472×10^{-1}	-6.209×10^{-1}	-7.452×10^{-1}	-7.894×10^{-1}	-7.334×10^{-1}	-5.808×10^{-1}	-3.673×10^{-1}	-1.544×10^{-1}	-8.233×10^{-3}	3.065×10^{-2}	2.009×10^{-2}	4.663×10^{-3}	0

TABLE 33.- COMPARISON OF RESULTS FOR THE 2 × 1 RECTANGULAR CAVITY FOR R = 100

(a) Vorticity at center of moving wall

Calculation method	Points	Vorticity
Spline	29 × 15	7.1603
Finite difference, divergence form	33 × 17	7.3929

(b) Upper vortex maximum stream function

Calculation method	Points	Upper-vortex maximum stream function
Spline	29 × 15	-0.10625
Finite difference, divergence form	33 × 17	-.99286
Reference 8	21 × 21	-.10204

(c) Lower vortex maximum stream function

Calculation method	Points	Lower-vortex maximum stream function
Spline	29 × 15	0.00094
Finite difference, divergence form	33 × 17	.00059
Reference 8	21 × 21	.00062

TABLE 34.- CALCULATED VORTICITY AND STREAM FUNCTION FOR THE 2 × 1 RECTANGULAR CAVITY FOR R = 100

(a) SADI calculated stream function, 29 × 15 points equally spaced

y \ x	0	0.0714	0.1428	0.2143	0.2857	0.3571	0.4286	0.5000	0.5714	0.6428	0.7143	0.7857	0.8571	0.9286	1.0
2.0000	0	0	0	0	0	0	0	0	0	0	0	0	0	0	0
1.8571	0	-9.805×10^{-3}	-2.805×10^{-2}	-4.436×10^{-2}	-5.752×10^{-2}	-6.822×10^{-2}	-7.682×10^{-2}	-8.335×10^{-2}	-8.757×10^{-2}	-8.890×10^{-2}	-8.644×10^{-2}	-7.850×10^{-2}	-6.065×10^{-2}	-2.721×10^{-2}	0
1.7143	0	-6.346×10^{-3}	-2.116×10^{-2}	-3.927×10^{-2}	-5.747×10^{-2}	-7.413×10^{-2}	-8.833×10^{-2}	-9.921×10^{-2}	-1.057×10^{-1}	-1.062×10^{-1}	-9.887×10^{-2}	-8.097×10^{-2}	-5.148×10^{-2}	-1.752×10^{-2}	0
1.5714	0	-5.117×10^{-3}	-1.736×10^{-2}	-3.293×10^{-2}	-4.923×10^{-2}	-6.449×10^{-2}	-7.732×10^{-2}	-8.636×10^{-2}	-9.007×10^{-2}	-8.681×10^{-2}	-7.521×10^{-2}	-5.531×10^{-2}	-3.057×10^{-2}	-8.919×10^{-3}	0
1.4286	0	-3.696×10^{-3}	-1.256×10^{-2}	-2.382×10^{-2}	-3.550×10^{-2}	-4.609×10^{-2}	-5.433×10^{-2}	-5.902×10^{-2}	-5.905×10^{-2}	-5.365×10^{-2}	-4.300×10^{-2}	-2.877×10^{-2}	-1.432×10^{-2}	-3.752×10^{-3}	0
1.2857	0	-2.186×10^{-3}	-7.497×10^{-3}	-1.424×10^{-2}	-2.107×10^{-2}	-2.690×10^{-2}	-3.088×10^{-2}	-3.230×10^{-2}	-3.077×10^{-2}	-2.632×10^{-2}	-1.966×10^{-2}	-1.216×10^{-2}	-5.558×10^{-3}	-1.323×10^{-3}	0
1.1428	0	-1.014×10^{-3}	-3.565×10^{-3}	-6.855×10^{-3}	-1.012×10^{-2}	-1.274×10^{-2}	-1.425×10^{-2}	-1.436×10^{-2}	-1.303×10^{-2}	-1.052×10^{-2}	-7.332×10^{-3}	-4.171×10^{-3}	-1.709×10^{-3}	-3.457×10^{-3}	0
1.0000	0	-3.292×10^{-4}	-1.230×10^{-3}	-2.449×10^{-3}	-3.667×10^{-3}	-4.591×10^{-3}	-5.016×10^{-3}	-4.855×10^{-3}	-4.152×10^{-3}	-3.079×10^{-3}	-1.894×10^{-3}	-8.759×10^{-4}	-2.297×10^{-4}	1.883×10^{-6}	0
.8571	0	-2.507×10^{-5}	-1.549×10^{-4}	-3.826×10^{-4}	-6.284×10^{-4}	-7.977×10^{-4}	-8.226×10^{-4}	-6.843×10^{-4}	-4.186×10^{-4}	-1.049×10^{-4}	1.577×10^{-4}	2.855×10^{-4}	2.479×10^{-4}	1.004×10^{-4}	0
.7143	0	6.816×10^{-5}	2.001×10^{-4}	3.325×10^{-4}	4.482×10^{-4}	5.517×10^{-4}	6.495×10^{-4}	7.369×10^{-4}	7.958×10^{-4}	7.989×10^{-4}	7.215×10^{-4}	5.565×10^{-4}	3.288×10^{-4}	1.058×10^{-4}	0
.5714	0	7.210×10^{-5}	2.361×10^{-4}	4.313×10^{-4}	6.188×10^{-4}	7.751×10^{-4}	8.858×10^{-4}	9.397×10^{-4}	9.279×10^{-4}	8.452×10^{-4}	6.941×10^{-4}	4.905×10^{-4}	2.681×10^{-4}	8.066×10^{-4}	0
.4286	0	4.897×10^{-5}	1.672×10^{-4}	3.160×10^{-4}	4.639×10^{-4}	5.877×10^{-4}	6.708×10^{-4}	7.031×10^{-4}	6.798×10^{-4}	6.023×10^{-4}	4.789×10^{-4}	3.269×10^{-4}	1.723×10^{-4}	5.002×10^{-5}	0
.2857	0	2.377×10^{-5}	8.445×10^{-5}	1.644×10^{-4}	2.464×10^{-4}	3.160×10^{-4}	3.623×10^{-4}	3.789×10^{-4}	3.632×10^{-4}	3.173×10^{-4}	2.474×10^{-4}	1.647×10^{-4}	8.418×10^{-5}	2.353×10^{-5}	0
.1428	0	5.613×10^{-6}	2.239×10^{-5}	4.650×10^{-5}	7.226×10^{-5}	9.448×10^{-5}	1.093×10^{-4}	1.144×10^{-4}	1.091×10^{-4}	9.407×10^{-5}	7.169×10^{-5}	4.591×10^{-5}	2.194×10^{-5}	5.443×10^{-6}	0
0	0	0	0	0	0	0	0	0	0	0	0	0	0	0	0

TABLE 34.- CALCULATED VORTICITY AND STREAM FUNCTION FOR THE 2 × 1 RECTANGULAR CAVITY FOR R = 100 – Concluded

(b) SADI calculated vorticity, 29 × 15 points equally spaced

y \ x	0	0.0714	0.1428	0.2143	0.2857	0.3571	0.4286	0.5000	0.5714	0.6428	0.7143	0.7857	0.8571	0.9286	1.0
2.0000	----------	3.293 × 10	2.130 × 10	1.591 × 10	1.253 × 10	1.015 × 10	8.404	7.160	6.407	6.202	6.677	8.026	1.114 × 10	2.418 × 10	----------
1.8571	-5.062	-2.301	6.570×10^{-2}	1.364	2.112	2.629	3.031	3.377	3.704	4.042	4.439	5.186	6.292	1.825	-1.669×10
1.7143	-2.924	-1.685	-6.642×10^{-1}	7.726×10^{-2}	6.473×10^{-1}	1.151	1.650	2.175	2.731	3.306	3.828	3.842	1.887	-3.078	-8.805
1.5714	-2.329	-1.340	-5.403×10^{-1}	4.972×10^{-2}	5.107×10^{-1}	9.297×10^{-1}	1.353	1.778	2.150	2.345	2.107	1.073	-8.344×10^{-1}	-2.809	-3.931
1.4286	-1.679	-9.823×10^{-1}	-4.307×10^{-1}	-3.968×10^{-2}	2.464×10^{-1}	4.834×10^{-1}	6.921×10^{-1}	8.481×10^{-1}	8.838×10^{-1}	7.046×10^{-1}	2.355×10^{-1}	-4.799×10^{-1}	-1.195	-1.565	-1.492
1.2857	-9.823×10^{-1}	-6.243×10^{-1}	-3.311×10^{-1}	-1.243×10^{-1}	1.071×10^{-2}	9.439×10^{-2}	1.334×10^{-1}	1.169×10^{-1}	2.547×10^{-2}	-1.504×10^{-1}	-3.864×10^{-1}	-6.126×10^{-1}	-7.343×10^{-1}	-6.820×10^{-1}	-4.708×10^{-1}
1.1428	-4.432×10^{-1}	-3.310×10^{-1}	-2.253×10^{-1}	-1.453×10^{-1}	-9.820×10^{-2}	-8.230×10^{-2}	-9.498×10^{-2}	-1.344×10^{-1}	-1.965×10^{-1}	-2.703×10^{-1}	-3.358×10^{-1}	-3.669×10^{-1}	-3.410×10^{-1}	-2.464×10^{-1}	-9.433×10^{-2}
1.0000	-1.344×10^{-1}	-1.371×10^{-1}	-1.270×10^{-1}	-1.142×10^{-1}	-1.080×10^{-1}	-1.118×10^{1}	-1.254×10^{-1}	-1.461×10^{-1}	-1.689×10^{-1}	-1.869×10^{-1}	-1.919×10^{-1}	-1.762×10^{-1}	-1.343×10^{-1}	-6.449×10^{-2}	2.778×10^{-2}
.8571	-2.320×10^{-3}	-3.486×10^{-2}	-5.591×10^{-2}	-6.849×10^{-2}	-7.764×10^{-2}	-8.616×10^{-2}	-9.476×10^{-2}	-1.024×10^{-1}	-1.071×10^{-1}	-1.059×10^{-1}	-9.625×10^{-2}	-7.563×10^{-2}	-4.287×10^{-2}	1.965×10^{-3}	5.599×10^{-2}
.7143	3.488×10^{-2}	6.337×10^{-3}	-1.606×10^{-2}	-3.238×10^{-2}	-4.421×10^{-2}	-5.273×10^{-2}	-5.843×10^{-2}	-6.119×10^{-2}	-6.041×10^{-2}	-5.524×10^{-2}	-4.489×10^{-2}	-2.879×10^{-2}	-6.852×10^{-3}	2.041×10^{-2}	5.137×10^{-2}
.5714	3.377×10^{-2}	1.610×10^{-2}	8.449×10^{-4}	-1.139×10^{-2}	-2.070×10^{-2}	-2.724×10^{-2}	-3.115×10^{-2}	-3.241×10^{-2}	-3.090×10^{-2}	-2.647×10^{-2}	-1.899×10^{-2}	-8.477×10^{-3}	4.819×10^{-3}	2.034×10^{-2}	3.716×10^{-2}
.4286	2.208×10^{-2}	1.340×10^{-2}	5.310×10^{-3}	-1.699×10^{-3}	-7.303×10^{-3}	-1.133×10^{-2}	-1.371×10^{-2}	-1.439×10^{-2}	-1.337×10^{-2}	-1.063×10^{-2}	-6.268×10^{-3}	-4.244×10^{-4}	6.607×10^{-3}	1.437×10^{-2}	2.234×10^{-2}
.2857	1.032×10^{-2}	7.678×10^{-3}	4.832×10^{-3}	2.084×10^{-3}	-2.432×10^{-3}	-1.959×10^{-3}	-2.972×10^{-3}	-3.251×10^{-3}	-2.799×10^{-3}	-1.639×10^{-3}	1.711×10^{-4}	2.512×10^{-3}	5.168×10^{-3}	7.805×10^{-3}	1.014×10^{-2}
.1428	2.109×10^{-3}	3.038×10^{-3}	3.501×10^{-3}	3.807×10^{-3}	4.156×10^{-3}	4.522×10^{-3}	4.810×10^{-3}	4.936×10^{-3}	4.862×10^{-3}	4.613×10^{-3}	4.263×10^{-3}	3.902×10^{-3}	3.555×10^{-3}	3.026×10^{-3}	2.017×10^{-3}
0	0	2.458×10^{-4}	2.007×10^{-3}	5.011×10^{-3}	8.347×10^{-3}	1.128×10^{-2}	1.318×10^{-2}	1.383×10^{-2}	1.312×10^{-2}	1.114×10^{-2}	8.219×10^{-3}	4.891×10^{-3}	1.926×10^{-3}	2.194×10^{-4}	0

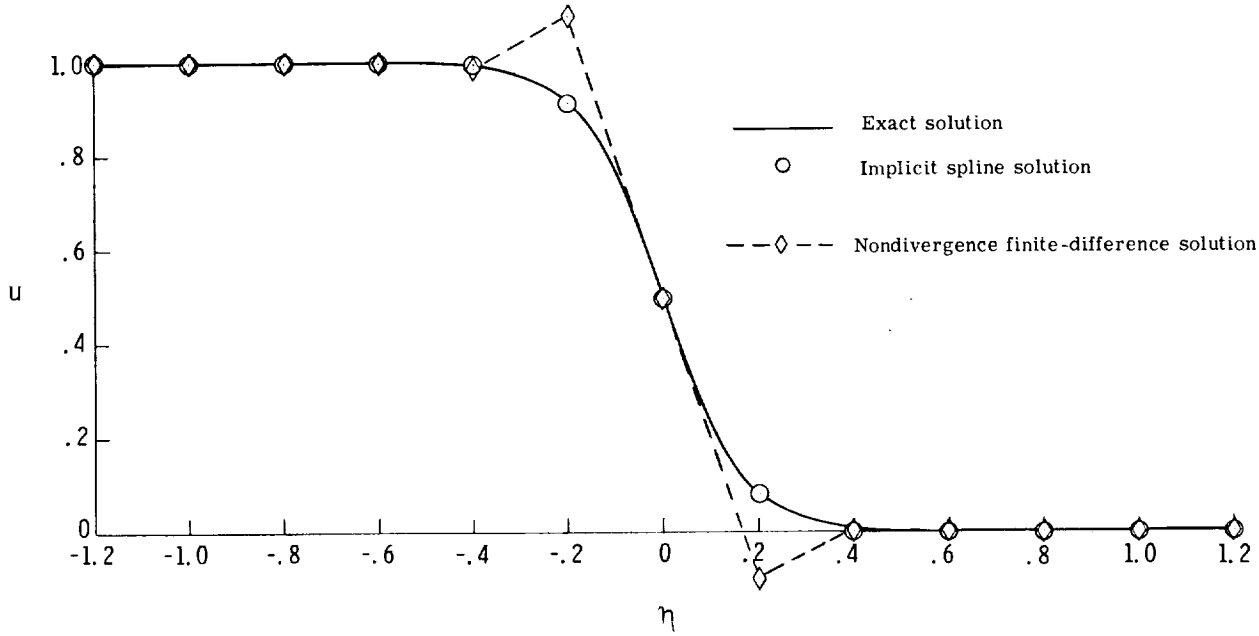

Figure 1.- Comparison of implicit spline and nondivergence finite-difference solutions with the exact solution to Burgers' equation for 51 points, $\nu = 1/24$, equal spacing, and $\sigma = 0$.

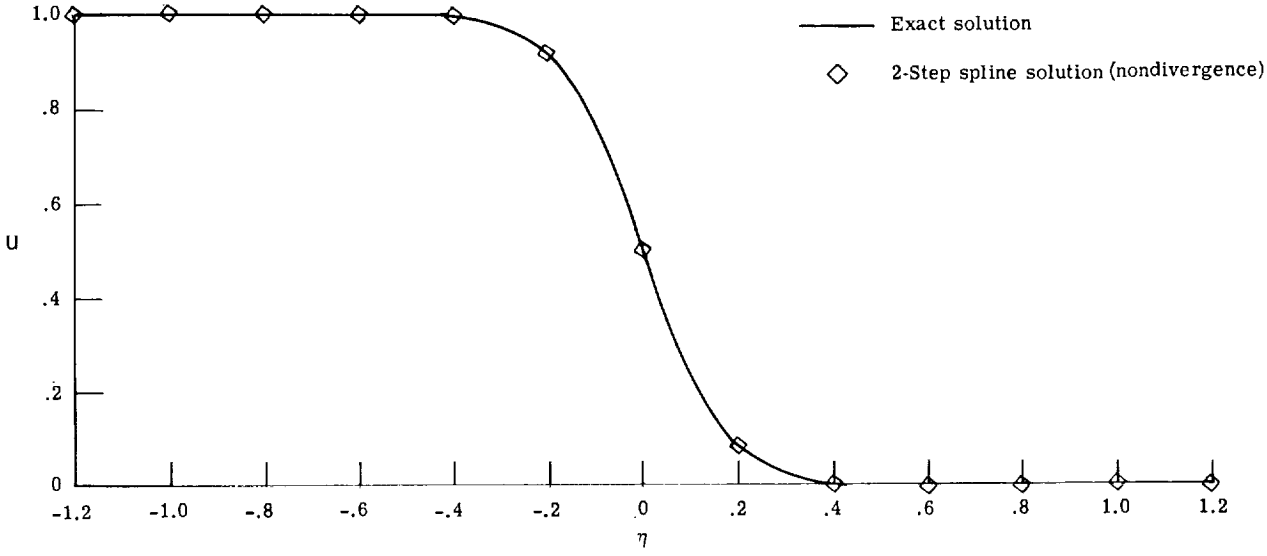

Figure 2.- Comparison of two-step spline solution with the exact solution to Burgers' equation for 51 points, $\nu = 1/24$, equal spacing, and $\sigma = 0$.

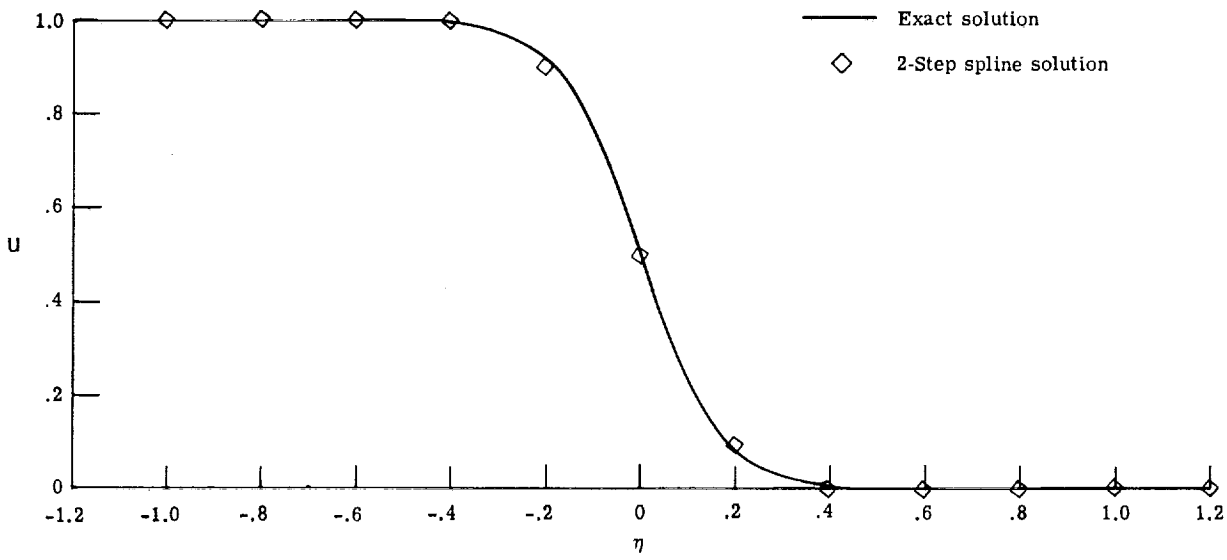

Figure 3.- Comparison of two-step spline solution with the exact solution to Burgers' equation for 51 points, $\nu = 1/24$, equal spacing, and $\sigma = 0$.

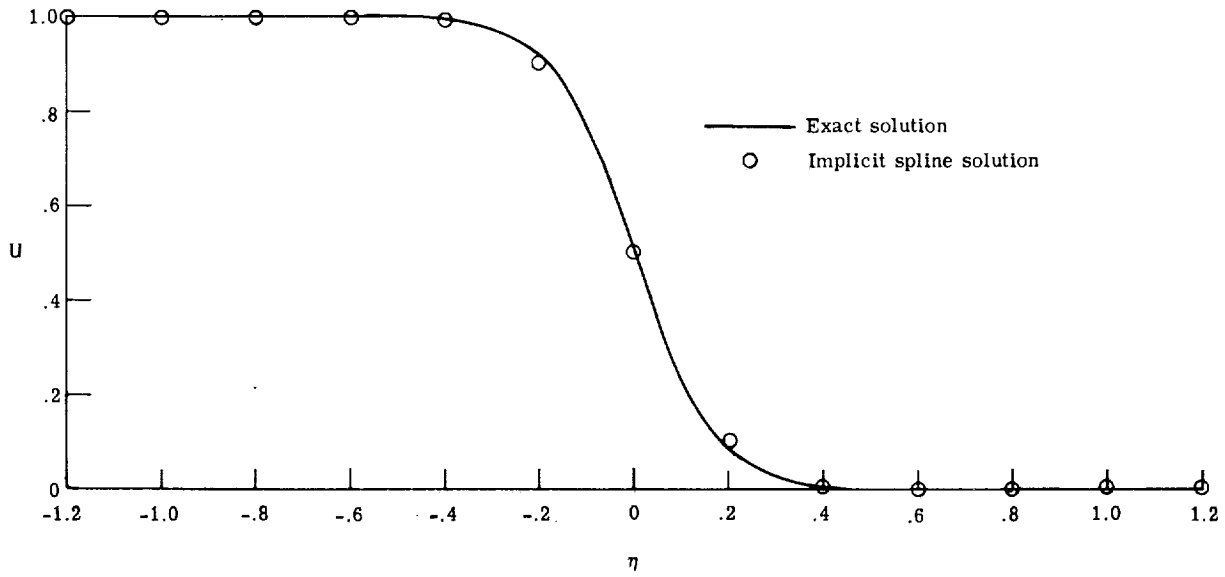

Figure 4.- Comparison of implicit spline solution with the exact solution to Burgers' equation for 51 points, $\nu = 1/24$, equal spacing, and $\sigma = 5$.

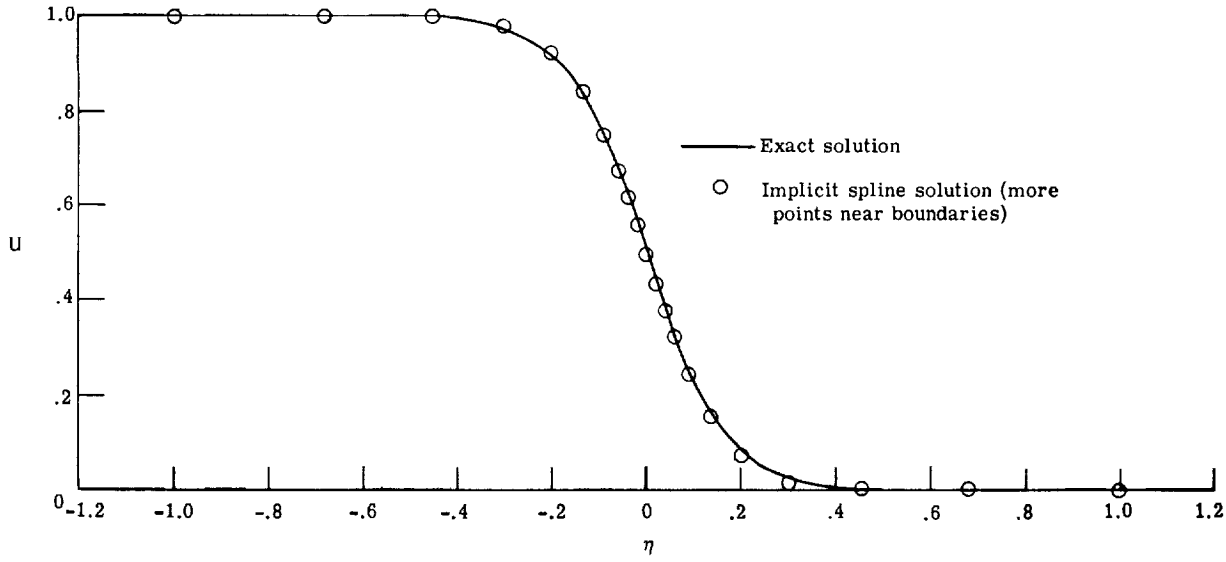

Figure 5.- Comparison of implicit spline solution with the exact solution to Burgers' equation for 37 points, $\nu = 1/24$, unequal spacing – more points near boundaries, and $\sigma = 0$.

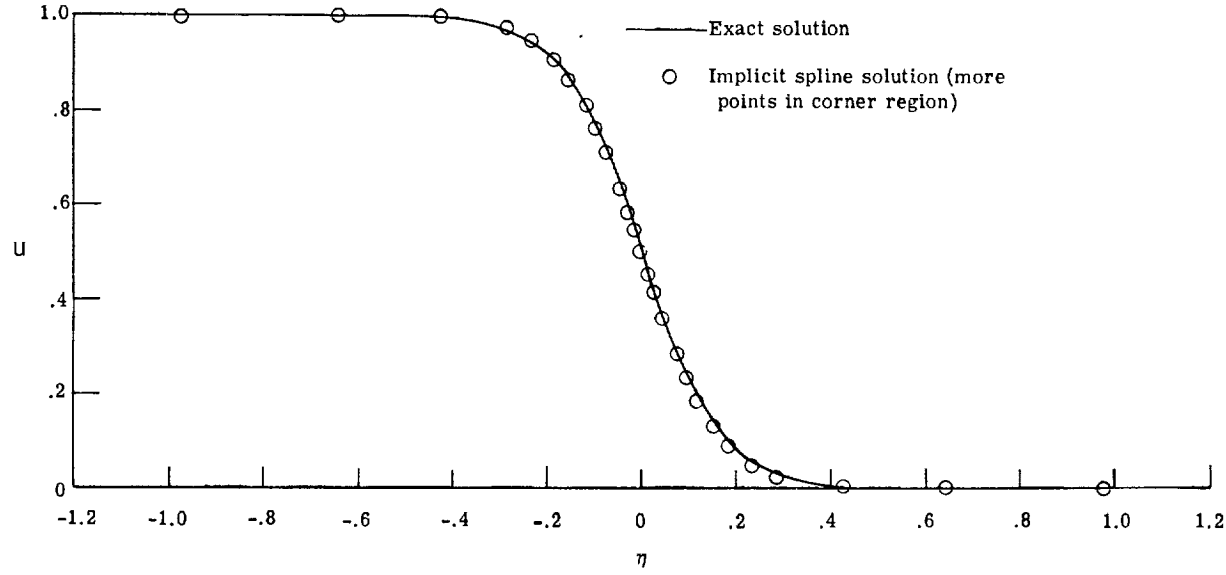

Figure 6.- Comparison of implicit spline solution with the exact solution to Burgers' equation for 37 points, $\nu = 1/24$, unequal spacing – more points in corner region, and $\sigma = 0$.

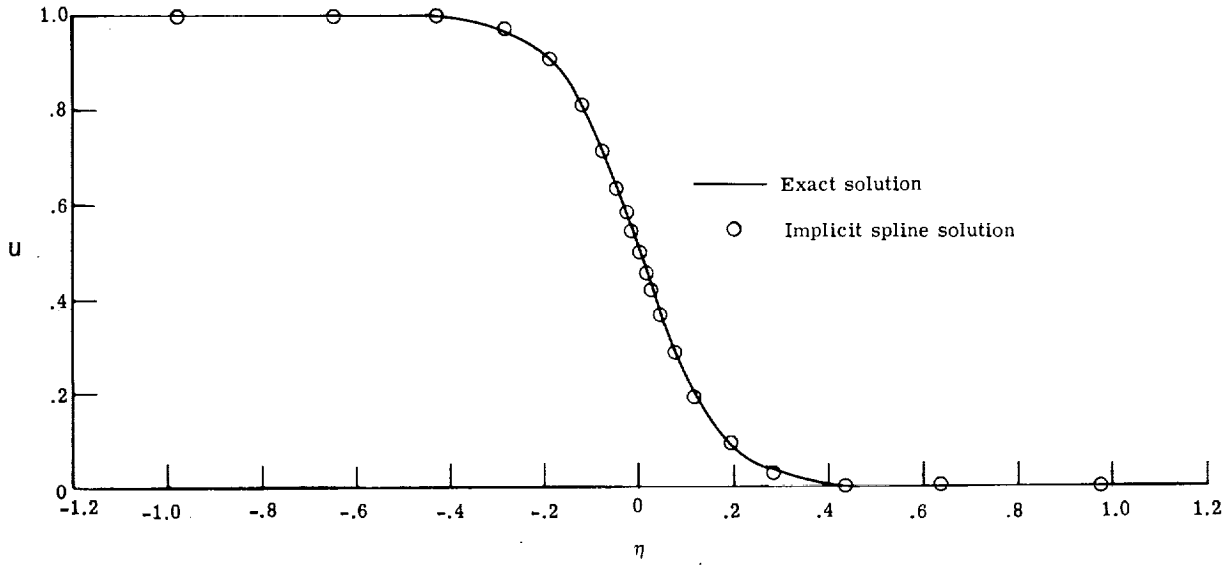

Figure 7.- Comparison of implicit spline solution with the exact solution to Burgers' equation for 31 points, $\nu = 1/24$, unequal spacing $\sigma_i = 1.5$, and $\sigma = 0$.

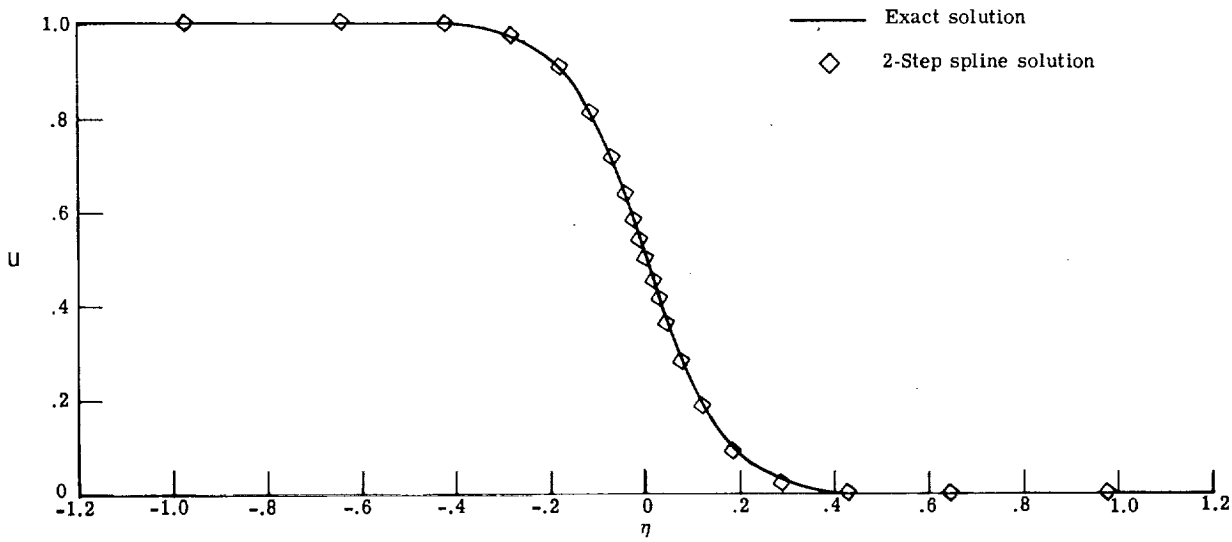

Figure 8.- Comparison of two-step spline solution with the exact solution to Burgers' equation for 31 points, $\nu = 1/24$, unequal spacing $\sigma_i = 1.5$, and $\sigma = 0$.

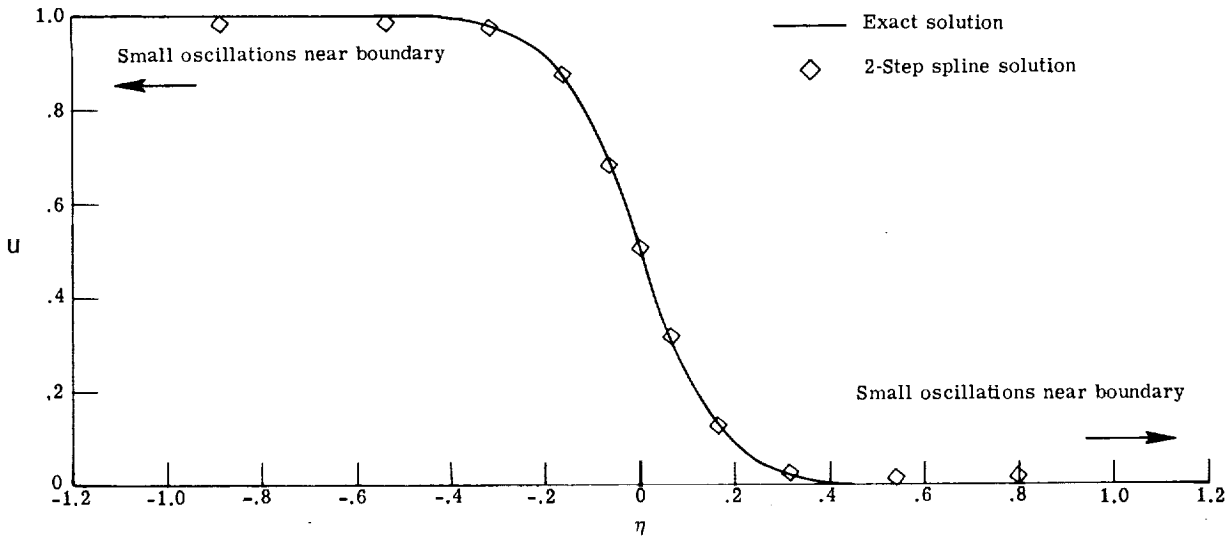

Figure 9.- Comparison of two-step spline solution with the exact solution to Burgers' equation for 19 points, $\nu = 1/24$, unequal spacing $\sigma_i = 1.5$, and $\sigma = 0$.

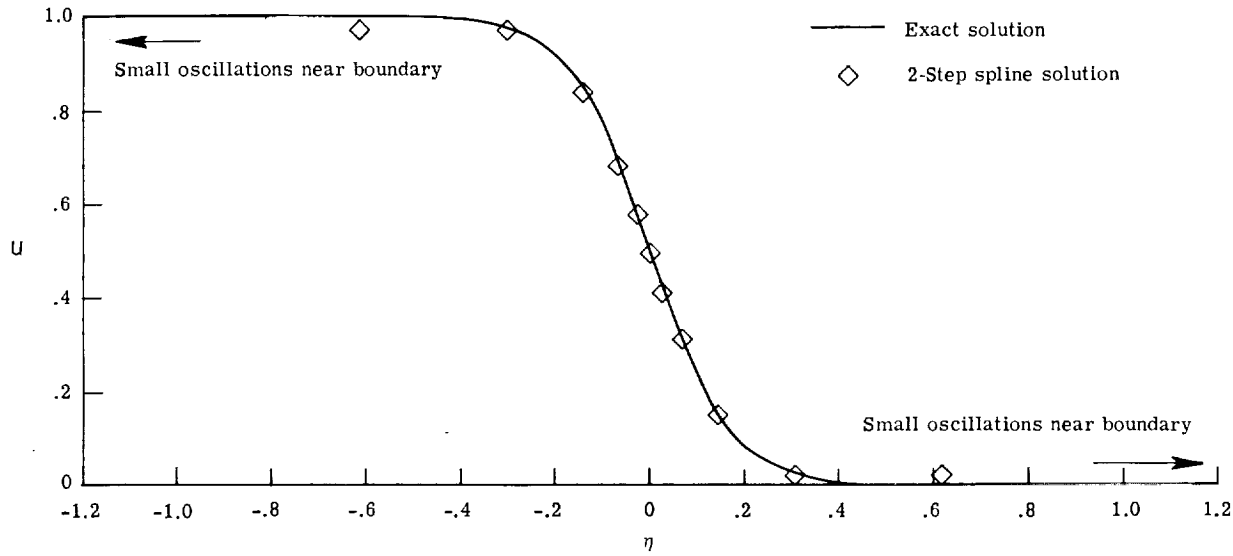

Figure 10.- Comparison of two-step spline solution with the exact solution to Burgers' equation for 19 points, $\nu = 1/24$, unequal spacing $\sigma_i = 2$, and $\sigma = 5$.

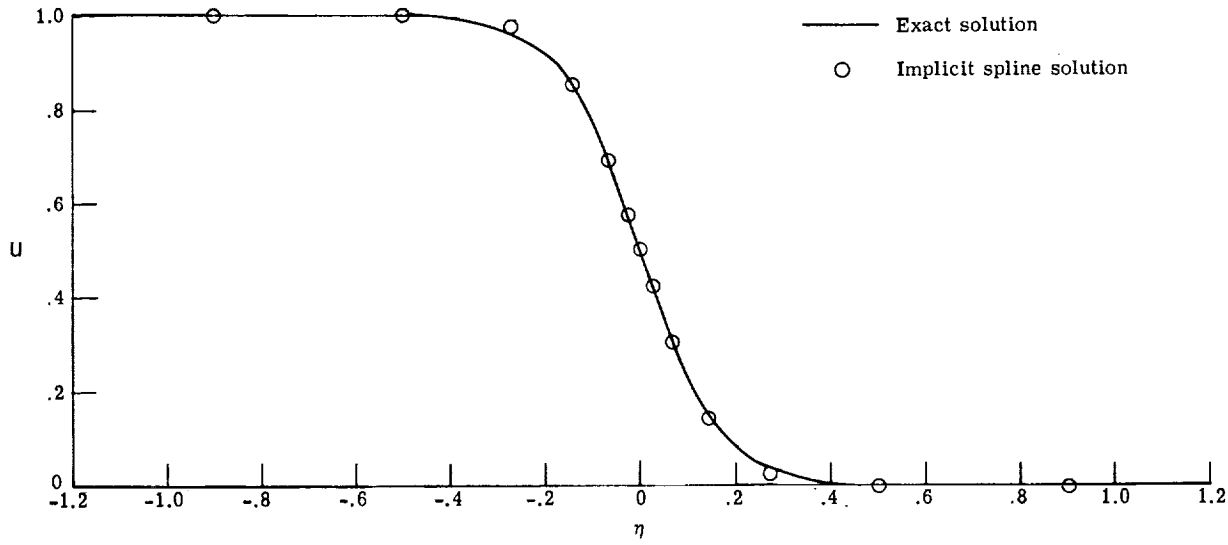

Figure 11.- Comparison of implicit spline solution with the exact solution to Burgers' equation for 19 points, $\nu = 1/24$, unequal spacing $\sigma_i = 1.75$, and $\sigma = 5$.

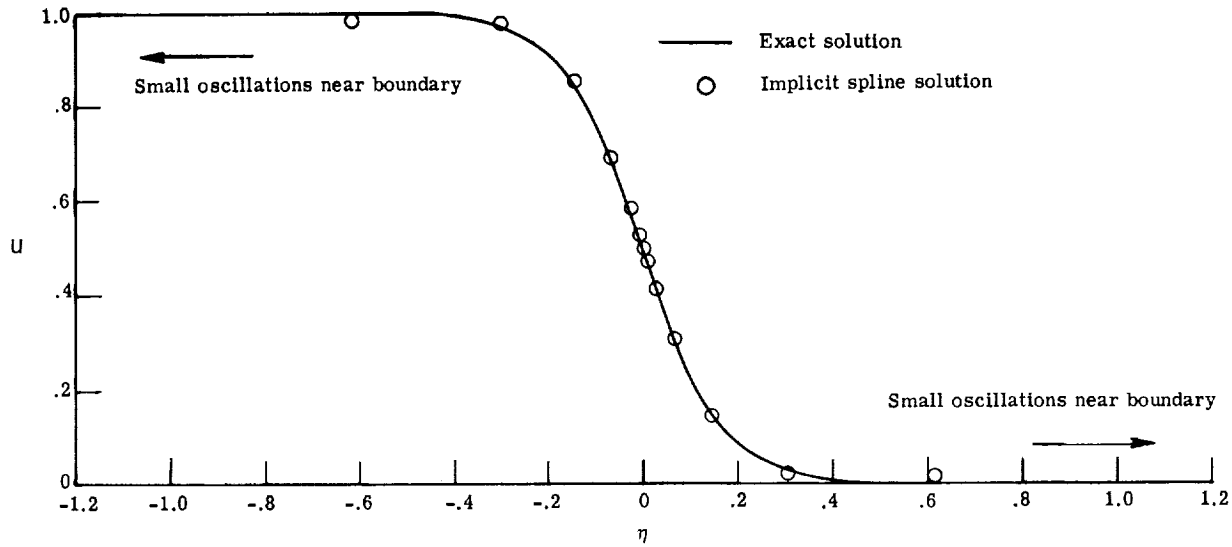

Figure 12.- Comparison of implicit spline solution with the exact solution to Burgers' equation for 19 points, $\nu = 1/24$, unequal spacing $\sigma_i = 2$, and $\sigma = 5$.

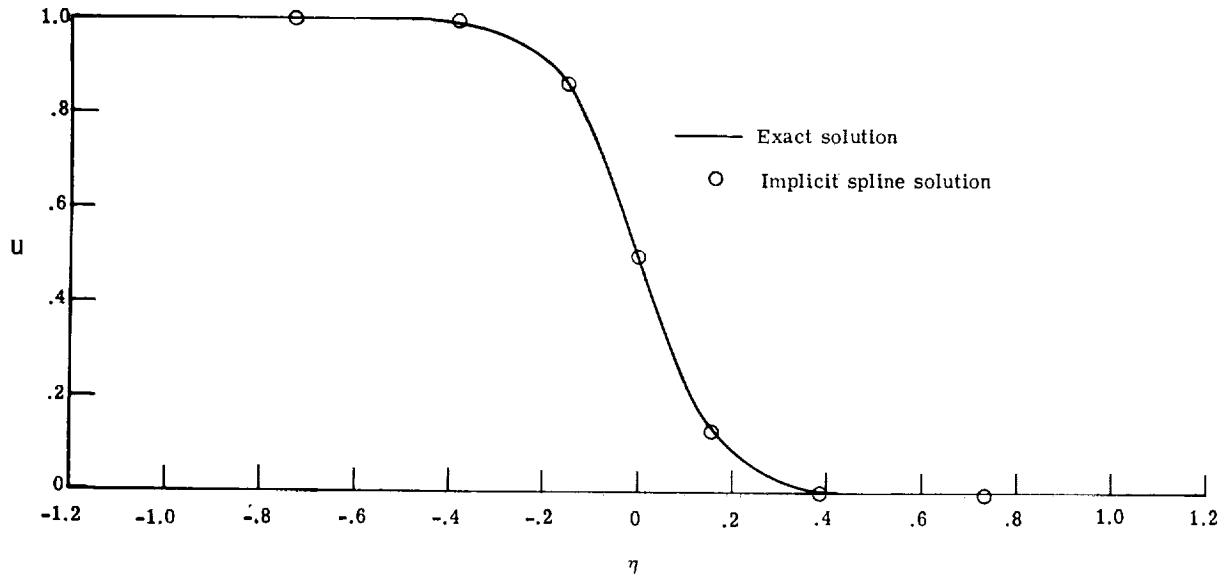

Figure 13.- Comparison of implicit spline solution with the exact solution to Burgers' equation for 15 points, $\nu = 1/24$, unequal spacing $\sigma_i = 1.5$, and $\sigma = 4.5$.

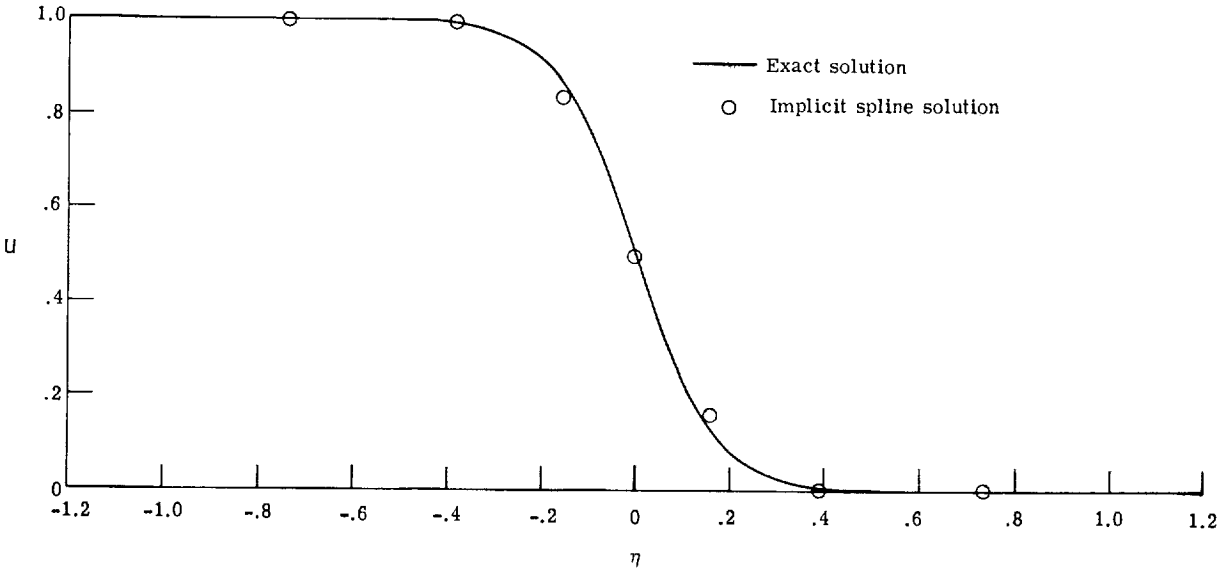

Figure 14.- Comparison of implicit spline solution with the exact solution to Burgers' equation for 15 points, $\nu = 1/24$, unequal spacing $\sigma_i = 1.5$, and $\sigma = 7.5$.

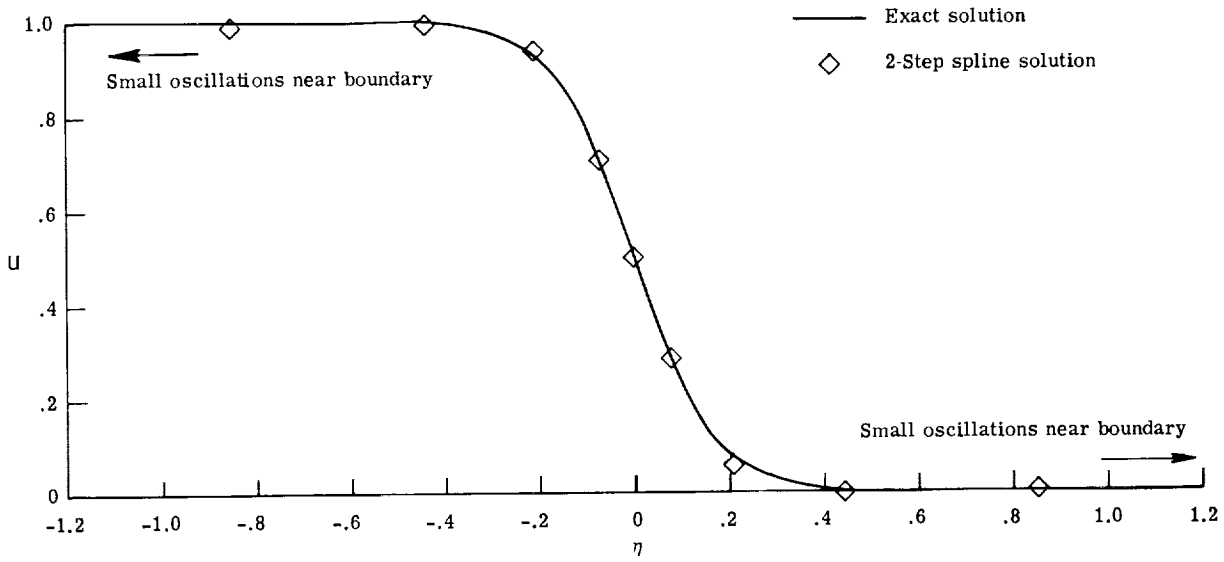

Figure 15.- Comparison of two-step spline solution with the exact solution to Burgers' equation for 15 points, $\nu = 1/24$, unequal spacing $\sigma_i = 1.75$, $\sigma = 0$, and $-3 \leq \eta \leq 3$.

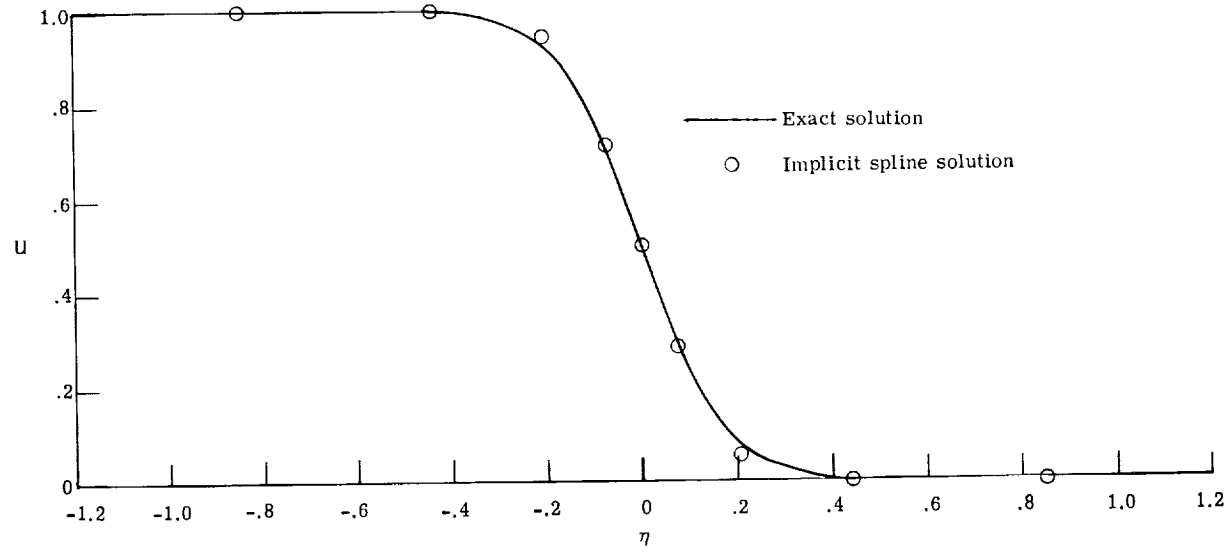

Figure 16.- Comparison of implicit spline solution with the exact solution to Burgers' equation for 15 points, $\nu = 1/24$, unequal spacing $\sigma_i = 1.75$, and $\sigma = 5$.

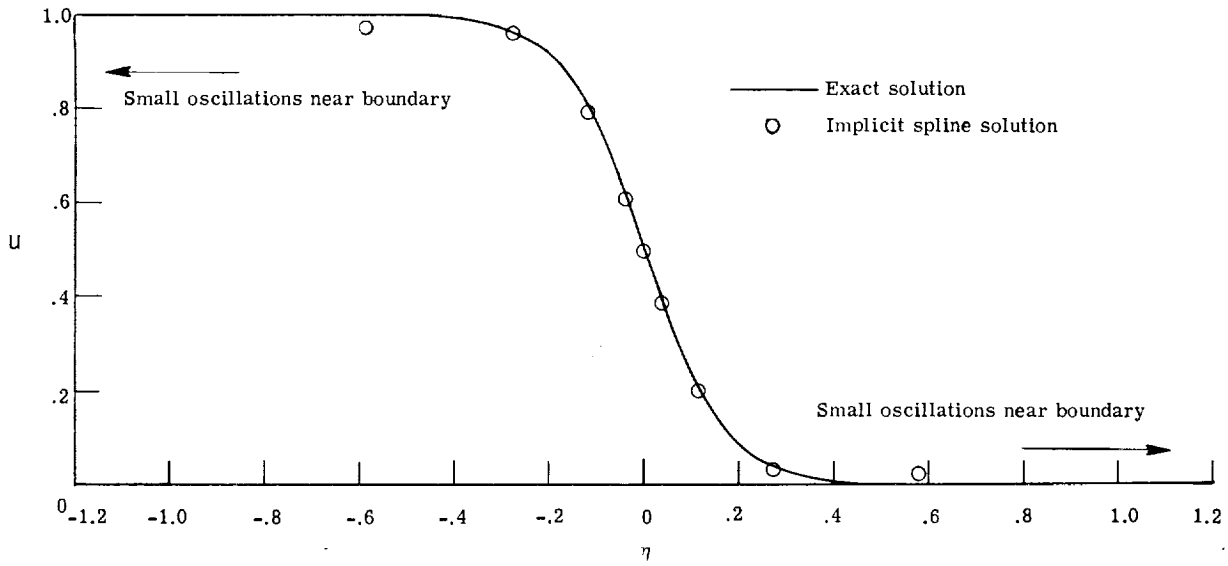

Figure 17.- Comparison of implicit spline solution with the exact solution to Burgers' equation for 15 points, $\nu = 1/24$, unequal spacing $\sigma_i = 2$, and $\sigma = 5$.

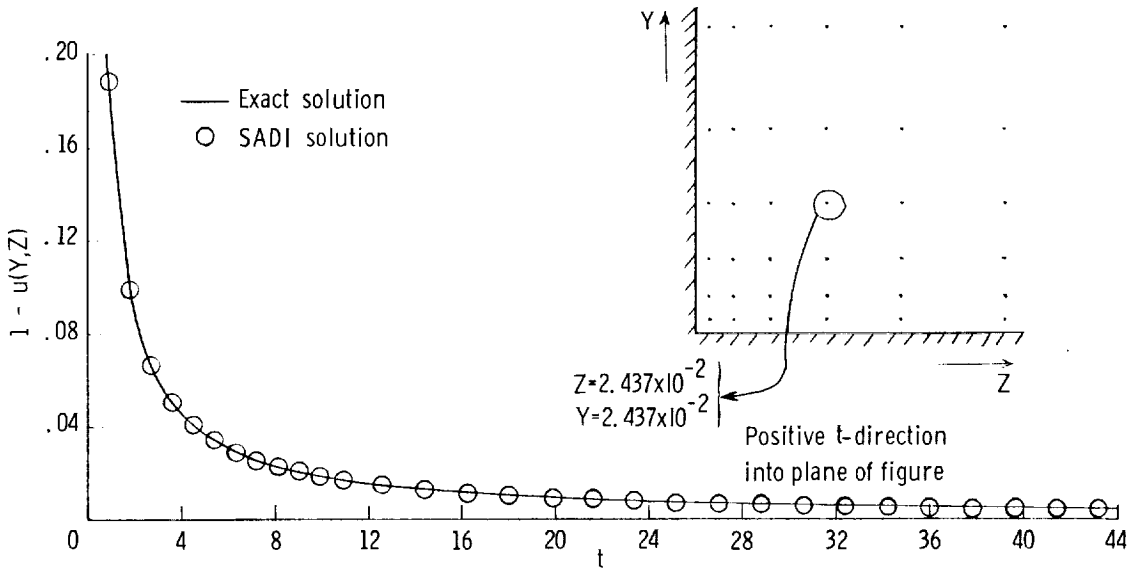

Figure 18.- Comparison of the SADI solution with the exact solution to the two-dimensional diffusion equation. $R = 1000$; $\Delta t = 9 \times 10^{-3}$; 17×17 grid; unequal spacing; $0 \leq Y,Z \leq 4$.

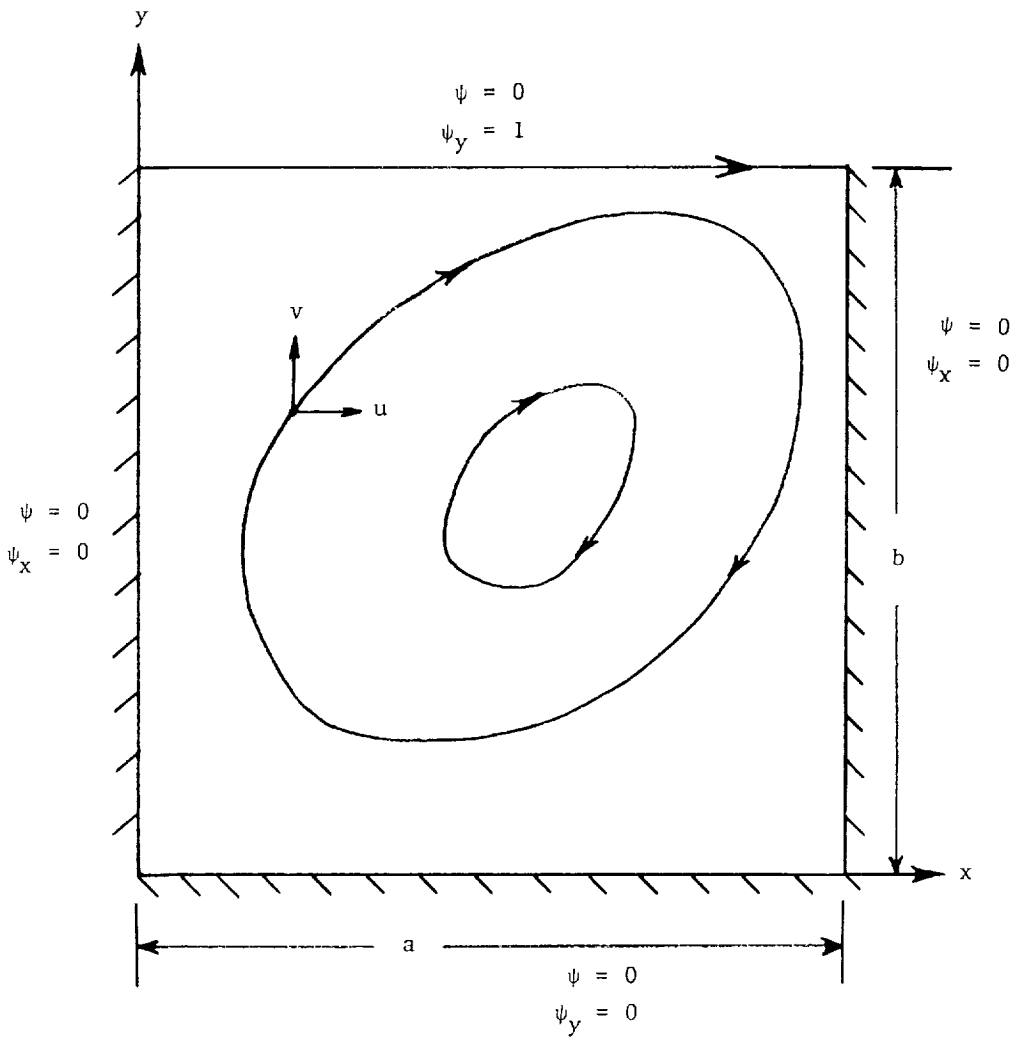

Figure 19.- Schematic of the driven cavity.

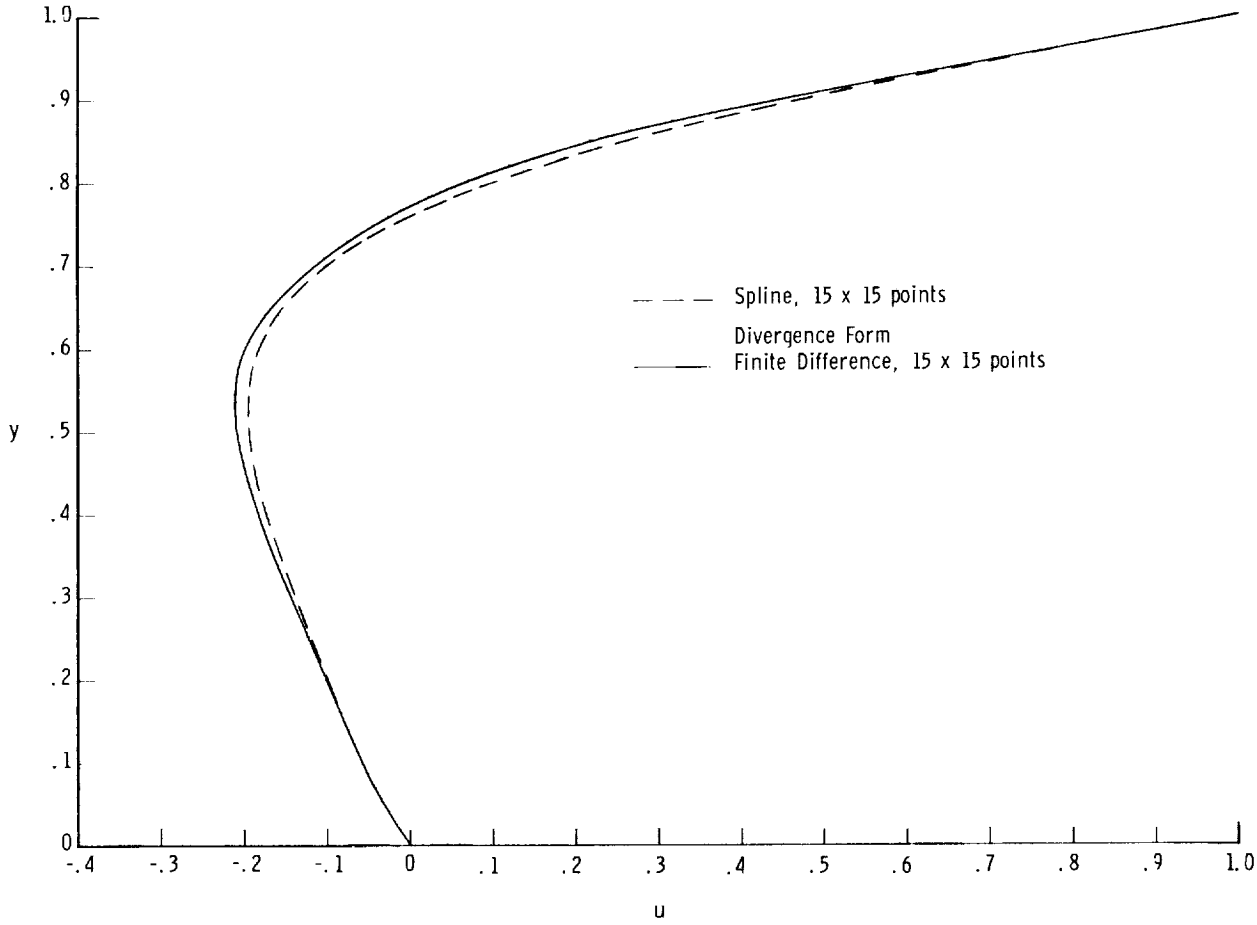

Figure 20.- Comparison of calculated velocity u through point of maximum ψ for R = 10. (Note: Nondivergence form results are virtually identical to divergence form.)

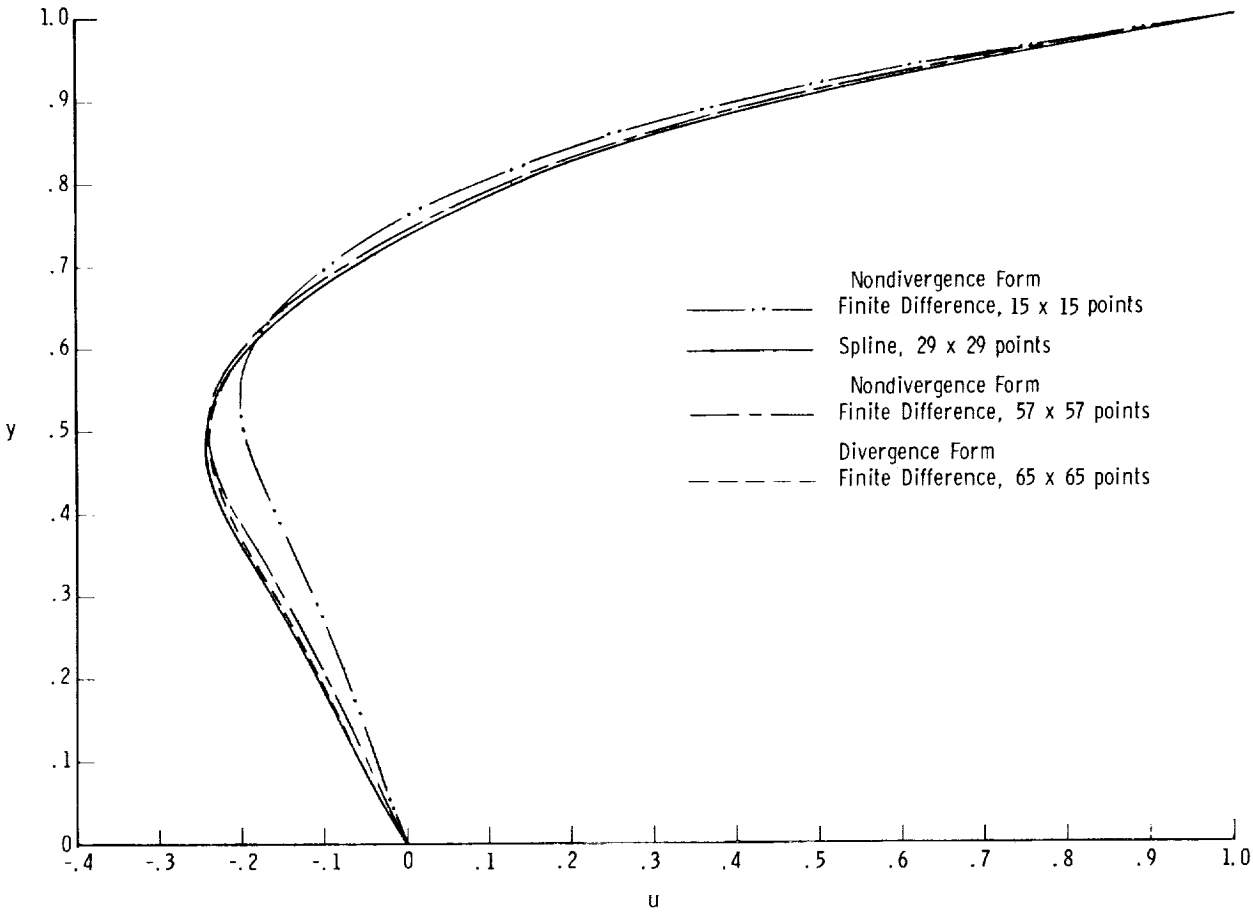

Figure 21.- Comparison of calculated velocity u through point of maximum ψ for R = 100.

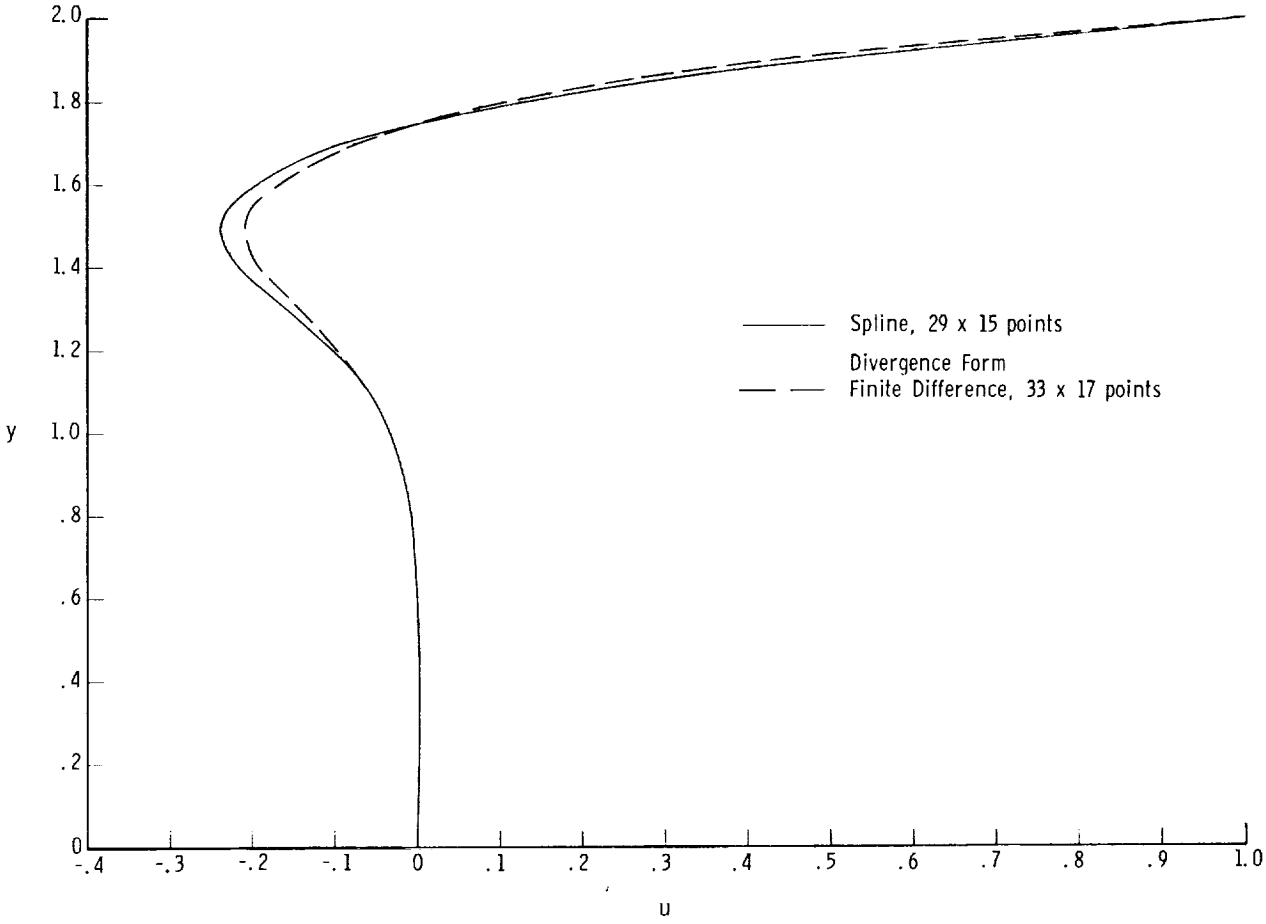

Figure 22.- Comparison of calculated velocity u through upper point of maximum ψ for R = 100 and 2 × 1 rectangular cavity.